20.3. DOWNSTREAM PROCESSING: SEPARATION AND PURIFICATION

20.3.1. INTRODUCTION

[1]Purification of bioproducts typically involves a long sequence of steps, and each step requires the use of one or more*unit operations,* such as filtration, precipitation, and chromatography. Each bioproduct has unique properties that differentiate it from other bioproducts. For bioseparation purposes, important properties include thermal stability, solubility, diffusivity, charge, isoelectric pH, molecular mass, hydrodynamic radius, hydrophobicity, reaction rate constants, and separation thermodynamics. A considerable amount of downstream process planning is based on the lability of most bioproducts. Temperature, pH, and concentration must be kept within specific limits to maintain product bioactivity.

Removal of solids (or recovery), isolation of product, purification, and polishing constitute a sequence of processing stages applied to nearly every product as it is prepared. These four stages make use of various unit operations. A *unit operation* is a single process and the equipment used therefor. These operations are applied in varying combinations to the four stages, approximately as indicated in Table 20-17.

Table 20-17 Objectives and Typical Unit Operations of the Four Stages in Bioseparations

Stage	Objective(s)	Typical unit operations
Separation of insolubles	Remove or collect cells, cell debris, or other particulates.	Filtration, sedimentation, extraction, adsorption
	Reduce volume (depends on unit operation).	
Isolation of product	Remove materials having properties widely different from those desired in product.	Extraction, adsorption, ultrafiltration, precipitation, affinity methods
	Reduce volume (depends on unit operation).	
Purification	Remove remaining impurities, which typically are similar to the desired product in chemical functionality and physical properties.	Chromatography, affinity methods, crystallization, fractional precipitation
Polishing	Remove liquids.	Drying, crystallization
	Convert the product to crystalline or other solid or concentrated form (not always possible).	
Reproduced from *Bioseparations Science and Engineering*, 2d. ed., by Roger G. Harrison, Paul W. Todd, Scott R. Rudge, and Demetri P. Petrides (2015). By Permission of Oxford University Press.		

The development and optimization of a bioseparation process involve the integration of the various unit operations in the most efficient way possible. The strategy for how to design a process to meet the desired objectives is presented along with a brief discussion of each unit operation. This is followed by a discussion of measures of process/product quality and the types of bioproducts that are on route to market. After this introduction section, more detailed treatments of key unit operations used in bioseparations are given that are not discussed elsewhere in this handbook.

Bioseparation Process Development The development of a process for the recovery and purification of a biological product is a creative activity that draws on the experience and imagination of the engineer. Attempts have been made to capture that experience on the computer in the form of expert systems [Petrides, *Comput. Chem. Eng.* **18:** S621 (1994)] and automate to some extent the process synthesis tasks. Experienced engineers rely heavily on certain *rules of thumb*, also known as *heuristics*, for putting together the skeleton of a recovery and purification process [Nfor et al.,*J. Chem. Technol. Biotechnol.* **83:** 124 (2008)]. A few such heuristics follow:

1. Remove the most plentiful impurities first.
2. Remove the easiest-to-remove impurities first.
3. Make the most difficult and expensive separations last.
4. Select processes that make use of the greatest differences in the properties of the product and its impurities.
5. Select and sequence processes that exploit different separation driving forces.
6. Sequence unit operations such that the product of one can serve as the feedstock for the next without dilution or intermediate treatment.

Approaches to process development (also known as *process synthesis*) must be made with future scale-up in mind. A biotechnology product production process is a set of sequential unit operations that produces a final product able to meet defined levels of quality, yield, and cost. The following criteria should therefore be used in evaluating and developing a bioseparation process:

- Product purity
- Cost of production as related to yield
- Scalability
- Reproducibility and ease of implementation
- Robustness with respect to process stream variables

Examples of the integration of unit operations for the efficient synthesis of bioseparation processes are presented later in the subsection Bioprocess Design and Economics.

Figure 20-29 provides a generalized structure for creating an initial block diagram representation of a product recovery process. For each product category (intracellular or extracellular), several branches exist in the main pathway. Selection among the branches and alternative unit operations is based on the properties of the product, the properties of the impurities, and the properties of the producing microorganisms, cells, or tissues. Bioprocess synthesis thus consists of sequencing steps according to the six heuristics above and the structure of Fig. 20-29. The majority of bioprocesses, especially those employed in the production of high-value and low-volume products, operate in batch mode. Conversely, continuous bioseparation processes are utilized in the production of commodity biochemicals, such as organic acids and biofuels.

Figure 20-29 Generalized block diagram of downstream processing. [Petrides et al., in Shuler (ed.), Chemical Engineering Problems in Biotechnology, American Institute of Chemical Engineers, 1989, p. 351.]

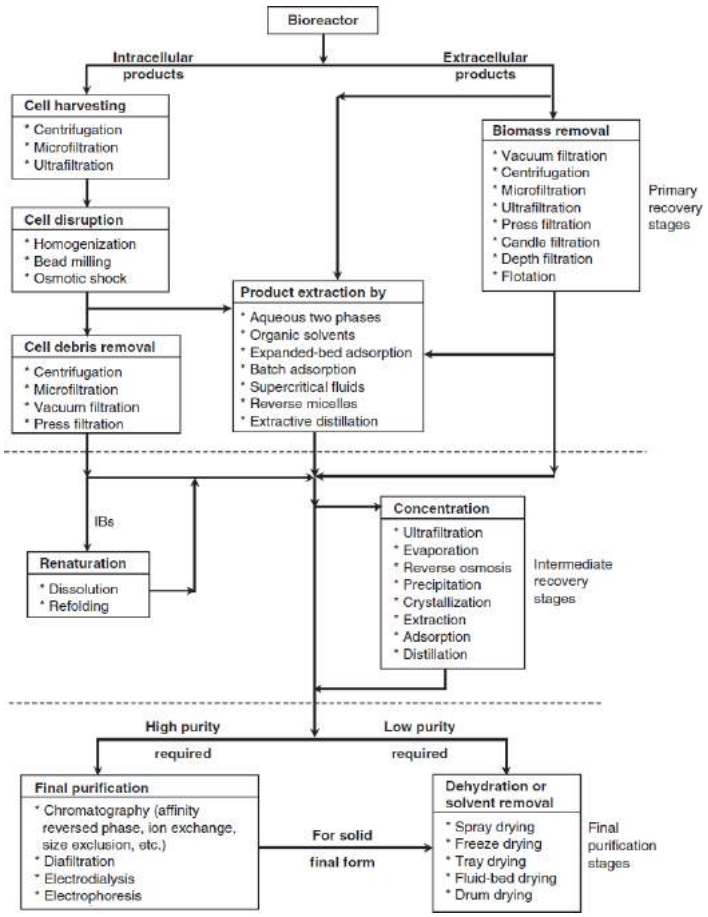

Primary Recovery Stage Primary recovery encompasses the first steps of downstream processing where some purification and broth volume reduction occurs. Primary recovery includes both the solids separation stage and parts of the product isolation stages shown in Table 20-17. According to Fig. 20-29, the selection of the first step depends on whether the product is intracellular (remains inside the microorganism or eukaryotic cell after its expression) or extracellular (is secreted into the solution). Almost all low-molecular-weight bioproducts are extracellular, as are many that have a high molecular weight. Recovery and purification are easier for these bioproducts than for intracellular products because of the lower amount of impurities present. Most recombinant eukaryotic proteins produced by prokaryotic microorganisms are intracellular products. These proteins accumulate inside the host cell in either native or denatured form; the denatured intracellular products often form insoluble *inclusion bodies* (IBs). A brief review of the most common primary recovery steps follows, and various rationales for unit operation selection are included. The human insulin process analyzed in this section provides additional information on the recovery and purification of intracellular products.

The first purification step for intracellular products is cell harvesting. Removal of the extracellular liquid is in agreement with the first general heuristic: *Remove the most plentiful impurities first.*

As seen in Fig. 20-29, centrifugation and membrane filtration (either microfiltration or ultrafiltration) are the primary techniques used for large-scale cell harvesting. Centrifugation has advantages for large, sturdy, and dense microorganisms (diameter >2 μm and density >1.03 g cm^{-3}), and it avoids the fouling that can occur with membrane filtration. For instance, centrifugation is very efficient for harvesting yeast. Centrifugation can lead to cell disruption (releasing additional impurities for extracellular products) with fragile cells, such as mammalian cells in suspension. Filtration has advantages for harvesting small, fragile, and light cells. Filtration operates with much lower shear rates compared to centrifugation. Another advantage of filtration is its superior product recovery. Cell loss and/or supernatant loss during centrifugation can be as high as 50 percent and is rarely less than 5 percent. However, with membrane filtration, essentially all cells are recovered unless there is cell disruption (lysis) or unless the membranes fail.

The second step for intracellular products is usually cell disruption, which serves to break open the host cells and release the intracellular product. Disruption of bacteria and yeast is carried out either by high-pressure homogenizers or bead mills [Kula and Horst, *Biotechnol. Prog*. **3:** 31 (1987)]. For large capacities (several cubic meters per hour) only high-pressure homogenizers are practical. Osmotic shock is often used for release of periplasmic products that accumulate between the cell membrane and the cell wall.

Prior to disruption, the concentrate is often diluted (to 5 to 10 percent by weight) with a "lysis buffer" to create conditions that minimize product denaturation upon release from the cell and maximize product solubility. For hard-to-disrupt microorganisms, multiple homogenization passes at 500 to 1000 bar are required. Multiple passes are also required if the product forms inclusion bodies. This allows the IBs to be released and breaks the cell debris into very small particles, facilitating the separation of IBs from cell debris further downstream. Some soluble product degradation often occurs during cell disruption as a result of high shear at interfaces and oxidation.

The cell debris generated by cell disruption is usually removed by centrifugation or microfiltration. Other options include rotary vacuum filtration, press filtration, depth filtration, extraction, and expanded-bed adsorption (EBA).

When the product is soluble, it is recovered during cell debris removal either in the light phase of a centrifuge or in the permeate stream of a filter. Centrifuges are only able to efficiently separate fairly large particles of cell debris (>0.5-μm Stokes diameter). Therefore, when a centrifuge is used for cell debris removal, a polishing filtration step must follow the centrifugation in order to remove small debris particles that might otherwise cause severe problems in processes downstream, such as chromatography. Filters of various types (e.g., depth, press, candle, rotary vacuum, membrane microfilters) can be used for polishing. Alternatively, these filters can be used for cell debris removal with no preceding centrifugation step. It is very difficult to predict a priori which filter will perform best for a specific product, so lab and pilot-scale testing are typically used to make this decision. In addition, when microfilters are used for cell debris removal, some degree of diafiltration is required to achieve an acceptable product recovery yield.

When the product is insoluble and forms inclusion bodies, it must first be separated from the cell debris particles, then dissolved and refolded (see insulin example later in this section for additional information on the subject). Fortunately, inclusion bodies usually have a large diameter (0.3 to 1.0 μm) and high density (1.3 to 1.5 g cm^{-3}) [Taylor et al., *Bio/Technol.* **4:** 553 (1986)] and can be separated from cell debris with a disk-stack centrifuge. The inclusion bodies are recovered in the heavy phase of the centrifuge, while most cell debris particles remain in the light phase. The heavy phase is usually resuspended and recentrifuged two or three times to reach a high degree of inclusion body purity. Resuspension in a solution of a low concentration of a chaotropic agent such as a detergent is often practiced to facilitate the removal of other contaminants without solubilizing the inclusion bodies. The pH and the ionic strength of the solution are adjusted to reduce the hydrophobicity of the cell debris particles and to enhance their removal in the light phase. Final product purity exceeding 70 percent is quite common.

Separation of soluble product from cell debris can be carried out by extraction and/or adsorption. Organic solvents are commonly used as extractants for low-molecular-weight products, such as various antibiotics. Aqueous two-phase systems have found applications for recovery of proteins. The criteria for extractant selection are as follows: (1) the partition coefficient of the product should be higher than the partition coefficient of the contaminants, (2) the extractant should not degrade the product, and (3) the extractant should not be expensive and should be easy to recover or dispose of.

Alternatively, product separation from debris and simultaneous concentration can be achieved by adsorptive techniques [Palmer, *Process Biochem.* **12:** 24 (1977)]. Adsorbents of various types (e.g., ion exchange, reversed phase, affinity) can be used. This type of purification requires the disrupted cells and product to be mixed in a stirred tank with an adsorbent. A washing step, where most of the cell debris particles and contaminants are washed out, follows product adsorption. Expanded-bed adsorption is an alternative technology for separating proteins from cell debris particles [Chang and Chase, *Biotechnol. Bioeng*. **49:** 512 (1996); Jin, *Pharm. Eng.*, Jan./Feb., p. 66 (2015)]. The feed is pumped upward through an expanded bed. Target proteins are bound to the adsorbent while cell debris and other contaminants pass through. A washing step removes all weakly retained material. An elution step follows that releases and further purifies the product.

In agreement with the second generic heuristic (*Remove the easiest-to-remove impurities first*), biomass removal is usually the first step of downstream processing of extracellular products. This step can be accomplished by using one (or more) of the following unit operations: rotary vacuum filtration, disk-stack or decanter centrifugation, press filtration, depth filtration, microfiltration, ultrafiltration, and flotation. Since each unit operation has advantages and disadvantages for different products and microorganisms, the selection of the best unit operation(s) for a given system can be difficult.

Rotary vacuum filtration, especially with precoat, is the classical method for removal of mycelial organisms [Dlouhy and Dahlstrom, *Chem. Eng. Prog.* **64:** 116 (1968)]. Rotary vacuum filters can operate continuously for long periods. In addition, the filtrate flux in these units is usually higher than 200 L m^{-2} h^{-1} and may reach 1000 L m^{-2} h^{-1}. The most important disadvantage of this type of unit is the problem with disposal of the mixture of filter aid and biomass. Filter aid is added in equal or higher amounts than biomass. Stringent environmental laws have made it costly to dispose of such solid materials. Therefore, if the disposal cost of filter aid is relatively high where a new plant is going to be built, alternative unit operations should be considered for biomass separation. However, if the disposal cost of filter aid is relatively low, a rotary vacuum filter is a good choice. The citric acid process, which is described later in this section, offers an example where rotary vacuum filtration is used for biomass removal.

Disk-stack and decanter centrifuges are frequently used at large scale [Brunner and Hemfort, in Mizrahi and Alan (eds.), *Advances in Biotechnological Processes*, vol. 8, Liss Inc., New York, 1988, p. 1]. Disk-stack centrifuges operate at higher rotational speeds and remove smaller and lighter microorganisms than decanters. However, with the use of flocculating agents, the decanter centrifuge performance improves, and choosing between the two types becomes more difficult. It appears that the only criterion being applied when disk-stack is chosen instead of decanter is the ability to remove small, light microorganisms. Centrifugation does not require filter aid, which is a significant advantage over rotary vacuum filtration. In general, the centrifuge paste contains 40 to 60 percent v/v extracellular liquid. To recover the product dissolved in that liquid, the paste is usually washed and recentrifuged.

With membrane filters (microfilters and ultrafilters), the extracellular product passes through the membrane while biomass and other particulate components remain in the concentrate. Concentration is usually followed by diafiltration to prevent product degradation and/or to improve the performance of the subsequent step. Membrane filters are used for biomass removal mainly in recovery of low-molecular-weight products, such as antibiotics from mycelia. For high-molecular-weight products, gel layer formation often limits application to cases in which the amount of solids is rather small (e.g., cell culture).

Depth filtration is commonly used in the recovery of antibodies from cell culture. New depth filtration media contains a layer of fiber and a layer of filter aid contained within another filter. These filters have shown a combination of high solids load and excellent retention of small particles at micrometer and submicrometer scales. Depth filtration can process solids- containing fluids at 1700 to 25,000 L m^{-2} min^{-1} [http://www.pall.com/main/biopharmaceuticals/product.page?id=28210].

Intermediate Recovery Stages The primary recovery stages just described are followed by the intermediate stages, where the product is concentrated and further purified. Intermediate recovery has similarities to the product isolation stages shown in Table 20-17. If the product is soluble, product capture and concentration is usually the first step. If the product is denatured and insoluble, it is first dissolved and refolded and then captured, concentrated, and purified.

After primary separation, the product is usually in a dilute solution. Volume reduction by concentration is in agreement with heuristics 1 and 2. Common concentration options include ultrafiltration, reverse osmosis, evaporation, adsorption, precipitation, extraction, and distillation.

Ultrafiltration is used extensively for protein solution concentration. The molecular weight cutoff of the membrane is selected to retain the product while allowing undesirable impurities (mainly low-molecular-weight solutes) to pass through the membrane. The low operating temperature and the purification achieved along with concentration are some of the advantages of ultrafiltration over evaporation. The typical operating transmembrane pressure is 2 to 5 bar, and the average flux is 20 to 50 L m^{-2} h^{-1}.

Membranes with smaller pore sizes are used for reverse-osmosis filters. The process of reverse osmosis may be used when concentrating medium- to low-molecular-weight products (e.g., antibiotics, certain amino acids).

Agitated film evaporators can operate at relatively low temperatures (40 to 50 C) under vacuum. These units compete in the market with ultrafiltration and reverse osmosis for concentrating both low- and high-molecular-weight compounds. Unlike ultrafiltration, however, evaporation lacks the capability to provide purification during concentration. Advantages include the ability to concentrate to a higher final solids concentration and the ability to handle large throughputs [Freese, in Vogel and Todaro (eds.), *Fermentation and Biochemical Engineering Handbook*, Noyes, Westwood, N.J., 1993, p. 227].

Precipitation is often used for concentration and purification. Blood protein fractionation and citric acid production (see later subsection Bioprocess Design and Economics) constitute typical applications. Addition of salts, solvents, and polymers and changes in pH, ionic strength, and temperature are commonly used to selectively precipitate compounds of interest [Chan et al., *Biotechnol. Bioeng*. **28:** 387 (1986)]. Precipitation often follows an extraction carried out in a polymer/salt (e.g., PEG and potassium phosphate) aqueous two-phase system. When the product is recovered in the polymer-rich phase, precipitation is accomplished by adding more polymer. It is important for economic reasons to recover and recycle the precipitating materials. Precipitation is also used to remove contaminants (i.e., nucleic acids) by adding manganese sulfate ($MnSO_4$) and streptomycin sulfate.

The process of distillation is used for concentrating and purifying low-molecular-weight and volatile compounds, such as acetone, ethanol, butanol, acetic acid, etc.

Pervaporation is a membrane-based process that has found applications in biofuels for the dehydration of ethanol and other alcohols. One component from a liquid mixture selectively permeates a membrane, driven by a gradient in partial vapor pressure and leaving the membrane as a vapor (Bruschke, in Nunes and Peinemann, *Membrane Technology in the Chemical Industry*, Wiley-VCH, Weinheim, Germany, 2006, p. 127). Dehydration of ethanol-water azeotropic solutions (around 90 percent ethanol) is facilitated by the use of hydrophilic membranes. Hydrophobic membranes are used for removal/recovery of small amounts of organics from aqueous solutions.

Eukaryotic proteins produced by prokaryotic microorganisms often form insoluble inclusion bodies in the host cell, and renaturation of the protein is required when this occurs. Inclusion bodies first need to be dissolved and usually reduced (to break disulfide bonds that have formed incorrectly in the inclusion body) and then oxidized to form the proper disulfide bonds. Inclusion bodies can be dissolved rapidly by using solutions of strong chaotropes, such as 6 *M* guanidine hydrochloride or urea. Detergents and surfactants can also be used. Common reducing agents are 0.5 *M* 2-mercaptoethanol or 50 *mM* dithiothreitol [Fish et al., *Biochemistry* **24:** 1510 (1985)]. The dissolved protein is then allowed to refold to its native conformation. This can be done with air or oxygen in the presence of copper ion as a catalyst, and by removing the chaotropic agents through diafiltration, dilution, or chromatography, with final protein concentrations in the range of 10 to 100 mg L^{-1}. Dilution is sometimes necessary for minimizing intermolecular interactions, especially when there are multiple cysteines in the protein. Intermolecular interactions that occur during product refolding can lead to product inactivation, dimerization, crosslinking, and poor yield. Regulation of the redox state of the refold through addition of small amounts of thiols such as reduced glutathione (1 to 5 *mM*) and oxidized glutathione (0.01 to 0.5 *mM*) and incubation at 35 to 40 C for 5 to 10 h completes the refolding process. Thus, choosing an upstream process that forms IBs entails consideration of the large volumes, hence large waste streams, that are produced. More information on IB solubilization and protein refolding can be found in the insulin example (see later subsection Bioprocess Design and Economics).

Final Purification Stages The final purification steps are dependent on the required final product purity. Pharmaceutical products require high purity, while commodity products require lower purity. For products of relatively low purity, such as industrial enzymes, the final purification step is dehydration or more generally a solvent removal step. For high-purity products, the final purification stages usually involve a combination of chromatographic and filtration steps [Bjurstrom, *Chem. Eng.* **92:** 126 (1985)]. If the final product is required in solid form, a dehydration or solvent removal step follows.

Chromatography is typically done later in a process in agreement with the third generic heuristic (*Make the most difficult and expensive separations last*). With the preceding separation steps, a large fraction of contaminants is removed, thereby reducing the volume of material that needs to be treated further. A sequence of chromatographic steps is usually required to achieve the desired final product purity, and the fourth and fifth generic heuristics are good guides for selecting and sequencing such steps [Wheelwright, *Bio/Technol*. **5:** 789 (1987)]. For instance, according to the fifth heuristic, an ion exchange step should not be followed by another step of the same type. Instead, it should be followed by a reversed-phase, affinity, or any other chromatography type that takes advantage of a different separation driving force. The insulin and monoclonal antibody examples presented later in this section provide additional information on selection, sequencing, and operation of chromatographic separation units.

Membrane adsorption units combine the high flux of membrane filters with the selective binding of chromatographic resins [Zhou and Tressel, *BioProcess Int*. **3:** 32 (2005)]. As a result, they have advantages compared to traditional column chromatography when operated in the flow-through mode for removing small amounts of specific contaminants. The membrane retains certain impurities (e.g., DNA molecule fragments) while the product molecules pass through the membrane. Such membrane systems are typically used as the last step of biopharmaceutical protein purification processes. More information about membrane chromatography is given in the subsection Liquid Chromatography and Adsorption.

Simulated moving-bed (SMB) chromatography is the method of choice for handling large volumes of material [Holzer et al., *BioProcess Int.* **6:** 74 (2008)]. It has found applications in the purification of amino acids, high-fructose corn syrup, cheese whey proteins, lactic acid, succinic acid, etc. In SMB systems, multiple columns operate out of phase using a complex system of valves. The feed stream usually passes through two columns, resulting in increased yield and resolution. One column is always out of use for cleaning/regeneration. SMB systems can handle feed streams of continuous flow, which is the preferred method of operation for the production of high-volume biochemicals. More information about SMB can be found in the subsection Simulated Moving-Bed Chromatography.

Membrane filtration can be used between chromatographic steps to exchange buffers, concentrate the dilute product solutions, and control bioburden. Dead-end filtration can also be used to remove contaminating particles in chromatography feed streams.

Crystallization and fractional precipitation can sometimes result in significant purification. Because these processes are cheaper to operate than chromatography, they should always be considered. The crystalline form of a bioproduct is especially advantageous, since the purity can be quite high and crystals can usually be stored for long periods. The citric acid process that is analyzed later in this section is a good example of a product that is recovered and purified using precipitation and crystallization.

Dehydration or solvent removal is achieved with dryers. Spray, fluidized-bed, and tray dryers are used when products can withstand temperatures of 50 to 100 C. Freeze dryers are used for products that degrade at high temperatures. Freeze dryers require high capital expenditures and should be avoided, if possible.

Pairing of Unit Operations in Process Synthesis It is often advantageous to consider how two different unit operations can be paired to improve process efficiency, which follows the sixth heuristic (*Sequence unit operations such that the product of one can serve as the feedstock for the next without dilution or intermediate treatment*). The following gives some examples of operations that are logical to pair:

- In the pairing of extraction and precipitation, the bioproduct is extracted with a solvent and then precipitated. To increase the yield, it is often desirable to concentrate the extract before the precipitation. The major hurdle to overcome for this pairing is to find a solvent that will work with both extraction and precipitation.
- The pairing of precipitation and hydrophobic interaction chromatography is usually accomplished for protein purification by using ammonium sulfate to precipitate impurities, leaving the desired bioproduct in the mother liquor. The ammonium sulfate is added to a concentration just below that needed to precipitate the bioproduct. After removal of precipitated impurities, the mother liquor can be applied directly to a hydrophobic interaction chromatography column, which was equilibrated to the concentration of ammonium sulfate in the mother liquor prior to the loading. The bioproduct adsorbs to the column under these conditions. The column is eluted with a decreasing gradient of ammonium sulfate, and the desired bioproduct is recovered in a fraction from the elution.
- When the bioproduct is contained in the filtrate after filtration, it can often be extracted with an immiscible solvent. For the extraction of small molecules such as antibiotics with organic solvents, the pH must usually be adjusted to obtain the bioproduct in either its free base or free acid form so it will partition into the organic phase. For the aqueous two-phase extraction of proteins, two polymers or a salt and a polymer must be added. If the additions to the filtrate can be made in-line, the filtration and extraction steps can be carried out simultaneously, reducing the processing time.

Process and Product Quality In the development of bioseparation processes, important measures of product quality due to processing are purity, fold purification, specific activity, and yield. Purity is defined as follows:

$$\text{Purity} = \frac{\text{amount of product}}{\text{amount of product} \ + \ \text{amount of total impurities}}$$

(20-19)

Fold purification is the ratio of the purity at any stage in the process to the purity at the start of the purification process. However, this factor is usually expressed in terms of the impurity itself, and is given in logs; for example,

$$\text{Fold DNA removal} = -\log\left(\frac{\text{DNA concentration}_{\text{stage of interest}}}{\text{DNA concentration}_{\text{beginning}}}\right)$$

(20-20)

Another measure of purity is

$$\text{Specific activity} = \frac{\text{units of biological activity}}{\text{mass}}$$

(20-21)

where units of biological activity are assayed by means of a biological test, such as moles of substrate converted per second per liter or fraction of bacterial cells killed. For proteins, the mass in Eq. (20-21) is usually total protein; on this basis, the specific activity reaches a constant value when the protein is pure.

Yield is given by

$$\text{Yield} = \frac{\text{amount of product produced}}{\text{amount of product in feed}}$$

(20-22)

Purity is a strictly quantitative measure and not always an expression of the quality of the product. A therapeutic protein can be 99.99 percent pure but still unacceptable if any pyrogen (a substance that produces a fever) is present. However, if the product is not a therapeutic protein but an industrial enzyme, then practically any impurities that do not inhibit the activity of the product or endanger the user are allowed. Figure 20-30 indicates this principle by comparing the level and range of purity acceptable for three different protein products. In short, two kinds of measurements of purity are required: activity, composition, and structure on the product itself; and host cell materials, degraded product, and excipients (additives) on the impurities.

Figure 20-30 Different levels of purity are required for different products. [Reproduced from Bioseparations Science and Engineering, 2d ed., by Roger G. Harrison, Paul W. Todd, Scott R. Rudge, and Demetri P. Petrides (2015). By Permission of Oxford University Press.]

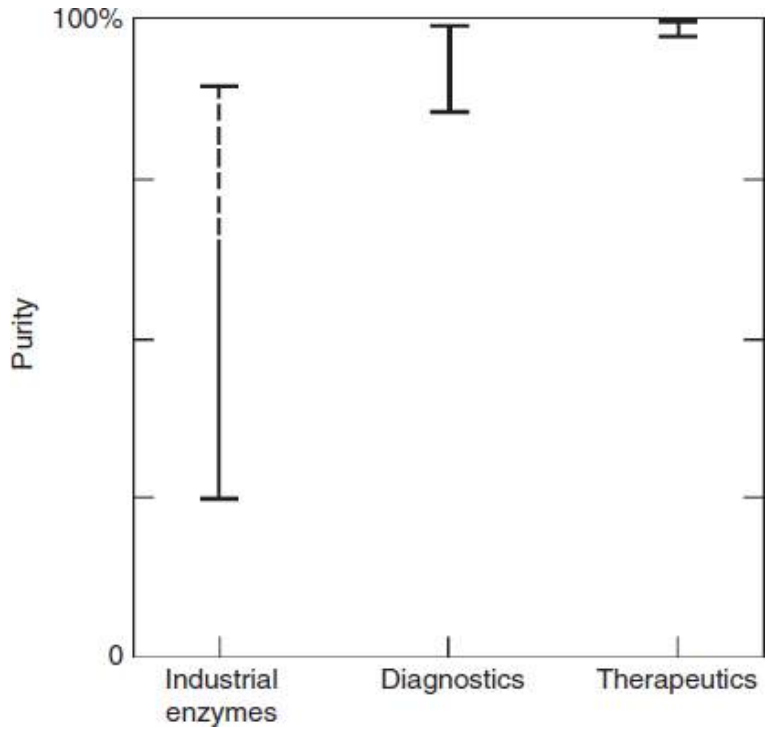

The Route to Market The route for a biotechnology product to be on the market is complex and can be lengthy. Figure 20-31 charts the pathway to market for a biotechnology product. Note that several years are required for the completion of the route from genetic discovery to marketing.

Figure 20-31 Pathway to market beginning with the discovery of a biotechnology product. [Reproduced from Bioseparations Science and Engineering, 2d ed., by Roger G. Harrison, Paul W. Todd, Scott R. Rudge, and Demetri P. Petrides (2015). By Permission of Oxford University Press.]

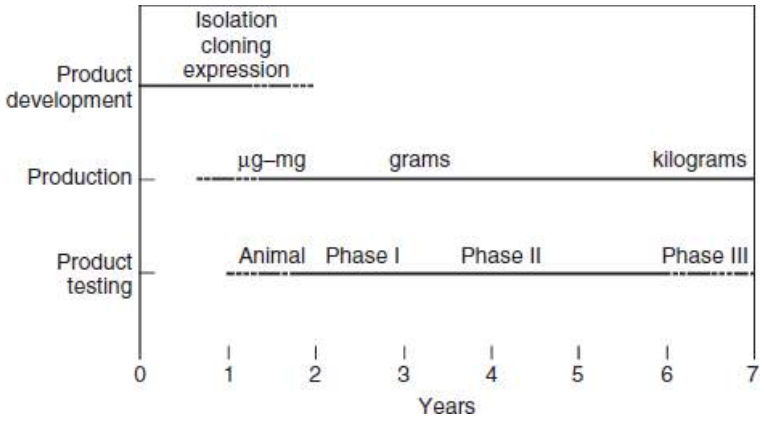

Besides identifying the market for the product and determining the optimal process for the expected production rate, the personnel involved in this effort must make sure that all the regulatory requirements are met. This is clearly an interdisciplinary task, involving not only engineers and bioscientists but also marketing and regulatory personnel. Often applications personnel, such as medical doctors and veterinarians, must also be involved.

As mentioned earlier, modern biotechnology produces the full range of substances for a wide range of applications; some well-known examples help emphasize this point:

Aspartame, a dipeptide nonnutritive sweetener

Paclitaxel, a triterpene from plants used in cancer treatment

Erythropoietin, a peptide hormone that stimulates red cell production in bone marrow

Oligonucleotides, which can be made to function according to shape and according to catalytic activity

Bacillus thuringiensis (Bt), whole bacterial cells that, when dried, can be sprayed on crops to prevent insect damage

Bioethanol, which can be produced by the anaerobic fermentation of starch

Note the categories: food, medicine, agriproducts, and biofuels. While most of the excitement in biotechnology and bioprocessing today is in the area of biopharmaceuticals produced by genetically engineered organisms, a much wider variety of products exist, usually with lower value per mass unit, including biopesticides, novel food products, polymer components, hydrogel polymers, industrial enzymes, commodity enzymes (laundry products), and fine chemicals. To know what product purity, cost, and FDA requirements must be met, the exact application of the proposed bioproduct must be identified early in process development, or even beforehand.

20.3.2. FILTRATION

Filtration is an operation that has found an important place in the processing of biotechnology products. In general, filtration is used to separate particulate or solute components in a fluid suspension or solution according to size by flowing under a pressure differential through a porous medium. There are two broad categories of filtration, which differ according to the direction of the fluid feed in relation to the filter medium. In *conventional* or *dead-end filtration,* the fluid flows perpendicular to the medium, which generally results in a cake of solids depositing on the filter medium. In *cross-flow filtration* (which is also called *tangential flow filtration*), the fluid flows parallel to the medium to minimize buildup of solids on the medium. Conventional and cross-flow filtration are illustrated schematically in Fig. 20-32.

Conventional filtration (Fig. 20-32*a*) is typically used when a product has been secreted from cells, and the cells must be removed to obtain the product that is dissolved in the liquid. Antibiotics and steroids are often processed by using conventional filtration to remove the cells. Conventional filtration is also commonly used for sterile filtration in biopharmaceutical production. Cross-flow filtration (Fig. 20-32*b*) has been used in a wide variety of applications, including the separation of cells from a product that has been secreted, the concentration of cells, the removal of cell debris from cells that have been lysed, the concentration of protein solutions, the exchange or removal of a salt or salts in a protein solution, and the removal of viruses from protein solutions.

Figure 20-32 Schematic diagrams for (a) dead-end or conventional filtration and (b) cross-flow filtration. For dead-end filtration the thickness of the solids buildup increases, and the permeate flux decreases with time, ultimately reaching zero. In cross-flow filtration, the feed can contain either a soluble or a solid solute, which becomes concentrated at the membrane surface; the permeate flux reaches a constant value at steady state. [Reproduced from Bioseparations Science and Engineering, 2d ed., by Roger G. Harrison, Paul W. Todd, Scott R. Rudge, and Demetri P. Petrides (2015). By Permission of Oxford University Press.]

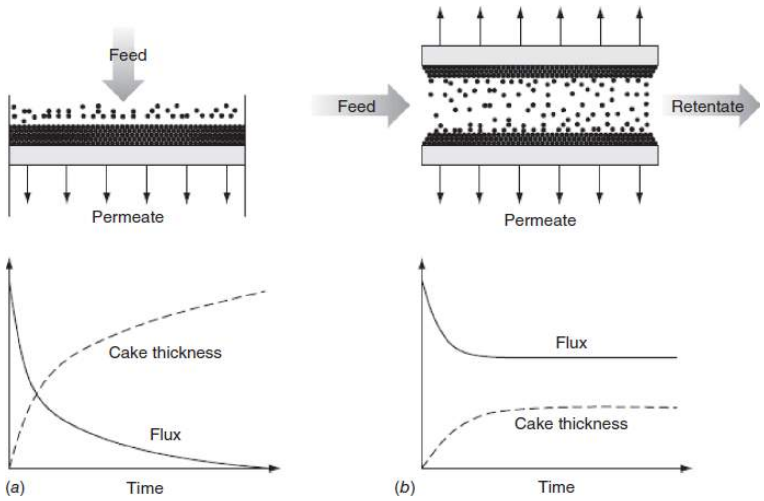

Filtration often occurs in the early stages of bioproduct purification, in keeping with the process design heuristic *Remove the most plentiful impurities first* (see Introduction). At the start of purification, the desired bioproduct is usually present in a large volume of aqueous solution, and it is desirable to reduce the volume as soon as possible to reduce the scale and thus the cost of subsequent processing operations. Filtration, along with sedimentation and extraction, is an effective means of accomplishing volume reduction.

The theory, equipment, and scale-up of conventional filtration are described in the subsection Filtration in Sec. 18. Here, additional topics that relate specifically to the filtration operations for bioproducts are discussed: (1) the principles, filter media, equipment, and scale-up of cross-flow filtration; and (2) the design of sterile filters, especially important in the pharmaceutical industry where products often need to be in sterile form.

Cross-flow Filtration As illustrated in Fig. 20-32*b*, the fluid in cross-flow filtration flows parallel to the membrane surface, resulting in constant permeate flux at steady state. The analysis of cross-flow filtration can be divided into two categories depending on whether the component being filtered is soluble or insoluble—see the discussion of filtration principles for each category later. When dissolved species such as proteins are being filtered, ultrafiltration membranes are generally used. The ultrafiltration membrane is selected so that the species of interest will not pass through these membranes. The retained species is carried to the surface of the membrane by the convective flow of fluid, and the concentration of the species builds up next to the membrane surface. The concentration of the species can be so high that it precipitates on the membrane surface, further impeding the flow of fluid through the membrane. The resulting layer of solids on the membrane surface has been called a *gel layer*. In addition, even without precipitation, the increased osmolarity near the membrane surface creates a solvent flux in the opposite direction of the flux due to the transmembrane pressure gradient.

When suspended micrometer-size particles are present, these particles are carried to the membrane surface and may form a thin cake layer at the surface, but do not significantly impact the osmotic pressure. In this situation, microfiltration membranes are generally utilized. These membranes let dissolved components pass through but retain particles above a certain size. There are instances, such as in the cross-flow filtration of cells that have been ruptured, where the layer at the membrane surface contains both suspended particles and precipitated solutes. More complete information about ultrafiltration and microfiltration membranes is given later in this section.

Dissolved Species In cross-flow filtration, a solution under pressure flows across the surface of a membrane. As a result of this pressure, fluid is forced through the membrane. This flow toward the surface of the membrane causes species dissolved in the solution also to be carried toward the membrane's surface. For a solute that is rejected by the membrane, there will be a concentration gradient of this solute across a stagnant boundary layer next to the surface of the membrane, as indicated in Fig. 20-33. The elevation of the solute concentration at the membrane surface (c_w) compared to that in the bulk solution (c_b) is known as *concentration polarization*.

Figure 20-33 Schematic representation of the boundary layer in cross-flow filtration with a dissolved solute in the feed. A solution flows parallel to the membrane surface, and fluid flows through the membrane under the influence of pressure. A fluid boundary layer forms next to the membrane surface, creating a gradient in the concentration c of solute. [Reproduced from Bioseparations Science and Engineering, 2d ed., by Roger G. Harrison, Paul W. Todd, Scott R. Rudge, and Demetri P. Petrides (2015). By Permission of Oxford University Press.]

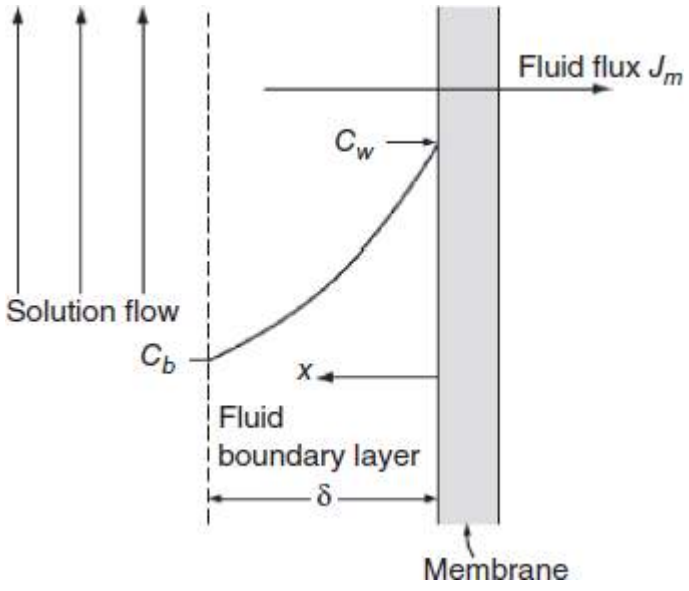

At steady state, the rate of convective mass transfer of solute toward the membrane surface must be equal to the rate of mass transfer of solute by diffusion away from the membrane surface, which is described as [Michaels, *Chem. Eng. Prog.* **64:** 31 (1968)]

$$J_m c = -\mathscr{D}\frac{dc}{dx}$$

(20-23)

where J_m is the transmembrane fluid flux, c is the concentration of the solute, and $\mathscr{D}$ is the diffusion coefficient of the solute. For a boundary layer thickness of δ, the solution of Eq. (20-23) is

$$J_m = \left(\frac{\mathscr{D}}{\delta}\right)\ln\left(\frac{c_w}{c_b}\right)$$

(20-24)

which can be also written as

$$\frac{c_w}{c_b} = \exp\left(\frac{J_m\delta}{\mathscr{D}}\right)$$

(20-25)

The term $\mathscr{D}/\delta$ can also be defined as a mass transfer coefficient k. The ratio c_w/c_b is sometimes called the *polarization modulus* and indicates the extent of concentration polarization. From Eq. (20-25), it can be seen that the polarization modulus is particularly sensitive to changes in J_m, δ, and $\mathscr{D}$ because of the exponential functionality involved. For high-molecular-weight solutes (small $\mathscr{D}$) and membranes with high solvent permeability (high J_m), concentration polarization can become severe, with c_w/c_b >10. At high concentration polarization levels, the solubility of the solute can be exceeded, resulting in the precipitation of the solute and the formation of a solids or gel layer on the membrane surface.

Experimental data have been obtained to support this simple model of concentration polarization. Figure 20-34 shows data for the ultrafiltration of the protein casein and dextran with a molecular weight of 110,000. For both species, a plot of ultrafiltration flux versus log of bulk concentration gives a straight line for bulk concentration varying by an order of magnitude. Estimates of the concentration of solute at the membrane surface can be obtained from the intercept of the straight line in Fig. 20-34 at zero flux. These estimates of c_w appear to be physically reasonable.

Figure 20-34 Decline in ultrafiltration flux with increasing concentration for solutions of casein and Dextran (MW 110,000). Data were obtained in thin-channel recirculating flow cells. [Data from Blatt et al., in flinn (ed.), Membrane Science and Technology, Plenum Press, 1970, p. 63.]

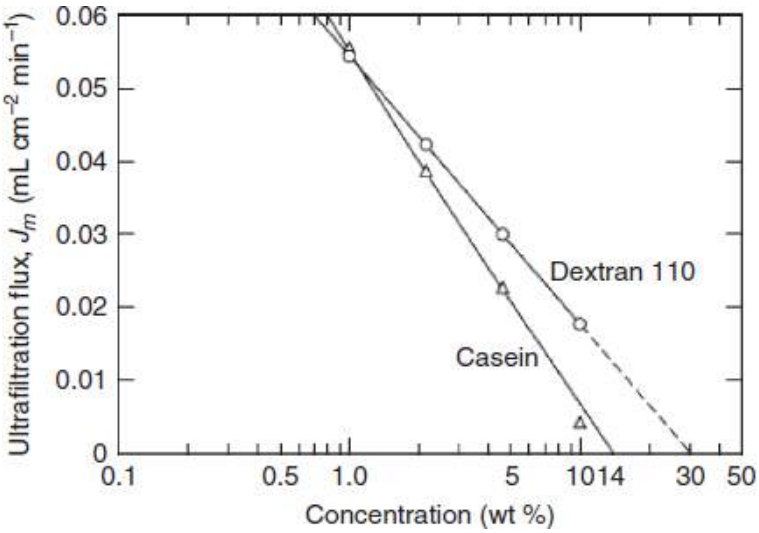

Correlations have been developed for the mass-transfer coefficient k. For laminar flow, boundary layer theory has been applied to yield analytical solutions (known as the Lévêque or Graetz solutions) for k [Blatt et al., in flinn (ed.), *Membrane Science and Technology*, Plenum Press, New York, 1970, p. 47]:

$$k = 0.816\left(\gamma_w \frac{\mathscr{D}^2}{L}\right)^{1/3}$$

(20-26)

where γ_w is the fluid shear rate at the membrane surface and L is the length of the flow channel over the membrane. The constant 0.816 is applicable for the gel-polarized condition of concentration polarization where the solute concentration at the wall is constant. For a rectangular slit of height $2h$ and bulk stream velocity u_b,

$$\gamma_w = \frac{3u_b}{h}$$

(20-27)

and the equation for a circular tube of diameter D is

$$\gamma_w = \frac{8u_b}{D}$$

(20-28)

For turbulent flow, empirical correlations have been developed for the mass-transfer coefficient. These correlations are based on dimensional analysis of the equations of change for forced convection mass transfer in a closed channel, which gives (Bird et al., *Transport Phenomena*, Wiley, Hoboken, N.J., 2002, p. 681):

$$\mathrm{Sh} = \frac{kD_h}{\mathscr{D}} = f(\mathrm{Re}, \mathrm{Sc}, L/D_h)$$

(20-29)

where $\mathrm{Re} = \dfrac{D_h u_b \rho}{\mu}$ = Reynolds number

Sc = $\dfrac{\mu}{\rho \mathscr{D}}$ = Schmidt number

D_h = equivalent diameter of the channel

= $4\left(\dfrac{\text{cross-sectional area}}{\text{wetted perimeter}}\right)$

u_b = bulk stream velocity

ρ, μ = density and viscosity of fluid, respectively

A typical correlation that has been developed for this Sherwood number [Calderbank and Moo-Young,*Chem. Eng. Sci.* **16:** 39 (1961)] is

$$\mathrm{Sh} = 0.082\mathrm{Re}^{0.69}\mathrm{Sc}^{0.33}$$

(20-30)

Note that the L/D_h term in the generalized dimensionless analysis solution is left out of the empirical correlation in Eq. (20-30).

Example

Example 20-1 Concentration Polarization in Ultrafiltration

Equipment is available for ultrafiltration of a protein solution at constant volume to remove low-molecular-weight species (achieved by the addition of water or buffer to the feed in an operation called diafiltration—see Example 20-3). The flow channels for this system are tubes 0.1 cm in diameter and 100 cm long. The protein has a diffusion coefficient of 9×10^{-7} cm^2/s. The solution has a viscosity of 1.2 cP and a density of 1.1 g/cm^3. The system is capable of operating at a bulk stream velocity of 300 cm/s. At this velocity, determine the polarization modulus for a transmembrane flux of 45 L m^{-2} h^{-1}.

We see from Eq. (20-25) that we can determine c_w/c_b if we know J_m $\delta/\mathscr{D} = J_m/k$, where J_m is as given in the problem statement. We can determine k from either Eq. (20-26) or Eqs. (20-29) and (20-30), depending on whether the flow is laminar or turbulent. We first need to calculate the Reynolds number to characterize the flow regime:

$$\mathrm{Re} = \frac{D_h u_b \rho}{\mu} = \frac{0.1\,cm \times \dfrac{300\,cm}{s} \times 1.1\dfrac{g}{cm^3}}{\dfrac{0.012\,g}{cm \cdot s}} = 2750$$

In the calculation of the Reynolds number, we see that the equivalent diameter of the channel D_h is the same as the diameter of the tubes. The flow is turbulent, since the Reynolds number is greater than 2100. For turbulent flow, we need to know Sc, the Schmidt number:

$$Sc = \frac{\mu}{\rho \mathscr{D}} = \frac{\dfrac{0.012\ g}{cm \cdot s}}{1.1\dfrac{g}{cm^3} \times 9 \times 10^{-7}\dfrac{cm^2}{s}} = 1.21 \times 10^4$$

From Eqs. (20-29) and (20-30),

$$\begin{aligned} k &= \frac{\mathscr{D}\mathrm{Sh}}{D_h} \\ &= \frac{\mathscr{D}}{D_h}(0.082)\mathrm{Re}^{0.69}\mathrm{Sc}^{0.33} \\ &= \left(\frac{9 \times 10^{-7}\dfrac{\mathrm{cm}^2}{\mathrm{s}}}{0.1\ \mathrm{cm}}\right)(0.082)(2750)^{0.69}(12,100)^{0.33} = 3.88 \times 10^{-3}\mathrm{cm/s} \end{aligned}$$

From Eq. (20-25), the polarization modulus can be estimated:

Thus, the concentration polarization is not severe.

Concentration polarization at the surface of the membrane can become great enough that it creates a significant resistance to fluid flow. This effect on the transmembrane fluid flux J_m can be modeled by using Darcy's law with the flow resistance made up of the sum of the membrane resistance R_m and the resistance R_p of the polarized boundary layer and any gel layer next to the surface of the membrane. For membranes, a correction needs to be made for the osmotic pressure $\Delta\pi$ of the solute that is being filtered, which results in the following equation:

$$J_m = \frac{\Delta p - \sigma\,\Delta\pi}{\mu_o(R_m + R_p)}$$

(20-31)

where Δp is the pressure difference between the bulk fluid and the permeate, μ_0 is the viscosity of the permeate, and σ is the reflection coefficient for the solute. A reflection coefficient of 1.0 indicates no passage of solute through the membrane, while a coefficient of 0 indicates free passage of the solute with the solvent through the membrane. For an ideal dilute solution,

$$\Delta\pi = RTc_w$$

(20-32)

where R is the ideal gas constant, T is the absolute temperature, and c_w is the solute concentration at the surface of the membrane.

Data for J_m versus Δp for the ultrafiltration of serum albumin in a stirred filtration cell are shown in Fig. 20-35 as a function of both cell stirrer speed and protein concentration. At high values of Δp for 3.9 percent and 6.5 percent protein concentrations, the ultrafiltration flux J_m is constant with increasing Δp. Constant flux as Δp increases can be interpreted as a condition in which the solute concentration at the membrane surface c_w has reached a solubility limit; this behavior is supported by Eq. (20-24), where J_m becomes constant when c_w reaches a constant.

Figure 20-35 ***Ultrafiltration flux as a function of pressure drop in a stirred cell with varying protein concentration and stirring rate. [Data from Perry (ed.), Progress in Separation and Purification, vol. 1, Wiley, 1968, p. 318.]***

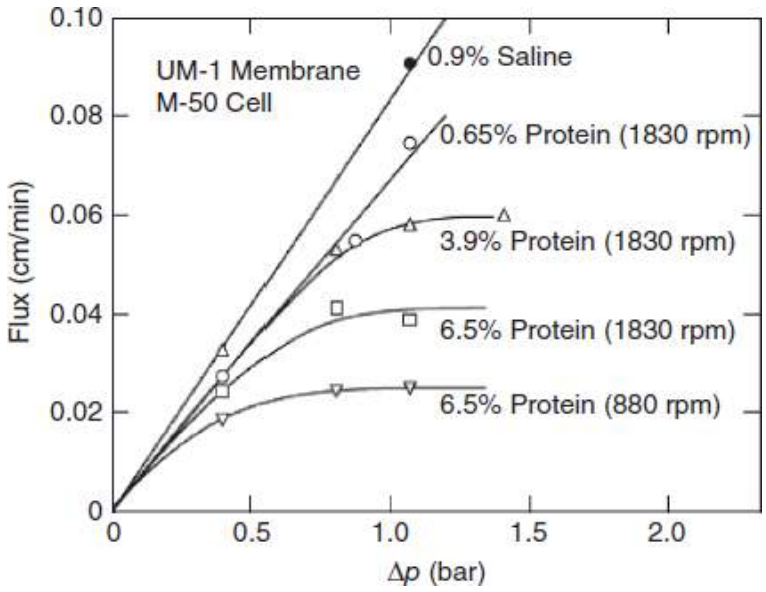

Suspended Particles In the cross-flow filtration of mixtures with suspended particles, the fluid flux toward the membrane carries particles to the membrane surface, where they are rejected and form a cake layer that is analogous to the gel layer in the ultrafiltration of dissolved species. The cake layer initially grows with time, thus reducing the permeate flux and constricting the channel. At steady-state conditions, the layer reaches a constant thickness, which is relatively thin if the shear exerted by the fluid flowing tangentially to the membrane surface is high enough.

The theory for the cross-flow filtration of dissolved species has been found to hold only for very small suspended particles up to approximately 1 μm in size [Belfort et al., *J. Membrane Sci*. **96:** 1 (1994)]. Beyond this size, experimental membrane flux values are often 1 to 2 orders of magnitude higher than those obtained from the Lévêque or Graetz theory given by Eq. (20-26) [Porter, *Ind. Eng. Chem. Prod. Res. Dev*. **11:** 234 (1972)]. Two different theories have been developed to more accurately predict membrane fluxes for particles larger than 1 μm, depending on the size of the particles: a shear-induced diffusion theory for small particles and an inertial lift theory for larger particles.

In the shear-induced diffusion theory, the concentration polarization model can be applied to the cross-flow filtration of suspended particles if the Brownian diffusivity is replaced by a shear-induced hydrodynamic diffusivity [Zydney and Colton, *Chem. Eng. Commun*. **47:** 1 (1986)]. In shear-induced hydrodynamic diffusion, the particles are randomly displaced from the streamlines in a shear flow and collide with other particles. In their model, Zydney and Colton employed an approximate relationship for the shear-induced diffusion $\mathscr{D}_s$ of spherical particles measured by Eckstein et al. [*J. fluid Mech*. **79:** 191 (1977)] for $0.2 < \phi < 0.45$

$$\mathscr{D}_s = 0.3\gamma_w a_p^2 \tag{20-33}$$

where ϕ is the particle volume fraction in the bulk suspension, a_p is the particle radius, and γ_w is the fluid shear rate at the membrane surface. Substituting for the diffusivity in the equation for the laminar flow mass-transfer coefficient in the concentration polarization model [Eq. (20-26)], we obtain

$$k = 0.366\gamma_w \left(\frac{a_p^4}{L}\right)^{1/3}$$

(20-34)

where L is the tube or channel length. Comparing this equation for k with the one for dissolved species in laminar flow, we see that the mass-transfer coefficient is much more strongly dependent on the shear rate at the wall. Shear-induced diffusion has been found to dominate for particles up to 30 to 40 μm, while inertial lift dominates for larger particles [Belfort et al., *J. Membrane Sci.* **96:** 1 (1994)].

Inertial lift arises when the Reynolds number based on the particle size is not negligible. Inertial lift produces a velocity that carries particles away from the membrane surface. For fast laminar flow of dilute suspensions with thin fouling layers, the steady-state transmembrane flux predicted by the inertial lift theory is [Belfort et al., *J. Membrane Sci.* **96:** 1 (1994)]:

$$J_m = \frac{0.036\rho_o {a_p}^3 \gamma_w^2}{\mu_o}$$

(20-35)

where ρ_0 and μ_0 are the density and viscosity, respectively, of the permeate. Thus, for transport by inertial lift, the transmembrane flux is strongly dependent on the particle size and shear rate at the membrane surface and not dependent at all on the length of the filter or on the concentration of particles in the bulk suspension.

Example

Example 20-2 Comparison of Mass-Transfer Coefficient Calculated by Boundary Layer Theory versus by Shear-Induced Diffusion Theory

Cells that are 5 μm in diameter are being concentrated by cross-flow filtration using hollow fibers that are 1.1 mm in diameter (inside) and 20 cm long. The velocity of the fluid in the hollow fibers is 100 cm/s. The fluid can be assumed to have the same density and viscosity as water. The temperature is 4 C. Compare the mass-transfer coefficient k calculated by using boundary layer theory with that using shear-induced diffusion theory.

Boundary layer theory We first calculate the Reynolds number in order to determine the flow regime. At 4 C for water, ρ = 1.00 g/cm^3 and μ = 1.56 cP (from Tables 2-92 and 2-139, respectively). Therefore,

$$\mathrm{Re} = \frac{D\, u_b \rho}{\mu} = \frac{0.11\,\mathrm{cm} \times \dfrac{100\ \mathrm{cm}}{\mathrm{s}} \times 1.00 \dfrac{\mathrm{g}}{\mathrm{cm}^3}}{\dfrac{0.0156\,\mathrm{g}}{\mathrm{cm}\cdot\mathrm{s}}} = 705$$

The upper limit of the Reynolds number for laminar flow in tubes is about 2100. Therefore, the flow is laminar in our case. For laminar flow in tubes, we can calculate k using Eqs. (20-26) and (20-28). Equation (20-26) requires the diffusion coefficient for the cells, which can be estimated from the Stokes-Einstein equation for spheres, Eq. (20-62):

$$\mathscr{D} = \frac{k_B T}{6\pi\mu a_p} = \frac{\left(1.38\times10^{-23}\dfrac{\text{J}}{\text{K}}\right)(277\text{ K})\left(\dfrac{10^7\text{g cm}^2\text{ s}^{-3}}{\text{J s}^{-1}}\right)}{6\pi\left(0.0156\dfrac{\text{g}}{\text{cm}\cdot\text{s}}\right)(2.5\times10^{-4}\text{ cm})} = 5.20\times10^{-10}\text{cm}^2\text{ s}^{-1}$$

From Eqs. (20-28) and (20-26), respectively,

$$\gamma_w = \frac{8u_b}{D} = \frac{8\times100\dfrac{\text{cm}}{\text{s}}}{0.11\text{ cm}} = 7273\text{ s}^{-1}$$

$$k = 0.816\left(\gamma_w\frac{\mathscr{D}^2}{L}\right)^{1/3}$$

$$= 0.816\left(\frac{7273\dfrac{1}{\text{s}}\times\left(5.20\times10^{-10}\dfrac{\text{cm}^2}{\text{s}}\right)^2}{20\text{ cm}}\right)^{1/3} = 3.77\times10^{-6}\text{ cm s}^{-1}$$

Shear-induced diffusion For laminar flow with shear-induced diffusion, Eq. (20-34) applies:

$$k = 0.366\,\gamma_w\left(\frac{a_p^4}{L}\right)^{1/3}$$

$$= 0.366\left(7273\frac{1}{\text{s}}\right)\left[\frac{(2.5\times10^{-4})^4\text{cm}^4}{20\text{ cm}}\right]^{1/3} = 1.54\times10^{-2}\text{cm}\cdot\text{s}^{-1}$$

Therefore, *k* is more than 4000 times greater when calculated using shear-induced diffusion theory than when calculated using Fickian diffusion theory for 5-μm cells.

Membrane Fouling Fouling of membranes results from physical and/or chemical interactions between the membrane and various components present in the process stream. Fouling leads to a decline in the permeate flux and a change in the membrane selectivity. Because of the high affinity of proteins for solid surfaces, proteins are the leading contributor to fouling in ultrafiltration (UF) and microfiltration (MF). The flux decrease caused by proteins can be attributed to one or more of the following processes [Belfort et al., *J. Membrane Sci.* **96:** 1 (1994)]:

- Protein adsorption, which involves the interaction of the proteins and the membrane and occurs with no convective flow through the membrane
- Protein deposition, which is the addition of more protein that is associated with the membrane, over and above the protein that would be adsorbed in a nonflowing system
- Protein accumulation on the membrane surface exposed to the flowing process stream as a result of concentration polarization, which can lead to formation of a gel layer

This last effect is governed by the mass-transfer coefficient [seeEqs. (20-26) and (20-30)] and thus can be minimized by increasing the fluid shear rate at the filtering surface of the membrane. These three processes can lead to pores in membranes that are constricted and even completely blocked, as illustrated in Fig. 20-36.

Figure 20-36 Mechanisms of membrane fouling. (a) Pore narrowing and constriction. (b) Pore plugging. (c) Solute deposition and formation of a gel or cake layer. Dimensions: d, protein or particle diameter; d_p, clean pore diameter; d'_p, effective pore diameter in the presence of adsorbed proteins or particles. [Reproduced from Bioseparations Science and Engineering, 2d ed., by Roger G. Harrison, Paul W. Todd, Scott R. Rudge, and Demetri P. Petrides (2015) By Permission of Oxford University Press.]

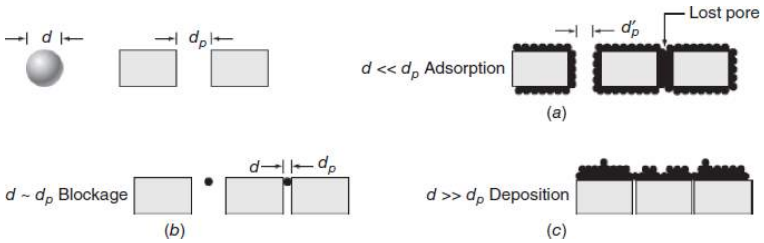

Protein adsorption studies have been performed for both MF and UF membranes to determine the extent to which the pores are constricted by adsorbed protein. To eliminate concentration polarization effects, these studies were done in the absence of flow. The work with MF membranes and a variety of proteins showed that there was approximately monolayer adsorption throughout the internal pores [Belfort et al., *J. Membrane Sci.* **96:** 1 (1994)]. Protein adsorption was reduced on the more hydrophilic membranes such as the hydrophilic PVDF type, with only a fraction of monolayer adsorption. A study of the adsorption of bovine serum albumin (molecular weight 69,000 Da) on UF membranes indicated the following extents of protein coverage within the ultrathin skin portion of the membrane: monolayer adsorption for the 300,000-Da MWCO membrane, only about half a monolayer for the 100,000-Da MWCO membrane, and no measurable protein adsorption for the 50,000-Da MWCO membrane [Robertson and Zydney, *J. Colloid Interface Sci.* **134:** 563 (1990)]. Thus, protein fouling within the membrane can be completely eliminated by making the pore size small enough.

To account for fouling caused by irreversible adsorption and deposition of proteins and other biological molecules to the membrane surface, it is useful to write Darcy's law [Eq. (20-31)] for the transmembrane flux in terms of the clean membrane resistance R_m, the resistance due to concentration polarization and a gel layer on the membrane surfaceR_p, and the resistance caused by irreversible fouling R_{if} [Rajabzadeh et al., *J. Membrane Sci.* **361:** 191 (2010)]:

$$J_m = \frac{\Delta p - \sigma \Delta \pi}{\mu_o (R_m + R_p + R_{if})}$$

(20-36)

In this model, irreversible fouling is considered the fouling that can only be removed by cleaning agents such as acids, bases, enzymes, surfactants, and disinfectants; and the resistance caused by concentration polarization and any gel layer is that which can be removed by physical means, such as circulation of feed through the system at zero transmembrane pressure and relatively high shear rate, or by backflushing using negative transmembrane pressure to remove foulants from the membrane surface [Zeman and Zydney, *Microfiltration and Ultrafiltration*, Dekker, New York, 1996, p. 452]. A comprehensive review of methods to control fouling in microfiltration and ultrafiltration membranes has been written by Hilal et al. [*Sep. Sci. Tech*. **40:** 1957 (2005)].

Filter Media and Equipment In the development of a filtration process, much effort is often devoted to the evaluation of the filter media and equipment that are available. The filter media and equipment selected can have a large impact on the process economics, in terms of both the capital outlay required and the operating expenses.

Filter media for cross-flow filtration are generally referred to as *membranes*. There are two general categories of membranes: ultrafiltration membranes and microporous membranes. The separation between ultrafiltration (UF) and microfiltration (MF) is based on the pore size of the membrane, with membranes having pores 0.1 μm and larger considered to be microporous. The pore sizes of UF membranes are in the range of 0.001 to 0.1 μm [Zeman and Zydney, *Microfiltration and Ultrafiltration*, Dekker, New York, 1996, p. 13], although these membranes are usually classified by their *molecular weight cutoff* (MWCO), which is the molecular weight of a globular solute at which the solute is rejected by the membrane. Typically, a 90 percent rejection level is used for establishing the MWCO. Ultrafiltration membranes can be obtained down to an MWCO level of 1000 daltons (Da) and up to as high as 1,000,000 Da. Ultrafiltration membranes are commonly used to concentrate and for changing the buffer for biomolecules such as proteins, while microfiltration is typically used to concentrate and wash cell suspensions. There is a class of membranes known as *nanofilters* that are used to remove virus particles based on their size. These membranes are typically operated in cross-flow mode due to the high resistance of the membrane. Virus filters are typically operated at about 100 kPa and achieve fluxes of about 60 L m^{-2} h^{-1}. Finally, there is also a category of membranes called *reverse-osmosis* (RO) or hyperfiltration membranes that pass only water and a very low flux of solutes. A very good RO membrane rejects 99.7 percent or more of sodium chloride (Henry et al., in *Perry's Chemical Engineers' Handbook*, 7th ed., McGraw-Hill, New York, 1997, pp. 22–49).

Three basic structures are commonly used for membranes: homogeneous, asymmetric, and composite. These three types are illustrated in Fig. 20-37. The homogeneous structure has no significant variation in pore diameter from the feed side to the filtrate side. In the asymmetric structure, there is a thin layer on the feed side of the filter that has very small pores. Below this layer is a much thicker layer that has much larger pores and serves as structural support for the membrane. The composite membrane is similar to the asymmetric membrane in having a thin layer containing very small pores next to the filtering surface; however, the thin and thick layers of this membrane are made of two different types of material.

Figure 20-37 Mechanisms of membrane fouling. (a) Pore narrowing and constriction. (b) Pore plugging. (c) Solute deposition and formation of a gel or cake layer. Dimensions: d, protein or particle diameter; d_p, clean pore diameter; d'_p, effective pore diameter in the presence of adsorbed proteins or particles. [Reproduced from Bioseparations Science and Engineering, 2d ed., by Roger G. Harrison, Paul W. Todd, Scott R. Rudge, and Demetri P. Petrides (2015) By Permission of Oxford University Press.]

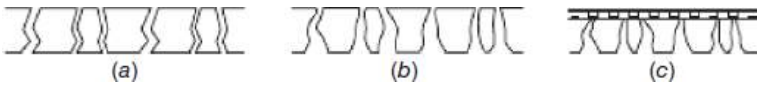

Backflushing composite filters is generally not recommended. The major element in pressure drop across the filter is due to the thin layer with very small pores, and so significantly more mechanical force is applied to the area of the thin layer, compared to the support layer. When operated in the intended direction, the thin layer is forced toward the support layer. But when operated in the opposite direction, the thin layer is forced away from the support layer, which can lead to delamination.

Filtration membranes are made from a wide variety of polymers and inorganic materials. The polymers that are used include cellulose acetate, polyamide, polyether, polycarbonate, polyester, polypropylene, polyethylene, regenerated cellulose, poly(vinyl chloride), poly(vinylidene fluoride) (PVDF), poly(tetrafluoroethylene) (PTFE), acrylonitrile copolymers, and polyethersulfones. The inorganic materials used include ceramics, zirconium oxide, borosilicate glass, stainless steel, and silver.

Cross-flow filtration membranes are available in a variety of configurations. The membranes are housed in a physical unit called a *module*. The membrane module must satisfy a number of mechanical, hydrodynamic, and economic requirements, the most important of which are the following [Zeman and Zydney, *Microfiltration and Ultrafiltration*, Dekker, New York, 1996, p. 327]:

Mechanical: It must obtain effective (physical) separation of the feed and permeate streams; provide the necessary physical support for the membrane (including the ability of the module to endure the required pressure drops and any backflushing).

Hydrodynamic: It must minimize pressure drops through the module (to reduce pumping costs); optimize solute mass transfer (reduce concentration polarization); minimize particulate plugging or fouling; avoid dead spots (for sanitary design); allow for or promote turbulence (for sanitary design and to reduce boundary layer thickness).

Economic: It must maximize the membrane packing density (ratio of membrane area to module volume); minimize manufacturing costs; permit easy access for cleaning and/or membrane replacement; provide sufficient chemical resistance and operational lifetime; incorporate modularity of design for easy scale-up, staging, or cascading.

Several of these criteria are in mutual opposition: for example, modules with high membrane packing density tend to be highly susceptible to plugging with particulates. Therefore, the choice of a particular module involves balancing these criteria to arrive at the most economic system for each particular application.

There are five types of module configuration for cross-flow filtration (Fig. 20-38): hollow fiber, tubular, flat plate, spiral wound, and rotating. The tubular module has the same general configuration as the hollow fiber module, but the tubes have much larger diameters than the fibers. Some key characteristics of these modules are compared in Table 20-18.

Table 20-18 Comparison of Key Characteristics of Cross-flow Membrane Modules*

Module type	Channel spacing (cm)	Packing density (m^2/m^3)	Energy costs	Particulate plugging	Ease of cleaning
Hollow fiber	0.02–0.25	1200	Low	High	Fair
Tubular	1.0–2.5	60	High	Low	Excellent
flat plate	0.03–0.25	300	Moderate	Moderate	Good
Spiral wound	0.03–0.1	600	Low	Very high	Poor to fair
Rotating	0.05–0.1	10	Very high	Moderate	Fair

*Zeman and Zydney, *Microfiltration and Ultrafiltration*, Dekker, New York, 1996. p. 331.

Reproduced from *Bioseparations Science and Engineering*, 2d ed., by Roger G. Harrison, Paul W. Todd, Scott R. Rudge, and Demetri P. Petrides (2015). By Permission of Oxford University Press.

Hollow fiber modules consist of an array of narrow-bore, self-supporting fibers that generally have an asymmetric membrane structure. The dense skin layer is usually on the lumen side of the fiber, but it can be placed on the outside. The feed flows through the lumen of the fibers when the dense skin layer is on the lumen side, and the flow is typically laminar, although hollow fiber systems by some manufacturers can be operated in turbulent flow. Since the hollow fibers are self-supporting, they can be cleaned by backflushing, that is, by reversing the direction of the permeate flow. One disadvantage of hollow fiber modules is that the entire module usually needs to be replaced upon the rupture of even a single fiber. Also, to avoid plugging of the small-diameter fibers, feed streams generally need to be prefiltered.

Except for some inorganic membranes, tubular membranes are not self-supporting and are usually cast in place within a porous support tube made of fiberglass, ceramic, plastic, or stainless steel. The feed flows through the inside of the tubes, while the permeate flows radially outward across the membrane and support tube. Inorganic membranes are usually constructed in a honeycomb monolith unit in which the membranes are arranged in a parallel array. Tubular systems are typically operated in the turbulent flow regime. Because of the large diameter of the tubes in these systems, the pumping costs are relatively high compared to other module configurations operated in turbulent flow. In addition, large-diameter tubes decrease the filter surface area to module volume ratio, leading to bigger equipment footprints. The chief advantages of tubular modules are that they are highly resistant to plugging by particulates, and they can be cleaned by backflushing. The diameter of the tubes can be selected to avoid prefiltration of the feed.

Most flat plate systems are in a rectangular configuration. The flow channels can be open or can have separator screens to improve the mass-transfer characteristics. Units with open channels are usually operated in laminar flow, while those with separator screens are often operated with flow in the turbulent regime. One disadvantage of these modules is that backflushing is often impractical because the membranes are effectively supported only on one side.

Spiral-wound modules are constructed from flat sheet membranes separated by spacer screens. The feed solution is fed into one end of the module and flows through the separator screens along the surface of the membranes. The retentate is then collected on the other end of the module. The permeate spirals radially inward, eventually to be collected through a central tube. The flow in these systems tends to be turbulent. The main disadvantage of spiral-wound modules is that they are susceptible to fouling by particulates because of the narrow and irregular flow through the spacer screens.

One effective rotating-type module is the rotating cylinder device originally proposed by Hallstrom and Lopez-Leiva [*Desalination* **24:** 273 (1978)]. The feed flows into a thin annular region between two concentric cylinders (Fig. 20-38*b*). Either cylinder or both can be porous and can have a membrane bound to the surface. With the membrane on the inner cylinder, permeate is collected in the central chamber. When the membrane is on the outer cylinder, permeate is collected in a separate annular permeate region adjacent to the outer porous cylinder. The inner cylinder is rotated at high speed (typically > 3000 rpm) to induce the formation of Taylor vortices, which effectively mix the fluid near the surface of the membrane and thereby increase the mass-transfer coefficient for the solutes/particles in the feed. The vortices also help reduce the thickness of the cake or gel layer at the membrane surface. One advantage of this system is that the rate of mass transfer is determined almost entirely by the rate of rotation of the inner cylinder, which effectively decouples the mass-transfer characteristics from the feed flow rate. As a result, the rotating devices can be operated at very low flow rates and with minimal pumping costs. Since, however, the energy requirements for rotating the device are usually very high, capital costs are high, and scale-up is very difficult, these systems have been limited to small-scale operation.

Figure 20-38 Schematic representations of filter modules. (a) Hollow fiber, plate, and spiral-wound membrane modules. (b) A rotating cylinder module. [Reproduced from Bioseparations Science and Engineering, 2d ed., by Roger G. Harrison, Paul W. Todd, Scott R. Rudge, and Demetri P. Petrides (2015). By Permission of Oxford University Press.]

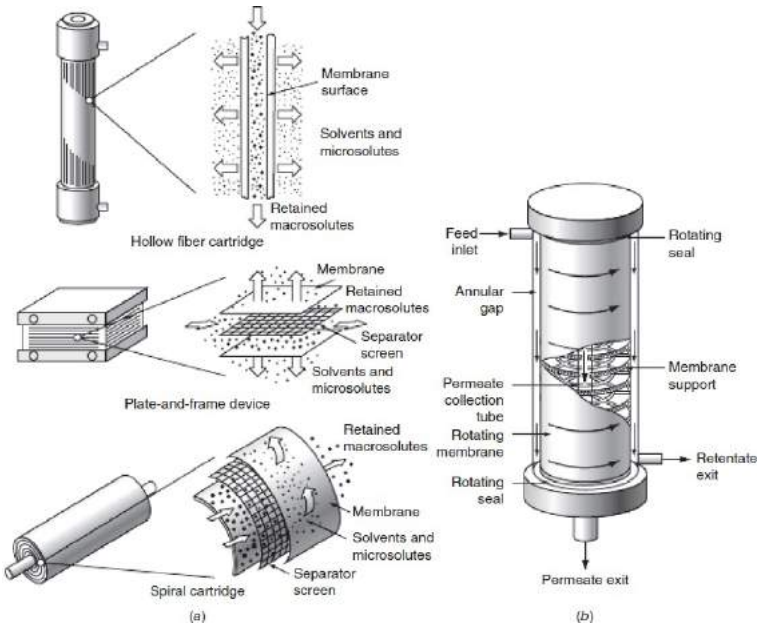

Scale-Up and Design Experimental testing is generally needed in the scale-up and design of cross-flow filtration systems. Cross-flow filtration modules are available from manufacturers for carrying out laboratory or pilot plant tests. The size of a plant unit can be determined by a direct scale-up of the filtration area based on the feed or permeate flow rate. For this scale-up, however, it is important that the following variables be kept constant [Datar and Rosen, in Rehm and Reed (eds.), *Biotechnology*, vol. 3, *Bioprocessing*, VCH, Weinheim, Germany, 1993, p. 486]:

- Inlet and outlet pressures
- Cross-flow (or tangential) velocity
- flow channel sizes (height and width)
- Feed stream properties—test slurries should be representative of the actual process streams
- Membrane type and configuration—test data from one design cannot directly be used to design another geometry

Maintaining the inlet and outlet pressures, the cross-flow velocity, and the flow channel size means that the length of the flow path is constant as well. It is also important to make an assessment of the rate of fouling of the membranes. Tests should be performed for several cycles of operation to estimate the fouling rate and to determine how fouling can be kept to a minimum.

There are four basic modes of operation of cross-flow filtration (Fig. 20-39): batch concentration, diafiltration, purification, and complete recycle. In the batch concentration mode, the retained stream containing the product suspended particles or dissolved macromolecules is reduced in volume. In diafiltration, the volume of the retained stream is kept constant by the continuous addition of water or buffer, which results in the removal of low-molecular-weight solutes into the permeate. Diafiltration is commonly used when salt removal or exchange is desired. In the purification mode, a low-molecular-weight product passes into the permeate and is thus separated from higher-molecular-weight impurities; or the product can be retained and impurities removed in the permeate. In the complete recycle mode, both the retained stream and the permeate are returned to the feed tank. Systems may be operated in complete recycle at start-up to reach steady state, saturate the membranes, test for leaks and blockage, and adjust the feed rate.

Figure 20-39 The four basic modes of operation of cross-flow filtration (CF = cross-flow filter): before the arrow, start of the operation; after the arrow, end of the operation. [Reproduced from Bioseparations Science and Engineering, 2d ed., by Roger G. Harrison, Paul W. Todd, Scott R. Rudge, and Demetri P. Petrides (2015). By Permission of Oxford University Press.]

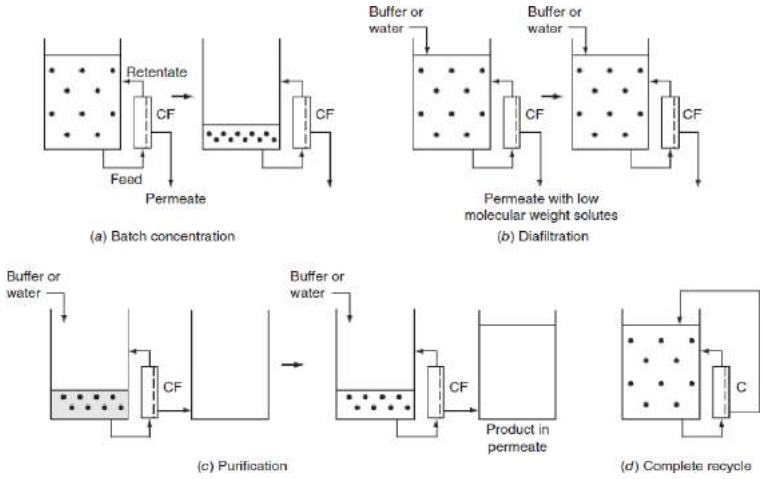

Diafiltration is similar to dialysis in that salts are exchanged or removed in both modes. Dialysis is a laboratory method that involves placing the feed in a bag made with an ultrafiltration membrane. The bag is placed in a large volume of the new solvent desired, and the new solvent is mixed until the system comes to equilibrium or near equilibrium. Complete equilibrium takes 3 to 5 h, while 90 percent equilibrium can be reached in 2 to 3 h (Scopes, *Protein Purification*, Springer-Verlag, 1982, p. 16). For a complete change of solvent, it is necessary to do the dialysis at least twice. It is frequently the job of the engineer to scale up a dialysis done in the laboratory to a diafiltration in the pilot plant or plant. For scaling and planning, it is customary to perform material balances on solids mass and liquid volume around any component of the operation.

Example

Example 20-3 Diafiltration Mode in Cross-flow Filtration

It is desired to use a cross-flow filtration system to desalt 1000 L of a protein solution containing NaCl. The system is capable of operating at a transmembrane flux of 30 L m^{-2} h^{-1}. A membrane is used that will allow complete passage of the salt but no passage of the protein. To remove 99.99 percent of the salt, determine the time required and the volume of water required using a cross-flow filtration unit with a membrane area of 100 m^2.

We operate the system in the diafiltration mode, which means that the volume of the solution being desalted is maintained constant. A material balance on the salt in the retained volume gives

$$V\frac{dc_s}{dt} = -Q\,c_s(1 - r_s)$$

where V = volume of solution being desalted

c_s = concentration of salt in volume V

r_s = fraction of salt rejected by the membrane

Q = filtration rate (volume/time)

For this case there is no rejection of salt by the membrane, so that $r_s = 0$. Integrating the differential equation with the initial time equal to 0 gives

$$\ln\frac{c_s}{c_{so}} = -\frac{Qt}{V}$$

where c_{so} = initial salt concentration. Solving for t, we obtain

$$t = \frac{V\,\mathrm{In}\dfrac{c_s}{c_{so}}}{Q} = -\frac{(1000\,\mathrm{L})(\mathrm{In}\,0.0001)}{\left(30\dfrac{\mathrm{L}}{\mathrm{m^2\,h}}\right)(100\,\mathrm{m^2})} = 3.07\,\mathrm{h}$$

$$\mathrm{Volume\ of\ water\ required} = (3.07\,\mathrm{h})\left(30\frac{\mathrm{L}}{\mathrm{m^2\,h}}\right)(100\ \mathrm{m^2}) = 9210\,\mathrm{L}$$

Thus, a relatively large volume of wastewater will be generated by this process.

In designing a diafiltration process, a decision must be made about the concentration of retained product at which to operate. As this concentration is increased, the filtration flux will decrease according to Eq. (20-24), and the total volume of filtrate will decrease for the removal of a given percentage of a low-molecular-weight solute. This leads to an optimum concentration to minimize the time required, which can be determined mathematically if the relation between filtrate flux and concentration in the bulk fluid (c_b) is known [Tutunjian, in Moo-Young (ed.), *Comprehensive Biotechnology,* vol. 2, *Principles of Biotechnology*, Pergamon, 1985, p. 411].

The basic components in the design of a cross-flow filtration system are shown inFig. 20-40. A pump flows the feed through the filtration module to give a permeate and a retentate or retained stream. The pump needs to be sized to provide the desired flow velocity and pressure. The transmembrane pressure is controlled by a back-pressure valve on the retentate stream exiting from the filtration module. Thus the transmembrane pressure drop is estimated by

Figure 20-40 Basic components of a cross-flow filtration system. [Reproduced from Bioseparations Science and Engineering, 2d ed., by Roger G. Harrison, Paul W. Todd, Scott R. Rudge, and Demetri P. Petrides (2015). By Permission of Oxford University Press.]

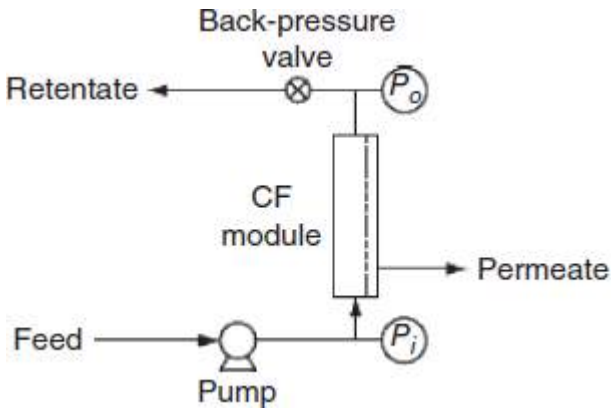

$$\Delta p_{TM} = \frac{1}{2}(p_i + p_o) - p_p$$

(20-37)

where p_i and p_o are the retentate pressures in and out of the module, respectively, andp_p is the pressure of the outlet permeate. In designing a cross-flow filtration system, it is important to minimize the occurrence of gas-liquid interfaces, since bioproduct denaturation, especially of proteins, can occur at these interfaces in the presence of mechanical shear and turbulent flow [Virkar et al., *Biotechnol. Bioeng*. **23:** 425 (1981)].

Cross-flow filtration systems may be designed to operate in the batch or the continuous mode (Fig. 20-41). In a batch system, feed is pumped through the filtration module and then back to the feed tank. In a variation of this mode (called *semibatch*) for diafiltration, fluid is continuously added to the feed tank to keep the feed volume constant (Fig. 20-39*b*).

Figure 20-41 Comparison of (a) batch and (b) single-stage continuous (feed-and-bleed) cross-flow filtration systems. [Reproduced from Bioseparations Science and Engineering, 2d ed., by Roger G. Harrison, Paul W. Todd, Scott R. Rudge, and Demetri P. Petrides (2015). By Permission of Oxford University Press.]

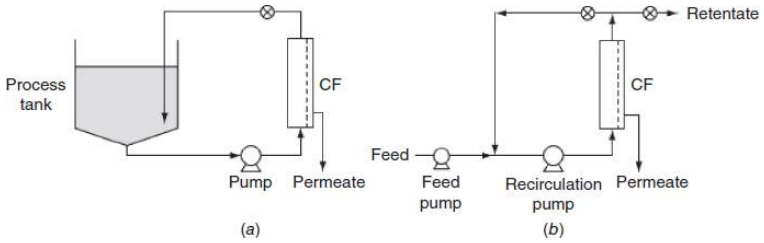

In the continuous mode of operation, also sometimes called the*feed-and-bleed* mode, or *retentate bleed* mode, feed is added to a recirculation loop by the feed pump, and concentrate exiting in the retained stream is withdrawn from the system so that the concentration factor (i.e., concentration in the retentate divided by the concentration in the feed) is at the desired value. When steady state has been achieved, the concentrate will be at its maximum concentration, which means that the filtration flux will be at a minimum throughout the run [Tutunjian, in Moo-Young (ed.), *Comprehensive Biotechnology,* vol. 2, *Principles of Biotechnology*, Pergamon, 1985, p. 411]. It is generally more economical to use a multistage system in a continuous process (Fig. 20-42). As more stages are added, the average filtration flux approaches that for a batch system, and thus the total filtration area decreases as more stages are added. This is illustrated in Table 20-19, where batch ultrafiltration operation is compared with continuous operation using one, two, three, and five stages.

Table 20-19 Comparison of Batch and Continuous Ultrafiltration Systems Using a Model of Flux as a Function of Bulk Concentration*

System†	Flux (L m^{-2} h^{-1})	Total area (m^2)
Batch	33.1 (average)	136
Continuous		
One-stage	8.1	555
Two-stage	31.1	243
	8.1	
Three-stage	38.7	194
	23.4	
	8.1	
Five-stage	44.7	165
	35.6	
	26.4	
	17.3	
	8.1	

*Tutunjian, in M. Moo-Young (ed.), *Comprehensive Biotechnology*, vol. 2, *Principles of Biotechnology*, Pergamon, Oxford, UK, 1985, p. 411.

†System design for 10× concentration factor and feed rate of 5000 L/h.

Flux from $J_m = 20 \ln (30/c_b)$.

Reproduced from *Bioseparations Science and Engineering*, 2d ed., by Roger G. Harrison, Paul W. Todd, Scott R. Rudge, and Demetri P. Petrides (2015). By Permission of Oxford University Press.

***Figure 20-42** Multistage cross- flow filtration system using the retentate bleed mode. [Reproduced from Bioseparations Science and Engineering, 2d ed., by Roger G. Harrison, Paul W. Todd, Scott R. Rudge, and Demetri P. Petrides (2015). By Permission of Oxford University Press.]*

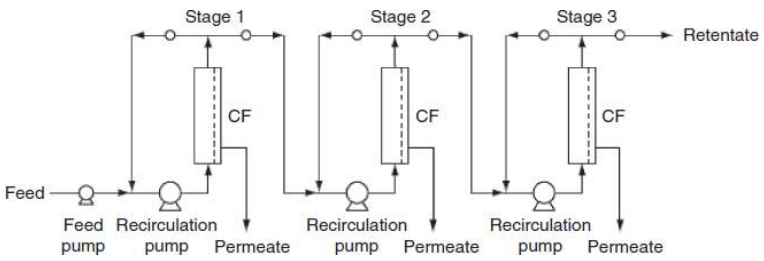

Because of the economic advantages of continuous operation and reduced tankage, this scheme is preferable to batch operation for most large-scale ultrafiltration operations (Henry et al., in *Perry's Chemical Engineers' Handbook*, 7th ed., McGraw-Hill, New York, 1997, pp. 22–56). Another advantage of continuous operation is that it permits the minimization of the residence time of the product in the cross-flow filtration unit, which is important for products that are sensitive to heat or shear. Dairy and food proteins are generally processed continuously, while most pharmaceutical and biological products are processed using batch operation [Tutunjian, in Moo-Young (ed.), *Comprehensive Biotechnology,* vol. 2, *Principles of Biotechnology*, Pergamon, 1985, p. 411].

Sterile Filter Design Sterile filtration is an important application of conventional filters in the pharmaceutical industry, where many products are sold in sterile form. It is sometimes desirable that other bioseparation processing steps besides the final one be carried out under sterile conditions, which requires the filtration of both liquids and air.

Sterile Liquid Filtration In typical sterile liquid filtration applications, there is no appreciable filter load, no cake buildup, and no contribution to filtration resistance from the filtrate that is reliable or reproducible. Further, there is no opportunity to add filter aids to form a cake, since this is usually the last step in a clean process.

Sizing of the filter is almost always based on the maximum allowable load in the solution to be filtered as well as the desired sterility assurance limit. The sterility assurance limit is the calculated probability of a single unit of product containing a single microorganism. This is expected to be a maximum of 10^{-4} for aseptic processes, and one usually designs in an extra order of magnitude at least. One determines the maximum load on the filter by knowing the bioburden or viral load specification of the purified pool from the preceding step, or by knowing the acceptable microbial or viral levels in the raw materials that make up that pool. The retentive requirement for the filter is then divided by the retention capability (per area) of the filter to be used. The resulting filter area is the minimum required to meet the sterility goal of fewer than one unit dose contaminated with one organism per million doses manufactured. The next step is to ensure that the filter is large enough to allow reasonable processing times. Typically, one does not want to filter for more than one shift (8 h). At 24 h, questions will be raised about "grow-through" (where retained microbes will have colonized the filter and "grown through" to the other side). The filtration time for the filter size is determined by finding the clean water flow rate for the filter, either through laboratory experiment or through the vendor's published data, and adjusting for the viscosity of the solution to be filtered relative to water (a correction for the effect of temperature on viscosity may be necessary). Once the flow rate is known, the time to filter a given size batch can be determined. The area of the filter can be increased to reduce the filtration time, but cannot be decreased without jeopardizing the sterility assurance.

For the ultimate filtration step, in which the product is rendered sterile, a depth filter can be added upstream of the membrane filter. This protects the sterile filter from fouling during use. This is a critical consideration in high-concentration process streams. It is very risky to replace a sterile filter once in place, with all the connections downstream sterilized. Depth filters with high "dirt loads" can keep particulate matter from reaching the membrane surface, keeping it clean for the removal of microbes. Two sterile filters are sometimes used in series, for added sterility assurance. This gives very high probability that dosage units will not be contaminated, but the arrangement sometimes becomes difficult to manage in other respects. For instance, multiple sterility assurance tests must be performed, a requirement that adds manipulations and increases chances for breaches in sterility.

Filters used for the purpose of sterilizing pharmaceutical products must be tested to ensure that they have been properly installed and have no defects that could allow sterility to be compromised. The two most common tests for a sterile filter for an aqueous product are the *bubble point* and the *pressure hold* or *diffusion* test. In both tests, a wetted, sterilized filter is pressurized with air or nitrogen. In the bubble point test, this pressure is increased until the lowest pressure is found at which a gas passes freely through the filter. It is assumed that this is the pressure required to overcome the surface tension and viscosity of water in the largest membrane pore (where the forces are the weakest). As the pore size of the membrane decreases, the bubble point increases. This test will also detect a sliced or unseated O-ring or other seal failure. The pressure hold test pressurizes a wetted filter to a pressure lower than the bubble point and measures either the total flow of gas through the membrane (by diffusion) or the rate of pressure decay. Both should be low, and both should meet the manufacturer's specifications for an intact, properly installed sterile filter.

Compatibility and extractable tests need to be performed on each filter type. Compatibility means that the filter does not adsorb an active ingredient or any other type of active excipient, such as a preservative. Such adsorption to the filter medium can change the strength (or biological potency) of the solution after the filtration step. Extractables and leachable chemicals, such as monomers from the membrane or support medium, filter coatings or mold release agents, and storage solutions, such as ethanol, must also be tested for in pilot studies with the product. These chemicals would be considered impurities in the final product and should be removed or prevented from leaching. Compatibility and extractables should be tested in a sample of the product solution. When this is not possible, because product or excipients would interfere with the analysis of the impurities, a placebo or similar solution should be used.

Air Sterile Filtration Air filters are also sized based on the anticipated flow rate. Airflows are specified with one or more of the following criteria: pressure differential between areas, air changes per hour, or linear flow rate. Pressure differentials are usually measured between rooms, or between rooms and corridors. These are specified when it is important for air to flow from a "cleaner" area to a "dirtier" area when doors, windows, or pass-throughs are opened between them. Pressure differentials are typically 50 to 150 Pa [= 0.5 to 1.5 cm of water, or 0.4 to 1.1 mm Hg (torr)]. Air changes per hour are often specified for rooms based on hazardous materials or clean operations the room is designed for. *Air changeover* is the airflow rate divided by the volume of the room. Air changeovers are different from *makeup rate*, which is the fraction of fresh air injected in the room's air handler.

Clean rooms often have very high changeover rates but low makeup rates. Rooms handling solvents or hazardous materials have high makeup rates (a 100 percent makeup rate is called *once-through air*) but low air cleanliness requirements. The changeover rate varies with the hazard of the material or the cleanliness requirement for the room. Linear flow rate is usually specified in hoods and smaller spaces. Linear flow rates of 5 to 20 ft/s (= 2.4 to 6.1 m/s) are found in laminar flow hoods, in aseptic areas where pharmaceuticals are sterile-processed, and in clean rooms where microelectronics are manufactured. Linear flow rates are established to prevent airborne microbes and particulate matter from settling in or on the materials being processed.

The air quality of a room or area is typically classified according to the number of airborne particles that can be measured in 1 m^3. Increasingly, rooms are being classified according to the International Organization for Standardization (ISO), which has published a series of documents numbered 14644 (volumes 1 to 5). These standards classify clean room space as 1 (cleanest) through 9 (dirtiest), with each classification allowing approximately one log more particles in a cubic meter of air than the previous. For biotechnology and pharmaceuticals, the most commonly used grades are ISO Class 5 (similar to the military standard Class 100) to ISO Class 8 (similar to the military standard class 100,000). ISO Class 5 is used for aseptic processing where products may be briefly exposed to the environment, and ISO Class 8 is used for areas containing primarily closed operations. High-efficiency particulate air (HEPA) filters are routinely tested for integrity by spraying a polyalphaolefin (PAO) aerosol on the feed side of the filters. The typical specification for a PAO test is a 10^3 reduction in aerosol particles.

Vent filters filter air on tanks and drainable equipment. Vent filters typically follow the same specification as the liquid filters used in the process. Vent filters are also sized based on the maximum airflow rate anticipated. The maximum flow rate is often encountered when the tanks are being filled or cleaned. Vent filters must allow flow in both directions. Integrity testing of vent filters is an evolving technology. These filters are typically hydrophobic, so aqueous-based bubble points and pressure holds are not appropriate. The PAO tests will not work because vent filters are typically membrane filters (which are the most compact), while HEPA filters are depth filters. Testing bubble points in solvents is feasible, and often performed, but is considered a destructive form of measurement.

20.3.3. SEDIMENTATION

Sedimentation is the movement of particles or macromolecules in an inertial field. Its applications in separation technology are widespread. Extremes of applications range from the settling due to gravity of tons of solid waste and bacteria in wastewater treatment plants to the high speed centrifugation of a few microliters of blood to determine packed blood cell volume in the clinical laboratory. Accelerations range from 1*g* in flocculation tanks to 100,000*g* in ultracentrifuges for measuring the sedimentation rates of macromolecules. In bioprocessing, the most frequent applications of sedimentation include the clarification of broths and lysates, the collection of cells and inclusion bodies, and the separation of fluids having different densities.

Unit operations in sedimentation include settling tanks and tubular centrifuges for batch processing, continuous centrifuges such as disk centrifuges, and less frequently used unit operations such as field-flow fractionators and inclined settlers. Bench-scale centrifuges that accommodate small samples can be found in most research laboratories and are frequently applied to the processing of bench-scale cell cultures and enzyme preparations. Certain high-speed ultracentrifuges are used as analytical tools for the estimation of molecular weights and diffusion coefficients.

The common types of production centrifuges are shown in Fig. 20-43, and a comparison of the advantages and disadvantages of the different centrifuge designs is given in Table 20-20 [Bell et al., in Fiechter (ed.), *Advances in Biochemical Engineering/Biotechnology*, vol. 26, Springer-Verlag, Berlin, 1983, p. 1]. The principles of sedimentation and more details about equipment for centrifugation are discussed in the Centrifuges subsection. Here, additional information on this topic that is specific for a bioproduct separation process is given, including the range of particle sizes and densities that are encountered, the concept of the sedimentation coefficient and its application, and the concept of equivalent time, which has been found to be useful for scale-up.

Table 20-20 Comparison of Production Centrifuges*

System	Advantages	Disadvantages
Tubular bowl	High centrifugal force	Limited solids capacity
	Good dewatering	Foaming unless special skimming or centripetal pump used
	Easy to clean	
	Simple dismantling of bowl	Recovery of solids difficult
Chamber bowl	Clarification efficiency remains constant until sludge space full	No solids discharge
	Large solids-holding capacity	Cleaning more difficult than with tubular bowl
	Good dewatering	Solids recovery difficult
	Bowl cooling possible	
Disk centrifuge	Solids discharge possible	Poor dewatering
	Liquid discharge under pressure eliminates foaming	Difficult to clean
	Bowl cooling possible	
Scroll or decanter centrifuge	Continuous solids discharge	Low centrifugal force
	High feed solids concentration	Turbulence created by scroll
Basket centrifuge	Solids can be washed well	Not suitable for soft biological solids
	Good dewatering	No solids discharge
	Large solids holding capacity	Recovery of solids difficult

*Bell et al., in Fiechter (ed.), *Advances in Biochemical Engineering/Biotechnology,* vol. 26, Springer-Verlag, Berlin, 1983, p. 1

Reproduced from *Bioseparations Science and Engineering*, 2d ed., by Roger G. Harrison, Paul W. Todd, Scott R. Rudge, and Demetri P. Petrides (2015). By Permission of Oxford University Press.

Figure 20-43 Common types of production centrifuges: (a) tubular bowl; (b) multichamber; (c) disk, nozzle; (d) disk, intermittent discharge; (e) scroll; and (f) basket. Arrows indicate the path of the liquid phase; dashed lines show where the solids accumulate. [Reproduced from Bioseparations Science and Engineering, 2d ed., by Roger G. Harrison, Paul W. Todd, Scott R. Rudge, and Demetri P. Petrides (2015). By Permission of Oxford University Press.]

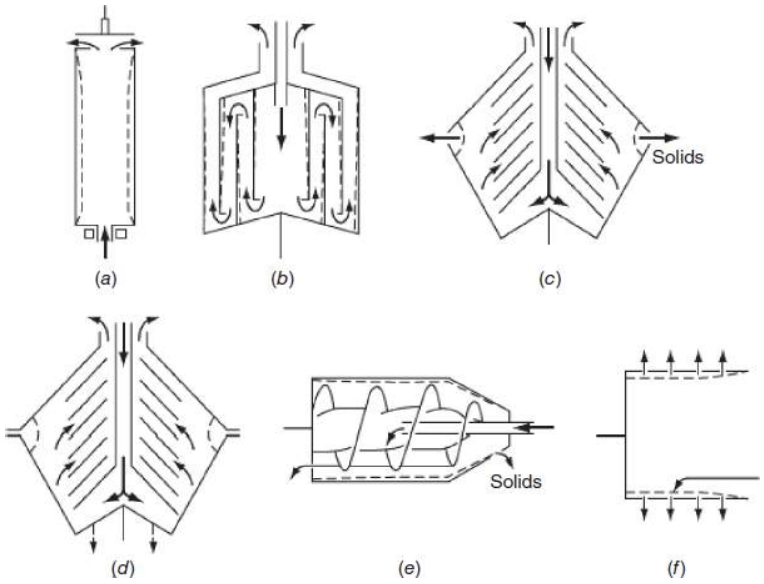

Fluid Dynamics During the sedimentation of a particle in the presence of a centrifugal field, the velocity of the particle reaches a constant value when all the forces are balanced. For a centrifugal field of acceleration $\omega^2 R$, where ω is the centrifuge's angular velocity and R is the distance of the particle from the center of rotation, at constant particle velocity$v$ for a particle of radius a_p and density ρ in a fluid of density ρ_0 and viscosity μ, an analysis using the equation of motion gives (Harrison et al., *Bioseparations Science and Engineering*, Oxford University Press, Oxford, UK, 2015, p. 187)

$$v = \frac{2a_p^2(\rho - \rho_o)\omega^2 R}{9\mu}$$

(20-38)

Creeping flow conditions are usually satisfied in sedimentation. The Reynolds number for sedimenting spherical particles is

$$\mathrm{Re} = \frac{2a_p v \rho}{9\mu}$$

(20-39)

Creeping flow occurs at Reynolds numbers less than about 0.1 (Bird et al.,*Transport Phenomena*, Wiley, Hoboken, N.J., 2002, p. 59).

Table 20-21 shows the sedimentation velocities for important bioparticles and biomolecules calculated from Eq. (20-38) with ρ_0 = 1.0 g/cm^3, μ = 0.01 g cm^{-1} s^{-1} (poise), and representative values of ρ and a_p. The sedimentation velocity and Reynolds number results shown in Table 20-21 for yeast cells and bacterial cells at gravitation acceleration can be multiplied by a centrifuge's centrifugal acceleration to give the corresponding values for operation in the centrifuge; for example, at a dimensionless acceleration of 10,000, the Reynolds number for yeast cells is 0.07, which means that the flow is still creeping.

Table 20-21 Calculated Settling Velocities and Reynolds Number for Example Bioproducts (Assumes ρ_0 = 1.0 g/cm^3 and μ = 1.0 cP)

Bioparticle or biomolecule	Sedimentation radius a_p (μm)	Density ρ (g/cm^3)	Dimensionless acceleration ($G = \omega^2 R/g$)	Sedimentation velocity v (cm/h)	Reynolds number Re
Yeast cell	2.5	1.1	1	0.5	7×10^{-6}
Bacteria cell	0.5	1.1	1	0.02	6×10^{-8}
Protein	0.005	1.3	10^4	0.06	2×10^{-9}

Reproduced from *Bioseparations Science and Engineering*, 2d ed., by Roger G. Harrison, Paul W. Todd, Scott R. Rudge, and Demetri P. Petrides (2015). By Permission of Oxford University Press.

It is clear from Table 20-21 that gravitational sedimentation is too slow to be practical for bacteria, and conventional centrifugation is too slow for protein macromolecules. In the case of true particles, flocculation is often used to increase the Stokes radius a_p, while ultracentrifugation is used in macromolecular separations (Harrison et al.,*Bioseparations Science and Engineering,* Oxford University Press, Oxford, UK, 2015, pp. 203, 205).

When particle density and solvent density are equal, the sedimentation velocity v is zero, and the process is called *isopycnic* or *equilibrium* sedimentation. This fact is exploited in the determination of molecular densities and in the separation of living cells. A density gradient or a density shelf is employed in such cases. Densities of representative cells, organelles, and biomolecules measured by this method are given in Table 20-22.

Table 20-22 Measured Values of Density of Representative Cells, Organelles, and Biomolecules

Cell, organelle, or biomolecule	Density ρ (g/cm^3)	Ref.
Escherichia coli	1.09*	1
Bacillus subtilis	1.12	2
Arthrobacter sp.	1.17	3
Saccharomyces pombe	1.09	1
Saccharomyces cerevisiae	1.11*	1
Amoeba proteus	1.02	1
Murine B cells	1.06*	1
Chinese hamster ovary (CHO) cells	1.06	1
Red blood cells	1.10*	4
White blood cells	1.02*	5
Peroxisomes	1.26*	6
Mitochondria	1.20*	6
Plasma membranes	1.15*	6

Cell, organelle, or biomolecule	Density ρ (g/cm)	Ref.
Proteins	1.30*	6
Ribosomes	1.57*	6
DNA	1.68*	6
RNA	2.00*	6

*Average value.

References

1. Kubitschek, *Crit. Rev. Microbiol*. **14:** 73 (1987).

2. Hart and Edwards, *Arch. Microbiol.* **147:** 68 (1987).

3. Illmer, *FEMS Microbiol. Lett.* **196:** 85 (2001).

4. Ponder, *J. Biol. Chem.* **144:** 333 (1942).

5. Barnkob et al., 15th International Conference on Miniaturized Systems for Chemistry and Life Sciences, Oct. 2–6, Seattle, Wash., 2011.

6. Sheeler, *Centrifugation in Biology and Medicine*, Wiley-Interscience, New York, 1981.

Reproduced from *Bioseparations Science and Engineering*, 2d ed., by Roger G. Harrison, Paul W. Todd, Scott R. Rudge, and Demetri P. Petrides (2015). By Permission of Oxford University Press.

An example of a density shelf used for the preparation of cells is the preparation of lymphocytes by sedimentation. The goal of this separation is to remove erythrocytes from a leukocyte population on the basis of a density shelf. By combining Ficoll, a high-molecular-weight polymer, and Hypaque, a heavily iodinated benzoic acid derivative, in appropriate proportions in aqueous buffers, it is possible to achieve a density around 1.07 g/cm^3 in isotonic solutions. At this density, most white blood cell subpopulations will float and nearly all red blood cells will sediment, which is in agreement with what would be expected for these cells based on their densities, shown in Table 20-22.

When the concentration of sedimenting particles increases, the sedimentation velocity has been found to decrease, a phenomenon known as *hindered settling*. This effect has been quantified by the following expression for particles of any shape [Richardson and Zaki, *Trans. Inst. Chem. Eng.* **32:** 36 (1954)]:

$$v_c = v(1-\phi)^n$$

(20-40)

where v_c is the sedimentation velocity of particles in a concentrated suspension, v is the velocity of individual particles [Eq. (20-38)], ϕ is the volume fraction of the particles, and n is a function of only the shape of the particle and the Reynolds number. For spherical particles with Re < 0.2 (usually satisfied during sedimentation), the exponent n has been found to be 4.65. Equation (20-40) may also be applied to particles of any size in a polydisperse system, using the volume fraction for all the particles in the calculation [Richardson and Shabi, *Trans. Inst. Chem. Eng.* **38:** 33 (1960)].

The magnitude of the hindered settling effect for spherical particles as a function of the particle volume fraction ϕ can be seen in Table 20-23. Note that hindered settling can be significant for particle concentrations of a few percent or greater.

Table 20-23 Effect of Particle Volume Fraction ϕ on the Particle Sedimentation Velocity for Spherical Particles

ϕ	$\frac{v_c}{v}$
0.01	0.95
0.05	0.79
0.10	0.61
0.20	0.35

Reproduced from *Bioseparations Science and Engineering*, 2d ed., by Roger G. Harrison, Paul W. Todd, Scott R. Rudge, and Demetri P. Petrides (2015). By Permission of Oxford University Press.

Sedimentation Coefficient When a body force is applied, velocity through a viscous medium is usually proportional to the accelerating field (examples are electric, magnetic, and inertial). In the case of sedimentation, the resulting constant, a property of both the particle and the medium, is the *sedimentation coefficient*, which is defined as

$$s \equiv \frac{v}{\omega^2 R}$$

(20-41)

where *v* is the steady state velocity of the particle,*R* is the distance of the particle from the center of rotation, and ω is the angular velocity. Comparing this equation with Eq. (20-38), we see that

$$s = \frac{2a_p{}^2(\rho - \rho_o)}{9\mu}$$

(20-42)

which defines *s* in terms of only properties of the particle and the medium. This coefficient is usually expressed at 20 C and under conditions (viscosity and density) of pure water as

$$s_{20,w}\,(units\,of\,S)$$

The sedimentation coefficient is often expressed in svedberg units, where 10^{-13} seconds = 1 svedberg unit (S), named after the inventor of the ultracentrifuge, Theodor Svedberg.

Example

Example 20-4 Application of the Sedimentation Coefficient

In 1974, D. E. Koppel determined the sedimentation coefficient $s_{20,w}$ for the smaller ribosomes from *Escherichia coli* to be 70 S [Koppel, *Biochemistry* **13:** 2712 (1974]. Estimate how long it would take to completely clarify a suspension of these ribosomes in a high-speed centrifuge operating at 10,000 rpm with a tube containing the ribosome suspension in which the maximum distance of travel of particles radially outward is 1 cm and the initial distance from the center of rotation to the particles nearest the center of rotation is 4 cm.

We can write Eq. (20-41) as

$$s = \frac{dR}{dt}\frac{1}{\omega^2 R}$$

or

$$\omega^2 s\, dt = \frac{dR}{R}$$

We integrate this equation with the initial condition at $t = 0$, $R = R_0$ (distance from center of rotation to the particles nearest the center of rotation) to give

$$\omega^2 s t = \ln\frac{R}{R_o}$$

To determine the maximum time required, we evaluate R at the maximum travel of the cells measured from the center of rotation (5 cm):

$$t = \frac{ln\left(\frac{R}{R_o}\right)}{\omega^2 s} = \frac{ln(5/4) \times \frac{1\ h}{3600\ s}}{\left(10{,}000\frac{rev}{min} \times \frac{2\pi\ rad}{rev} \times \frac{1\ min}{60\ s}\right)^2 (70 \times 10^{-13} s)} = 8.1\ h$$

This should not be an unreasonable amount of time to centrifuge the ribosomes. However, since the time varies inversely with the square of the rotation speed, the time can be reduced to 2 h by doubling the speed.

Equivalent Time To assess the approximate properties of a particle type to be separated, it is sometimes convenient to calculate an "equivalent time." To do this, we first define a dimensionless acceleration G, the ratio of the centrifugal to gravitational acceleration for a particular centrifuge:

$$G \equiv \frac{\omega^2 R}{g}$$

(20-43)

where R is usually defined as the radius of the centrifuge bowl. Thus, this dimensionless unit is measured in "g's"—multiples of the earth's gravitational acceleration. A rough approximation of the difficulty of a given separation by centrifugation is the product of the dimensionless acceleration and the time required for the separation. This product is called the *equivalent time* for the separation and is written as

$$\text{Equivalent time} = \frac{\omega^2 R}{g} t$$

(20-44)

Typical values of equivalent time are as follows: 0.3 × 10^6 s for eukaryotic cells, 9 × 10^6 s for protein precipitates, 18 × 10^6 s for bacteria, and 1100 × 10^6 s for ribosomes (Belter et al.,*Bioseparations*, Wiley, Hoboken, N.J., 1988, p. 63).

The equivalent time for the centrifugation of cells or biological particles of unknown sedimentation properties may be estimated in a laboratory centrifuge. Samples are centrifuged for various times until a constant volume of packed cells is reached. The equivalent time *Gt* is calculated as the product of the *G* for the particular centrifuge and the time required to reach constant packed cell volume. A centrifuge that has commonly been used for this determination is the Gyro-Tester (Alfa Laval, Inc.).

One approach to scale-up of a centrifugal operation is to assume constant equivalent time:

$$(Gt)_1 = (Gt)_2$$

(20-45)

where the subscripts refer to centrifuges 1 and 2, respectively.

Example

Example 20-5 Scale-Up Based on Equivalent Time

If bacterial cell debris has *Gt* = 54 × 106 s (Belter et al., Bioseparations, Wiley, Hoboken, N.J., 1988, p. 63), how large must the centrifuge bowl be and what centrifuge speed is needed to effect a full sedimentation in 2 h?

From Eq. (20-44) for *Gt*, we can estimate the centrifuge speed ω if we know the centrifuge bowl size and the time of centrifuging. It is reasonable to have a centrifuge that is 10 cm in diameter. Solving Eq. (20-44) for ω by using these values gives

$$\omega = \left(\frac{Gtg}{Rt}\right)^{1/2} = \left(\frac{54 \times 10^6 s \times 9.81 \frac{m}{s^2}}{0.05\,\mathrm{m} \times 2(3600)^s}\right)^{1/2}$$

$$= 1213 \frac{\mathrm{rad}}{s} \times \frac{1\,\mathrm{rev}}{2\pi\,\mathrm{rad}} \times \frac{60\,s}{\mathrm{min}} = 11{,}590\,\mathrm{rpm}$$

This speed can be achieved in a production tubular bowl centrifuge.

Another commonly used method to scale up centrifugation is the *sigma analysis* method, as discussed under the subsection Sedimentation Centrifuges in Sec. 18. This method uses the velocity of particles at 1*g* and a sigma factor that represents the geometry and speed of the centrifuge.

20.3.4. PRECIPITATION

Precipitation, which is the process of coming out of solution as a solid, is an important method in the purification of proteins that usually comes early in the purification process. Precipitation is frequently used in the commercial separation of proteins. The primary advantages of precipitation are that it is relatively inexpensive, can be carried out with simple equipment, can be done continuously, and leads to a form of bioproduct that is often stable in long-term storage. Since precipitation is quite tolerant of various impurities, including nucleic acids and lipids, it is used early in many bioseparation processes.

The goal of precipitation is often concentration to reduce volume, although significant purification can sometimes be achieved. For example, all the protein in a stream might be precipitated and redissolved in a smaller volume, or a fractional precipitation might be carried out to precipitate the protein of interest and leave many of the contaminating proteins in the mother liquor.

In this section, first the focus is upon protein solubility, which is the basis of separations by precipitation. Then we discuss the basic concepts of particle formation and breakage and the distribution of precipitate particle sizes. The specific methods that can be used to precipitate proteins are treated next. Finally, the methodology to use for the design of precipitation systems is discussed.

Protein Solubility The most important factors affecting the solubility of proteins are structure and size, protein charge, and the solvent. Explanations follow for each of these factors.

Structure and Size In the native state, a protein molecule in an aqueous environment assumes a structure that minimizes the contact of the hydrophobic amino acid residues with the water solvent molecules and maximizes the contact of the polar and charged residues with the water. The major forces acting to stabilize a protein in its native state are hydrogen bonding, van der Waals interactions, and solvophobic interactions. In aqueous solution, these forces tend to push the hydrophobic residues into the interior of the protein and the polar and charged residues to the protein's surface. For example, one study of 36 globular proteins has shown that 95 percent of the ionizable groups are solvent accessible [Rashin and Honig, *J. Mol. Biol.* **173:** 515 (1984)]. In other studies of 69 proteins, the average solvent-(water-) accessible atomic surface was found to be 57 percent nonpolar, 25 percent polar, and 19 percent charged [Miller et al., *J. Mol. Biol.* **196:** 641 (1987); Janin et al., *J. Mol. Biol.* **204:** 155 (1988)]. Thus, in spite of the forces operating to force hydrophobic residues to the protein's interior, the surface of proteins usually contains a significant fraction of nonpolar atoms.

The forces acting on a protein lead to the achievement of a minimum Gibbs free energy. For a protein in its native configuration, the net Gibbs free energy is on the order of only 10 to 20 kcal/mol. This is a relatively small net free energy, which means that the native structure is only marginally stable and can be destabilized by relatively small environmental changes [Privalov, *Annu. Rev. Biophys. Biophys. Chem.* **18:** 47 (1989)].

Water molecules bind to the surface of the protein molecule because of association of charged and polar groups and immobilization by nonpolar groups. For example, a study of the hydration of human serum albumin found two layers of water around the protein [Van Oss and Good, *J. Protein Chem.* **7:** 179 (1988)]. In the layer next to the protein, the water molecules are almost totally oriented, with the hydrogen atoms adjacent to and facing the albumin surface, while the oxygen atoms face away from the protein surface. In the second layer of water molecules, most of the water molecules (70 percent) are nonoriented. These hydration layers are thought to promote solubility of the protein by maintaining a distance between the surfaces of protein molecules.

The size of a protein becomes important with respect to solubility when the protein is excluded from part of the solvent. This can happen when nonionic polymers that are added to the solution result in steric exclusion of protein molecules from the volume of solution occupied by the polymer. Juckes [*Biochim. Biophys. Acta* **229:** 535 (1971)] developed a model for this phenomenon based on the protein molecule being in the form of a solid sphere and the polymer molecule in the form of a rod, which gave the following equation for *S*, the solubility of the protein:

$$\ln S = \beta' - K' c_p \tag{20-46}$$

where

$$K' = \frac{\overline{V}}{2.303}\left(\frac{r_s + r_r}{r_r}\right)^3$$

(20-47)

Here, r_s and r_r are the radius of the protein solute and polymer rod, respectively, $\overline{V}$ is the partial specific volume of the polymer, c_p is the polymer concentration, and β' is a constant. Based on this model, we can expect the lowest protein solubility for large proteins.

Molecular size is the predominant factor in a type of precipitation known as *affinity precipitation*. When affinity groups or antibodies to a specific biomolecule (antigen) are added to a solution, the antibody-antigen interaction can form large multimolecular complexes, as shown in Fig. 20-44. Such complexes are usually insoluble and cause selective precipitation of the antigen. The average size of the complex agglomerates is maximized when there is a 1:1 stoichiometric ratio of antibody and antigen. If either is present in great excess, only bimolecular complexes will be formed; and there may be no precipitation, or low recovery, even if a precipitate is formed.

Figure 20-44 Schematic representation of antibody–antigen (Ab–Ag) interaction. [Reproduced from Bioseparations Science and Engineering, 2d ed., by Roger G. Harrison, Paul W. Todd, Scott R. Rudge, and Demetri P. Petrides (2015). By Permission of Oxford University Press.]

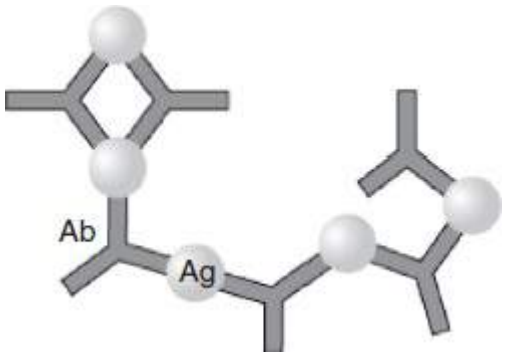

Charge The net charge of a protein has a direct bearing upon the protein's solubility. The solubility of a protein increases as its net charge increases, a result of greater interaction with dipolar water molecules. A repulsive reaction between protein molecules of like charge further increases solubility.

A simple way to vary the charge on a protein is by changing the pH of the solution. The pH of the solution in which a protein has zero net charge is called the *isoelectric pH* or *isoelectric point*. The isoelectric pH is known as the pI of the protein. The solubility of a protein is, in general, at its minimum at the isoelectric point. A typical example is shown in Fig. 20-45. Nonuniform charge distribution, however, results in a dipole moment on the molecule, which leads to an increase in solubility and a move in the minimum solubility away from the isoelectric point. The effect of the dipole moment is discussed further in the following subsection.

Figure 20-45 The solubility S of insulin in 0.1 N NaCl as a function of pH. The charge Z is the average protonic charge per 12,000 g of insulin at the pH values indicated. Insulin's pI corresponds to a zero net charge where its solubility is near minimum. (Data from Tanford, Physical Chemistry of Macromolecules, Wiley, New York, 1961.)

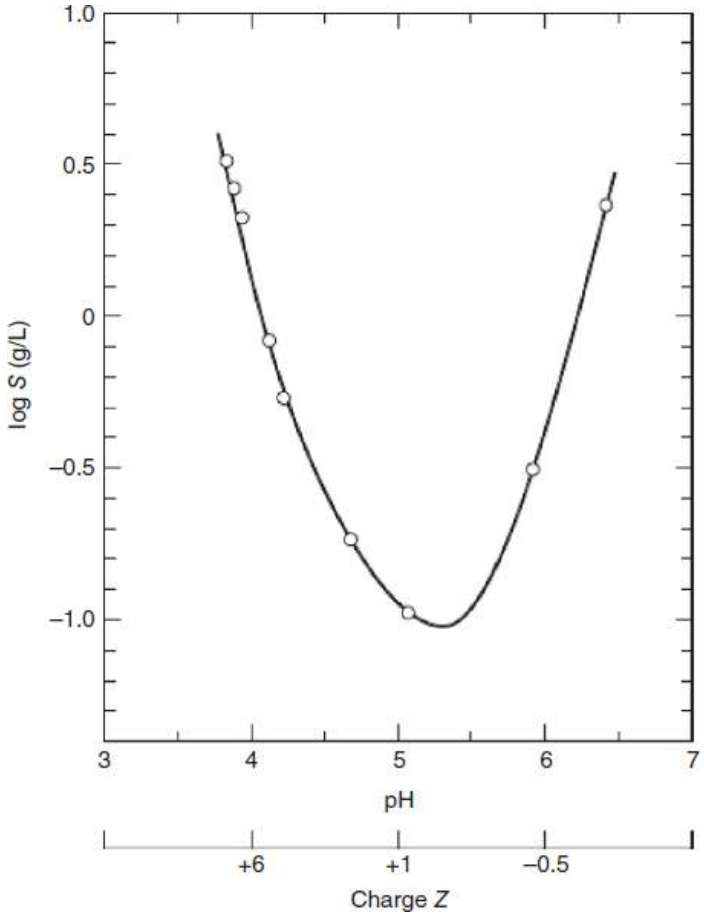

The net charge of a protein is determined by the following factors: the total number of ionizable residues, the accessibility of the ionizable residues to the solvent, the dissociation constants (or pK_a values) of the ionizable groups, and the pH of the solution [Rothstein, in Harrison (ed.), *Protein Purification Process Engineering*, Dekker, New York, 1994, p. 115]. Besides the chemical makeup of the ionizable groups, factors that can influence the pK_a values are the chemical nature of the neighboring groups (e.g., inductive effects), the temperature, the chemical nature of the solvent as partially reflected by its dielectric constant, and the ionic strength of the solvent.

Solvent The solvent affects the solubility of proteins primarily through two parameters, hydrophobicity and ionic strength. The first parameter has been well studied through observations of single-phase solutions of water and primary alcohols. Although these solutions can cause protein denaturation at room temperature, denaturation can be avoided at sufficiently low temperatures. Studies of primary alcohols have shown that denaturing efficiency is as follows:

$$\text{methanol} < \text{ethanol} < \text{propanol} < \text{butanol}$$

This led to the conclusion that the alcohols with longer alkyl chains are binding more effectively to nonpolar groups on the protein, weakening intraprotein hydrophobic interactions and thus leading to denaturation [Bull and Breese, *Biopolymers* **17:** 2121 (1978)]. It is thought that when the temperature is low, the primary alcohols compete for the water of hydration on the protein and cause the protein molecules to approach more closely, so that van der Waals interactions lead to aggregation.

The ionic strength of the solvent can have both solubilizing and precipitating effects. The solubilizing effects are referred to as *salting in*, while the precipitating actions are called *salting out*. The salting-in effect has been observed for several proteins, including the class of proteins named *euglobulins*. These proteins are insoluble in the absence of salt at their isoelectric points, but become soluble when salt is added. In contrast, members of another class of proteins, the *albumins,* are very soluble in water as well as in high concentrations of salt. It is believed that the solubilities of the euglobulins and the albumins differ because the euglobulins have a much higher dipole moment than the albumins [Oncley, in Cohn and Edsall (eds.), *Proteins, Amino Acids, and Peptides*, Reinhold, New York, 1943, p. 543].

A theoretical treatment of the interactions between ions and dipoles developed in 1943 by Kirkwood [Cohn and Edsall (eds.), *Proteins, Amino Acids, and Peptides*, Reinhold, New York, 1943, p. 276] accounts for salting-in effects by considering the solute size, solute shape, solute dipole moment, solvent dielectric constant, solution ionic strength, and temperature. One of Kirkwood's models was for a spherical dipolar ion with a point dipole moment u located at the center of the sphere. The equation derived to describe the interactions is as follows:

$$\ln\left(\frac{S_p}{S_o}\right) = K_i I - K_s I$$

(20-48)

where S_p is the solubility of the dipolar ion at ionic strength I, S_0 is the solubility of the dipolar ion in the absence of salt, K_i is the salting-in constant, and K_s is the salting-out constant. Ionic strength is defined by

$$I = \frac{1}{2}\sum_i c_i z_i^2$$

(20-49)

where c_i is the molar concentration of any ion and z_i is its charge. The salting-in and salting-out constants can be related to other variables as follows:

$$K_i \propto \left(\frac{u}{\varepsilon T}\right)^2$$

(20-50)

$$K_s \propto \frac{V_e}{\varepsilon T}$$

(20-51)

where ε is the dielectric constant of the solvent, T is absolute temperature, and V_e is the excluded volume of the dipolar ion. Equations (20-48) and (20-50) confirm the observed strong relationship between the solubility of dipolar proteins and the size of their dipole moment u, as well as the greater salting-in effect observed with proteins with high dipole moments. Also it can be seen that the salting-in term increases more than the salting-out term as the dielectric constant decreases. The dielectric constant decreases as the polarity of the solvent decreases. Therefore, the salting-in effect tends to predominate in relatively nonpolar solvents, while the salting-out effect is more dominant in aqueous solvents.

At high ionic strength, the salting-out effect becomes predominant and can be described empirically by the Cohn equation [Cohn, *Physiol. Rev.* **5:** 349 (1925)]:

$$\ln S = \beta - K_s' I$$

(20-52)

where *S* is the solubility of the protein and K_s' is a salting-out constant characteristic of the specific protein and salt that is independent of temperature and pH above the isoelectric point. The constant β, the hypothetical solubility of the protein at zero ionic strength, depends on only temperature and pH for a given protein and is a minimum at the isoelectric point. It is interesting that the Cohn equation is identical in form to the equation that describes the precipitation of proteins by the addition of nonionic polymers, Eq. (20-46). In addition, the Kirkwood equation for the solubility of dipolar ions [Eq. (20-48)] can be arranged to give

$$\ln S_p = \ln S_o - (K_s - K_i) I$$

(20-53)

which is also identical in form to the Cohn equation, with

$$\beta = \ln S_o$$

(20-54)

$$K_s' = K_s - K_i$$

(20-55)

Both salting in and salting out are illustrated in Fig. 20-46 for hemoglobin with ammonium sulfate or sodium sulfate being added. From zero ionic strength, the solubility of the protein increases to a maximum as salt is added and then continuously decreases as even more salt is added.

Figure 20-46 The effect of $(NH_4)_2SO_4$ and Na_2SO_4 on the solubility of hemoglobin: S_0 is the solubility in pure water, and S is the solubility in the salt solution. [Data from Tanford, Physical Chemistry of Macromolecules, Wiley, 1961, p. 244.]

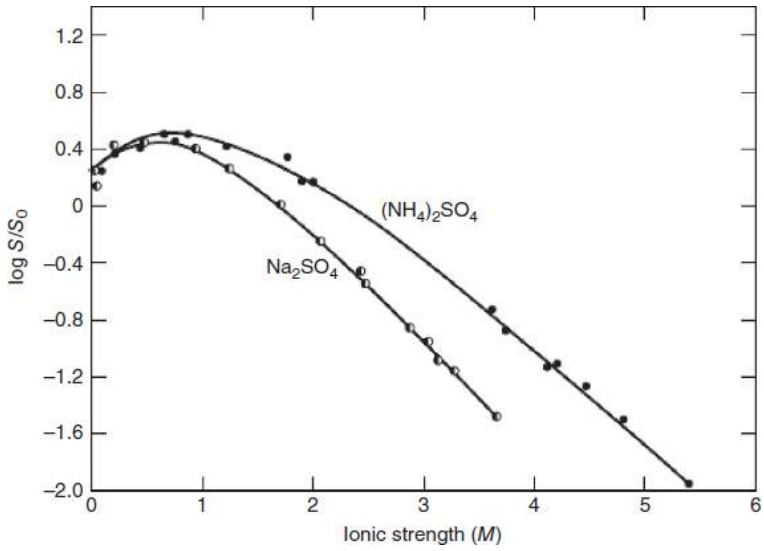

Example

Example 20-6 Salting Out of a Protein with Ammonium Sulfate

Data were obtained on the precipitation of a protein by the addition of ammonium sulfate. The initial concentration of the protein was 15 g/L. At ammonium sulfate concentrations of 0.5 and 1.0 M, the concentrations of the protein remaining in the mother liquor at equilibrium were 13.5 and 5.0 g/L, respectively. From this information, estimate the ammonium sulfate concentration to give 95 percent recovery of the protein as precipitate.

We can use the Cohn equation [Eq. (20-52)], to solve this problem if we can determine the constants in the equation. Since ionic strength is directly proportional to concentration c for a given salt [Eq. (20-49)], we can rewrite the Cohn equation as

$$\ln S = \beta - K''_s c$$

Substituting the experimental data into this equation gives

$$\ln(13.5) = \beta - 0.5K''_s$$
$$\ln(5.0) = \beta - 1.0K''_s$$

Solving these equations for the constants yields

$$\beta = 3.60$$
$$K''_s = 1.99\ \mathrm{M}^{-1}$$

For 95 percent recovery, the protein solubility in the mother liquor at equilibrium is 5 percent of the initial protein concentration. At this solubility, from the Cohn equation

$$c = \frac{\beta - \ln S}{K''_s} = \frac{3.60 - \ln(0.05 \times 15)}{1.99} = 1.95 \text{ M}$$

Precipitate Formation Phenomena By studying the phenomena of precipitate formation, we can maximize control over the characteristics of the final protein precipitate. Important characteristics of protein precipitates are the particle size distribution, density, and mechanical strength. Normally, it is desired to avoid having a large fraction of particles in the small size range. For proteins, particle sizes near or below 1 μm are considered to be small. Protein precipitates that consist largely of particles with small particle sizes can be difficult to filter or centrifuge. Low particle densities also can lead to filtration or centrifugation problems and can give excessive bulk volumes of the final dried precipitate. Particles with low mechanical strength can give problems with excessive attrition when the dry particles are moved. Low strength can also be interpreted as gel formation, which leads to major problems in filtration and centrifugation.

Precipitates form by a series of steps that occur in sequence, which are the following: (1) initial mixing, (2) nucleation, (3) growth governed by diffusion, and (4) growth governed by fluid motion. There is often some overlap between these steps. The final size of the precipitate particles during step 4 is subject to the limits imposed by particle breakage during mixing. The completion of the growth by fluid motion step can be followed by an "aging" step, where the particles are mixed until reaching a stable size.

Initial Mixing Initial mixing is the mixing required to achieve homogeneity after the addition of a component to cause precipitation. It is important to bring precipitant and product molecules into collision as soon as possible. This is a problem in micromixing, which is also important in fermentation. This subject was studied by the Russian statistician Kolmogoroff in the form of the homogeneous isotropic turbulence model, which assumes that mixing between randomly dispersed eddies is instantaneous and the mixing within eddies is diffusion-limited. It is therefore important to know the mean length of eddies, also known as the *Kolmogoroff length*, here designated l_e. It can be calculated from [Bell et al., in Fiechter (ed.),*Advances in Biochemical Engineering/Biotechnology*, vol. 26, Springer-Verlag, 1983, p. 1].

$$l_e = \left(\frac{\rho \nu^3}{P/V} \right)^{1/4}$$

(20-56)

where ρ is the liquid density, v is the liquid kinematic viscosity, andP/V is the agitator power input per unit volume of liquid.

It is necessary to mix until all molecules have diffused across all eddies. This time can be estimated from the Einstein diffusion relationship

$$t = \frac{\delta^2}{2\mathscr{D}}$$

(20-57)

where δ is the diffusion distance and $\mathscr{D}$ is the diffusion coefficient for the molecule being mixed. For spherical eddies of diameter l_e, this becomes

$$t = \frac{l_e^2}{8\mathscr{D}}$$

(20-58)

Thus, precipitation is initiated in a well-stirred tank for a period of time determined on the basis of isotropic turbulence.

Nucleation Nucleation is the generation of particles of ultramicroscopic size. For particles of a given solute to form, the solution must be *supersaturated* with respect to the solute. In a supersaturated solution, the concentration of the solute in solution is greater than the normal equilibrium solubility of the solute. The difference between the actual concentration in solution and the equilibrium solubility is called the *degree of supersaturation*, or just *supersaturation*. The rate of nucleation increases exponentially up to the maximum level of supersaturation, or supersaturation limit, which is illustrated in Fig. 20-47. Note that the rate of nucleation increases to a very high value at the supersaturation limit.

Figure 20-47 ***Nucleation rate as a function of degree of supersaturation. The normal equilibrium solubility is at A, and the supersaturation limit is at B. [Reproduced from Bioseparations Science and Engineering, 2d ed., by Roger G. Harrison, Paul W. Todd, Scott R. Rudge, and Demetri P. Petrides (2015). By Permission of Oxford University Press.]***

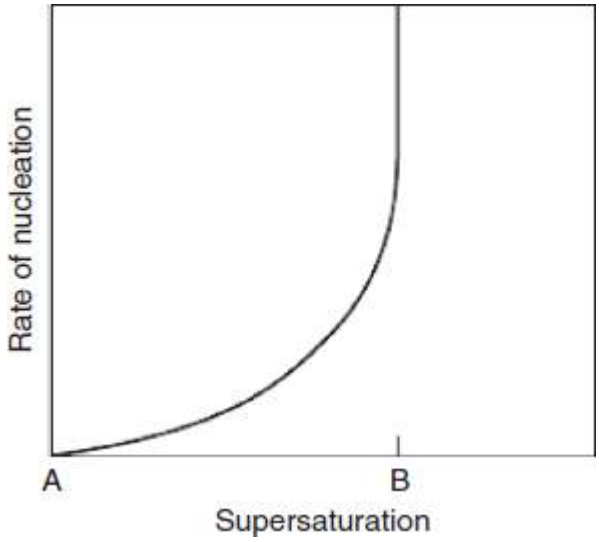

High supersaturations generally have negative consequences in carrying out precipitations. When the supersaturation is high, the precipitate tends to be in the form of a colloid, a gel, or a highly solvated precipitate. To obtain precipitate particles having desirable characteristics, the supersaturation should be kept relatively low.

Growth Governed by Diffusion The growth of precipitate particles is limited by diffusion immediately after nucleation and until the particles grow to a limiting particle size defined by the fluid motion, which generally ranges from 0.1 to 10 μm for high and low shear fields, respectively [Ives, in Ives (ed.), *Scientific Basis of flocculation*, Sijthoff and Noordhoff, Alphen aan den Rijn, 1978, p. 37]. In a dispersion of particles of uniform size that are growing as dissolved solute diffuses to the particles, the initial rate of decrease of particle number concentration N can be described by a second-order rate equation that was first derived by Smoluchowski [*Z. Phys. Chem.* **92:** 129 (1917)]:

$$-\frac{dN}{dt} = K_A N^2$$

(20-59)

Here N is the number of mono-sized particles at any given time$t$. The constant K_A is determined by the diffusivity $\mathscr{D}$ and diameter L_{mol} of the molecules that are adding to the particles as follows:

$$K_A = 8\pi \mathscr{D} L_{\text{mol}}$$

(20-60)

Integrating Eq. (20-59) gives

$$N = \frac{1}{K_A t + 1/N_o}$$

(20-61)

For convenience, N_o is taken as the initial number concentration of dissolved solute molecules. The Stokes-Einstein equation can be used to estimate the diameter of globular proteins, which can be modeled as spheres

$$L_{\text{mol}} = \frac{k_B T}{3\pi \mathscr{D} \mu}$$

(20-62)

where k_B is the Boltzmann constant, T is the absolute temperature, and μ is the liquid viscosity.

Equation (20-61) can be rewritten as

$$\frac{N}{N_o} = \frac{1}{1 + N_o K_A t}$$

(20-63)

With M as the molecular weight of particles at time t and M_o as the molecular weight of the solute,

$$\frac{M}{M_o} = \frac{N_o}{N}$$

(20-64)

so that

$$M = M_o(1 + K_A N_o t)$$

(20-65)

This equation has been verified experimentally by measuring the molecular weight of precipitating α-casein. The data plotted in Fig. 20-48 indicate good agreement with Eq. (20-65) after an initial lag time.

Figure 20-48 Molecular weight–time plots for three concentrations of α_s-casein (concentrations as indicated on graph in kilograms per cubic meter), aggregating in the presence of 0.008 M $CaCl_2$. Molecular weight was determined from light-scattering and turbidity measurements. (Data from Bell et al., Adv. Biochem. Eng. ***26:*** *20, Springer-Verlag, 1983, p. 20.)*

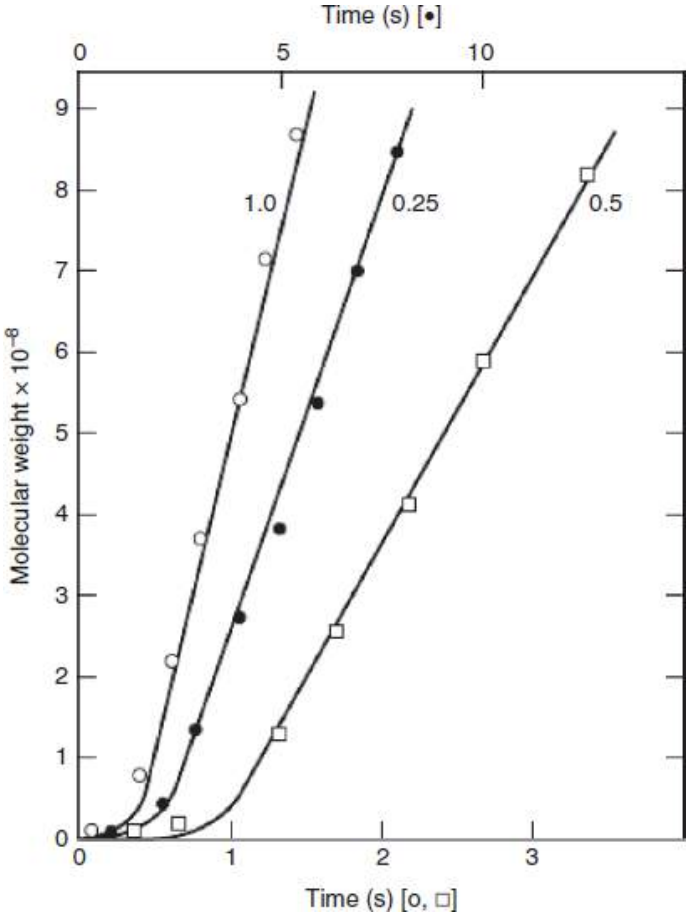

Growth Governed by fluid Motion Growth of particles is governed by fluid motion after the particles have reached a critical size, typically 1 μm in diameter [Bell et al., in Fiechter (ed.), *Advances in Biochemical Engineering/Biotechnology*, vol. 26, Springer-Verlag, 1983, p. 1]. In this growth regime, particles tend to grow by colliding and then sticking together. This is a flocculation process, which is enhanced when electrostatic repulsion between particles is reduced in comparison to the attractive van der Waals force. This can be accomplished by raising the ionic strength and lowering the temperature, to reduce the thickness of the electrical double layer, or Debye length, around particles.

For particles of uniform size in a suspension, the initial rate of decrease of particle number concentration N due to collisions can be described by a second-order rate equation

$$-\frac{dN}{dt} = \frac{2}{3}\alpha L^3 \gamma N^2$$

(20-66)

which was also derived by Smoluchowski [*Z. Phys. Chem.* **92:** 129 (1917)]. Here α is the collision effectiveness factor (fraction of collisions that result in permanent aggregates), L is the diameter of the particles, and γ is the shear rate (velocity gradient). Assuming that the volume fraction of the particles ($\phi = \pi L^3 N/6$) is constant during particle growth governed by fluid motion and integrating yields

$$\frac{N}{N_o} = \exp\left(-4\alpha\phi\gamma t/\pi\right)$$

(20-67)

where N_0 is now the particle number concentration at the time [t = 0 in Eq. (20-67)] at which particle growth starts to be governed by fluid motion. For turbulent flow, the average shear rate γ can be estimated by the following equation, developed by Camp and Stein [*J. Boston Soc. Civ. Engrs.* **30:** 219 (1943)]:

$$\gamma = \left(\frac{P/V}{\mu}\right)^{1/2}$$

(20-68)

where *P/V* is power dissipated per unit volume and μ is the viscosity of the liquid, respectively. Information about the determination of the collision effectiveness factor α has been given by Bell [Bell et al., in Fiechter (ed.), *Advances in Biochemical Engineering/Biotechnology*, vol. 26, Springer-Verlag, 1983, p. 1].

Precipitate Breakage When precipitate particles grow large enough by colliding and sticking together, they become susceptible to breakage during collisions. The rate of precipitate breakage has been shown to depend on the shear rate and particle concentration. In a study of soy protein precipitate particles, for example, particle breakup dominated at sizes greater than 16 μm, and breakup became negligible at low particle volume fractions (<0.0002) [Brown and Glatz, *Chem. Eng. Sci.* **42:** 1831 (1987)].

A model that has successfully described the breakup of protein precipitates is the displacement model, which depicts the rate of aggregate size change as a function of displacement from an equilibrium aggregate diameter L_e [Twineham et al., *Chem. Eng. Sci*. **39:** 509 (1984)]:

$$\frac{dL}{dt} = k(L_e - L)^n$$

(20-69)

where the rate constant *k* would be expected to depend on the volume fraction of particles ϕ and the shear rate γ. This model with *n* = 1 (first-order) fits data well for the mean diameter of soy protein particles at constant shear and various particle volume fractions (Fig. 20-49). The equilibrium diameter L_e has been shown to depend on the shear rate. For isoelectric soy protein precipitate in laminar Couette shear flow,

$$\overline{L}_{e,v} \propto \gamma^{-0.14} \qquad 2000\,s^{-1} \le \gamma \le 80{,}000\,s^{-1}$$

(20-70)

and for casein precipitated by salting out in a continuous stirred-tank reactor [Twineham et al.,*Chem. Eng. Sci.* **39:** 509 (1984)],

$$\overline{L}_{e,v} \propto \gamma^{-0.21} \qquad 12\ \mathrm{s}^{-1} \le \gamma \le 154\ \mathrm{s}^{-1}$$

(20-71)

where $\overline{L}_{e,v}$ is the equilibrium particle size at the volume mean of the particle size distribution. It is remarkable that both correlations are relatively similar, given the varation in protein precipitation type, protein type, and shear rate range. Particle breakage is also discussed later in the analysis of the particle size distribution in a continuous flow stirred-tank reactor.

Precipitate Aging As indicated in Fig. 20-49, protein precipitate particles reach a stable size after a certain length of time in a shear field. The time period for reaching this stable size is called the aging time. The strength of protein particles has been correlated with the product of the mean shear rate and the aging time, γt, which is known as the *Camp number.* As indicated in Fig. 20-50 for soy protein particles, the mean particle size becomes approximately constant after reaching a Camp number of 105. Aging of precipitates helps the particles withstand processing in pumps and centrifuge feed zones without further size reduction.

*Figure 20-49 Volume mean aggregate diameter as a function of time for soy precipitate particles exposed to shear rate of 1340 s^{-1} at different particle volume fractions ϕ. Lines are drawn for the displacement model. Points are experimental data. [Data from Brown and Glatz, Chem. Eng. Sci.**42:** 1831 (1987).]*

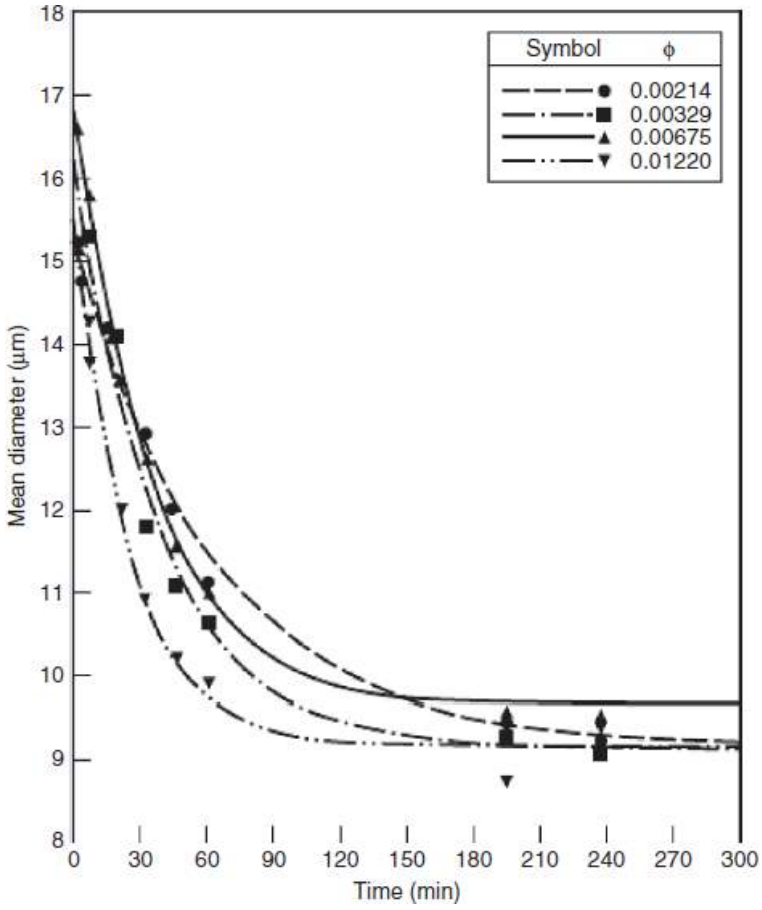

*Figure 20-50 The effect of aging on the change in the volume mean diameter of soy protein precipitate particles exposed to capillary shear. Average capillary rate of shear, 1.7×10^4 s^{-1}; average time of exposure in capillary, 0.065 s; protein concentration, 30 kg m^{-3}; initial mean diameter $\overline{L}_{0,v}$ (μm) prior to exposure to capillary shear: ○, 53.5; Δ, 23.4; ◊, 19.5; ⊗, 15.2; □, 10.2; •, 8.8. [Data from Bell and Dunnill, Biotechnol.Bioeng.**24:** 1271 (1982).]*

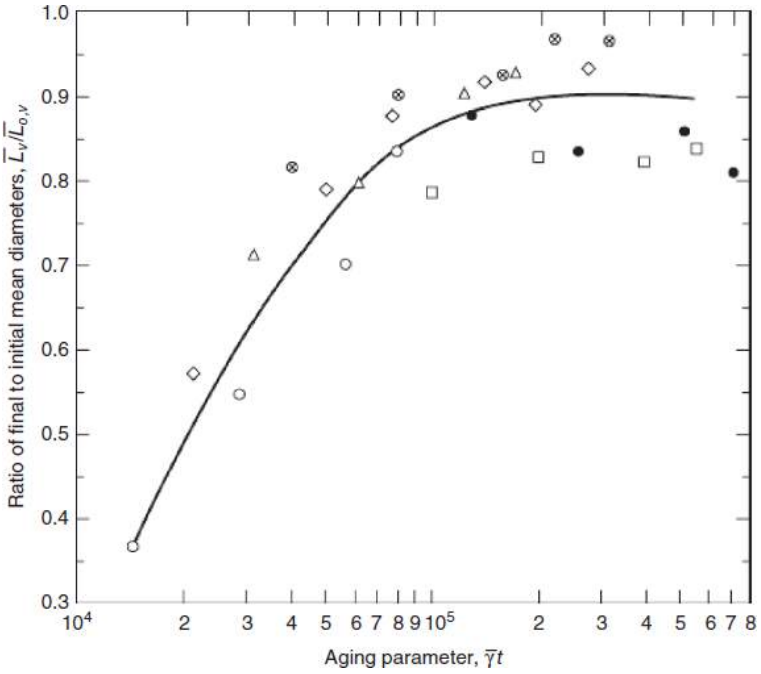

Particle Size Distribution in a Continuous flow Stirred-Tank Reactor The equations describing precipitate formation and breakage in the preceding subsection are convenient to use when the size of the precipitate is changing with time. In addition to being applicable to the batch reactor, these equations can be used to describe precipitate growth in the tubular reactor (see the Design of Precipitation Systems subsection). However, for one important type of reactor—the *continuous flow stirred-tank reactor* (CSTR)—operation is at steady state. Because precipitated protein leaves the CSTR at the same time as the feed protein solution enters, the product stream leaving the CSTR will have a *range of particle sizes*, which does not vary with time for operation at steady state. The distribution of particle sizes can be characterized by performing a population balance for precipitate particles in the CSTR (Randolph and Larson, *Theory of Particulate Processes*, Academic Press, Cambridge, Mass., 1971, p. 49). Before writing the population balance, it is first necessary to define the population density distribution function $n(L)$ and the linear growth rate G:

$$n(L) = \frac{dN}{dL} \tag{20-72}$$

$$G = \frac{dL}{dt} \tag{20-73}$$

Thus, if we know $n(L)$, we can take the integral of $n(L)dL$ to find the total number of particles bracketed by two given particle diameters, a minimum and a maximum, for example.

Making a balance on the number ΔN of precipitate particles within a given size range ΔL and taking the limit as $\Delta L \to 0$, we obtain for constant reactor volume V

$$\frac{d(nG)}{dL} + \frac{n}{\tau} + B = 0$$

(20-74)

where τ is the mean residence time (= V/Q) and B is the volumetric breakage or death rate of particles in the size range L to ΔL, such that the net rate of disappearance of particles due to breakage per volume is $B\,\Delta L$.

The growth of protein precipitate particles in a CSTR has been successfully described by Petenate and Glatz [*Biotechnol. Bioeng*. **25:** 3059 (1983)], who used the following expression for the linear growth rate:

$$G = \frac{dL}{dt} = \left(\frac{A}{4\pi}\right)\gamma\phi_1 L = K_o L$$

(20-75)

where A is a constant and ϕ_1 is the volume fraction of submicrometer-sized "primary" particles. In this model, aggregates above a critical diameter L_0 grow because small primary particles collide with aggregates and stick (see Fig. 20-51). Primary particles typically have diameters of about 0.2 μm for protein precipitation in a CSTR [Petenate and Glatz, *Biotechnol. Bioeng*. **25:** 3059 (1983)].

Figure 20-51 Schematic drawing of the growth of a precipitate aggregate by collisions of the aggregate with small primary particles: L_0 is the critical diameter above which particles grow by colliding with and sticking to small primary particles. [Reproduced from Bioseparations Science and Engineering, 2d ed., by Roger G. Harrison, Paul W. Todd, Scott R. Rudge, and Demetri P. Petrides (2015). By Permission of Oxford University Press.]

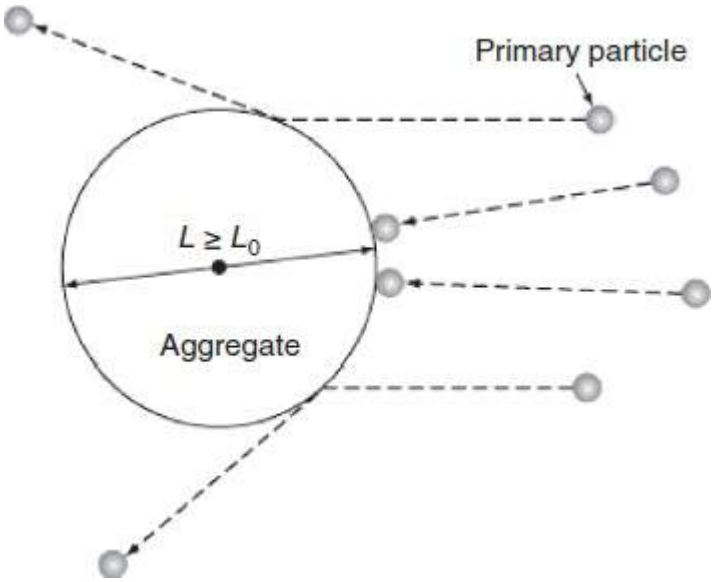

The larger a precipitate aggregate becomes, the more susceptible it is to being broken up by the local shear stresses encountered in turbulent flow. For the conditions under which local shear stresses are dominant, the following equation for the volumetric breakage or death rate *B* has been successfully used by Petenate and Glatz to describe the breakup of protein aggregates:

$$B = K\mu\gamma^2 n L^3 = K_1 n L^3$$

(20-76)

where *K* is a constant and μ is the viscosity.

A useful parameter to know for the precipitation in a CSTR is the mass-averaged particle size. For spherical particles, the total mass concentration M_T in terms of the mass-averaged diameter $\overline{L}_m$ is

$$M_T = \rho_p \pi \left(\frac{\overline{L}_m^3}{6} \right) N$$

(20-77)

where ρ_p is the density of individual particles and *N* is the total particle number concentration. From *n*(*L*), we can determine M_T and *N* for spherical particles equal to or greater than L_o in size as follows:

$$M_T|_{L \geq L_o} = \frac{\rho_p \pi}{6} \int_{L_o}^{\infty} L^3 n(L) dL$$

(20-78)

$$N|_{L \geq L_o} = \int_{L_o}^{\infty} n(L) dL$$

(20-79)

Combining Eqs. (20-77), (20-78), and (20-79) gives the mass-averaged particle diameter for $L \geq L_0$:

$$\overline{L}_m|_{L \geq L_o} = \left[\frac{\int_{L_o}^{\infty} L^3 n(L) dL}{\int_{L_o}^{\infty} n(L) dL} \right]^{1/3}$$

(20-80)

Example

Example 20-7 Dependence of Population Density on Particle Size and Residence Time in a CSTR

For the precipitation of protein in a CSTR, determine the dependence of the population density distribution n on the particle diameter L and residence time τ. Consider both particle growth by aggregation and particle breakup.

Use the expressions for the linear growth rate and particle breakup [Eqs. (20-75) and (20-76)] in the population balance equation [Eq. (20-74)]. This gives

$$\frac{d(K_o L n)}{dL} + \frac{n}{\tau} + K_1 n L^3 = 0$$

Differentiating and rearranging, we have

$$\frac{dn}{n} = -dL \left[\frac{\left(1 + \frac{1}{K_o \tau}\right)}{L} + \frac{K_1 L^2}{K_o} \right]$$

With lower limits of integration of n_0 (the population density function at $L = L_0$) and critical diameter L_0, we obtain

$$\frac{n}{n_o} = \left(\frac{L_o}{L}\right)^{\left(1+\frac{1}{K_o\tau}\right)} \exp\left[\frac{-K_1}{3K_o}\left(L^3 - L_o^3\right)\right]$$

Methods of Precipitation Methods that have been developed to precipitate proteins are based on a knowledge of the solubility of proteins. Based on the previous discussion of protein solubility, the most obvious methods that emerge are pH adjustment to the isoelectric point of the protein (called *isoelectric precipitation*), addition of organic solvents, salting out, and addition of nonionic polymers.

Isoelectric precipitation is based on the fact that the solubility of a given protein is generally at a minimum at the isoelectric point (pI) of the protein, which is the pH at zero charge (see Fig. 20-45). This is a convenient method to use when fractionating a protein mixture. For this situation the pH should be adjusted above the highest pI or below the lowest pI of all the proteins present. The pH is then changed to the nearest pI, where precipitate is allowed to form and is then removed. This procedure is repeated for as many proteins as one desires to precipitate. Local extremes of pH should be avoided during pH adjustment to minimize protein denaturation (Harrison et al., *Bioseparations Science and Engineering,* Oxford University Press, Oxford, UK, 2015, p. 32). There are two advantages of isoelectric precipitation when acids are added to cause precipitation: mineral acids are cheap, and several acids (e.g., phosphoric, hydrochloric, sulfuric) are acceptable in protein food products. This method, however, will not work for all proteins; for example, gelatin, which is a very hydrophilic protein, does not precipitate at its isoelectric point in solvents having low ionic strength [Bell et al., in Fiechter (ed.), *Advances in Biochemical Engineering/Biotechnology*, vol. 26, Springer-Verlag, 1983, p. 1].

Several organic solvents have been used to precipitate proteins, including alcohols, acetone, and ether. Alcohols, however, have been the most widely used in industry. One of the most important processes utilizing alcohol to precipitate proteins is the Cohn process to purify therapeutic proteins from human plasma [Strong, in Kirk and Othmer (eds.), *Encyclopedia of Chemical Technology*, Interactive Encyclopedia System, 1948, p. 566]. This process uses ethanol at temperatures below 0 C to minimize denaturation by the organic solvent. The variables that are manipulated in the Cohn process are pH, ionic strength, and ethanol concentration. Ionic strength is kept low, which leads to a salting-in effect (see the Protein Solubility subsection). This salting-in effect is enhanced when ethanol is added. Cohn's method has been used to obtain albumin, plasminogen, prothrombin, isoagglutinins, and γ-globulin starting with blood plasma.

In the salting out of proteins, salt is dissolved in the solution containing the proteins. The protein solubility decreases as the salt ionic strength rises according to the Cohn equation [Eq. (20-52)]. The most important consideration in salting out is the type of salt used. Salts with multiply charged anions such as sulfate, phosphate, and citrate are the most effective; for the cation, monovalent ions should be used (Scopes, *Protein Purification*, Springer-Verlag, 1982, p. 47). Following the Hofmeister or lyotropic series, the salting-out ability of the common multiply charged anions is citrate^{2-} > phosphate^{3-} > sulfate^{2-}; for the common monovalent cations, the order is $NH_4^+ > K^+ > Na^+$.

The salt that has the most desirable properties in general for precipitating proteins is ammonium sulfate. The solubility of this salt is very high (approximately 4 *M* in pure water) and varies very little in the range of 0 to 30 C. The density of a saturated solution of ammonium sulfate is 1.235 g cm^{-3}, which is enough below the density of protein aggregates (approximately 1.29 g cm^{-3}) to allow centrifugation. Another advantage of using ammonium sulfate is that protein precipitates are often very stable for years in 2 to 3 *M* salt; in fact, many commercial enzymes are normally sold in ammonium sulfate solution at high molarity. Furthermore, proteolysis and bacterial action are prevented in concentrated ammonium sulfate solutions. The only disadvantage of ammonium sulfate is that it cannot be used above pH 8 because of the buffering action of ammonia. Sodium citrate is very soluble and is a good alternative to ammonium sulfate when the precipitation must be performed above pH 8 (Scopes, *Protein Purification*, Springer-Verlag, 1982, p. 48).

Several nonionic polymers have been used to precipitate proteins, including dextran, poly(vinyl pyrrolidone), poly(propylene glycol), and poly(ethylene glycol) (PEG). Of these polymers, by far the most extensively studied is PEG. Several guidelines have been developed for the use of PEG as a protein precipitant. Solutions of PEG up to 20 percent w/v can be used without viscosity becoming a problem. PEGs with molecular weights above 4000 have been found to be the most effective (Scopes, *Protein Purification*, Springer-Verlag, 1982, p. 59). Protein destabilization in PEG solutions does not occur until the temperature is significantly higher than room temperature (>40 C) [Rothstein, in Harrison (ed.), *Protein Purification Process Engineering*, Dekker, New York, 1994, p. 115].

Design of Precipitation Systems Once a precipitating agent has been chosen for the protein of interest, it may be necessary to design a large-scale precipitation process. The safest procedure is to base the design on a laboratory or pilot plant system that has given acceptable results. Important considerations in obtaining the best possible plant design are the following: the type of precipitation reactor, processing conditions (flow rates, concentrations, etc.), and assumptions used to scale up to the plant scale. There are three basic types of precipitation reactor: the batch reactor, the continuous stirred-tank reactor (CSTR), and the tubular reactor. These types are discussed and compared.

The batch reactor is the simplest of the three types and is often the one that is tried first at small scale. Batch precipitation is carried out by slowly adding the precipitating agent to a protein solution that is being mixed. Addition of the precipitating agent continues until the desired level of supersaturation is reached with respect to the protein being precipitated. At this point nucleation begins, and precipitation proceeds through the steps of particle growth and aggregation. Mixing continues until the precipitation is complete. The mixing in a batch reactor is generally turbulent. Protein particles precipitated in a batch reactor tend to be more compact and regular in shape than those precipitated in a tubular reactor, apparently because of the different shear profiles existing in the two reactors and the length of time the particles are exposed to this shear [Bell and Dunnill, *Biotechnol. Bioeng.* **24:** 2319 (1982)]. The shear field in a tubular reactor is essentially homogeneous; by contrast, in the batch reactor the precipitate particles are exposed to a very wide range of shears and to much longer times of exposure than in the tubular reactor, resulting in improved precipitate mechanical stability.

In a tubular reactor, precipitation takes place in volume elements that approach plug flow as they move through the tube. Thus, the distance–particle size distribution history of the particles in a volume element moving through a tubular reactor is comparable to the time–particle size distribution history of a stationary volume element in a batch reactor. In the tubular reactor, the feed protein solution and the precipitating agent are contacted in a zone of efficient mixing at the reactor inlet. Good mixing can be accomplished, for example, by flowing the protein solution through a convergent nozzle to a biplanar grid and then introducing the precipitating agent just downstream of the biplanar grid [Virkar et al., *Biotechnol. Bioeng.* **24:** 871 (1982)]. The flow pattern in the reactor can be turbulent, a property that can be promoted by wire meshes at intervals along the reactor. In comparison to either the batch reactor or the CSTR, the tubular reactor has the advantages of short fluid residence times, an absence of moving mechanical parts, uniformity of flow conditions throughout the reactor, a simple and inexpensive design, and a relatively small holdup of fluid. For particles that grow relatively slowly, however, the length of the tubular reactor can be excessive.

In the CSTR, fresh protein feed contacts a mixed slurry containing precipitate aggregates. The mixing conditions in a CSTR are similar to those in a batch reactor. Upon entering the CSTR, fresh protein feed nucleates, the nucleate particles grow by diffusion, and the submicrometer-size “primary” particles collide with and adhere to growing aggregates. The degree of supersaturation can be more easily controlled than in the batch or tubular reactor, which means that the formation of precipitates with undesirable properties is less likely.

A few general statements can be made regarding the processing conditions in precipitation systems. flows are normally turbulent; flow must be high enough to avoid inadequate mixing and high supersaturation but low enough to avoid excessive particle breakage, leading to particles that are smaller than desirable. For both the batch and tubular reactors, the flow regime can be changed from turbulent to laminar during the particle growth phase to avoid excessive particle breakage. The rate of addition of precipitant is especially important. This rate should be kept low enough to avoid high supersaturations that lead to colloidal, highly solvated precipitates. The concentration of the precipitant being added is also important, with lower concentrations leading to lower supersaturations [Rothstein, in Harrison (ed.), *Protein Purification Process Engineering*, Dekker, New York, 1994, p. 115].

The key parameter for scale-up of precipitation is mixing. One recommended approach to scale up mixing is to first consider using geometric similarity and constant power per unit volume (*P/V*) (Oldshue, *fluid Mixing Technology*, McGraw-Hill, New York, 1983, p. 198). For geometric similarity, all important dimensions are similar and have a common constant ratio. As seen in Fig. 20-52, this method gave reasonable agreement for the d_{90} particle size (the particle size for which all particles that are larger account for 90 wt% of the total; d_{90} is also referred to as *D10* in describing particle size distributions) as a function of *P/V* for the batch isoelectric precipitation of soy protein for vessels ranging in size from 0.27 to 200 L. If the precipitate is susceptible to shear breakage, however, the assumption of constant *P/V* for scale-up may not be satisfactory. The impeller tip speed, which determines the maximum shear rate, rises when *P/V* is held constant upon scale-up of the reactor volume, as seen in Table 20-24. These results assume turbulent flow, where the power number is constant, so that

Figure 20-52 The relationship between aggregate size and power per unit volume for the preparation of isoelectric soy protein precipitate in batch-stirred tanks: d_{90} is the particle size for which all particles that are larger account for 90 wt% of the total. Protein concentration is 30 kg m^{-3}. Vessel volumes: △, 0.27 L; ○, 0.67 L; ⊓, 200 L. [Data from Bell et al.,Adv. Biochem. Eng. ***26:*** *40, Springer-Verlag, 1983, p. 40.]*

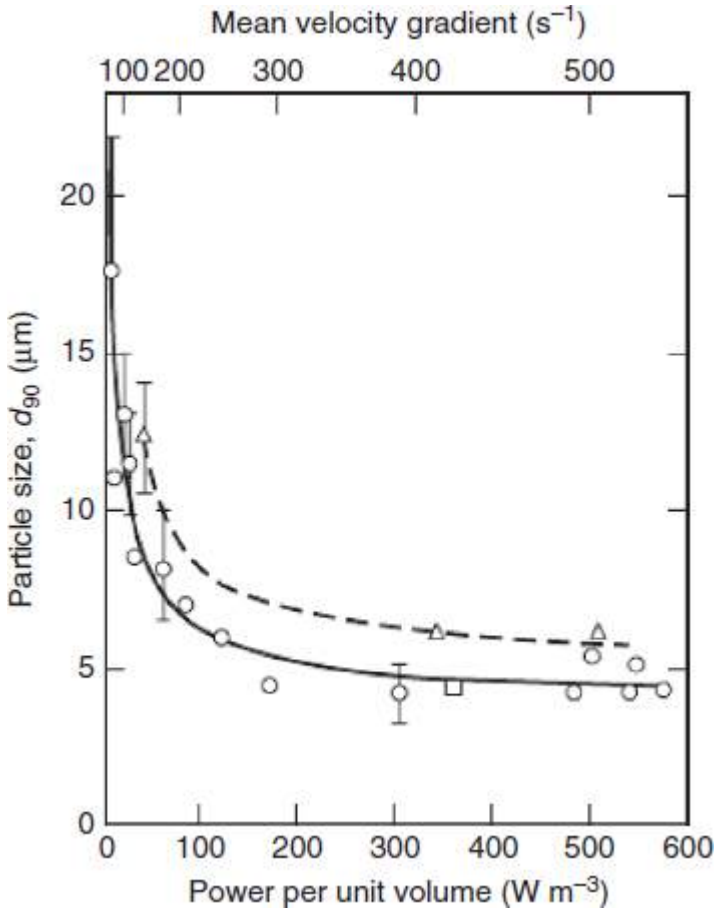

Table 20-24 Scale-Up of Turbulent Agitation, Assuming Constant *P/V*

Volume scale-up factor	$\frac{(\text{Tip speed})_{large}}{(\text{Tip speed})_{small}}$
10	1.3
100	1.7
1000	2.2
10,000	2.8

Reproduced from *Bioseparations Science and Engineering*, 2d ed., by Roger G. Harrison, Paul W. Todd, Scott R. Rudge, and Demetri P. Petrides (2015). By Permission of Oxford University Press.

$$P \propto N_i^3 d_i^5$$

(20-81)

Here, N_i is the impeller rotation rate, and d_i is the impeller diameter. It is also assumed that the maximum shear rate is proportional to the impeller tip velocity (= $\pi N_i d_i$) and that the volume is proportional to d_i^3. From Table 20-24 we see that even for a volume scale-up of 10,000 for constant *P/V*, the tip speed increases by less than a factor of 3. A volumetric scale-up factor of 10,000 is typical in scaling up from the lab to the plant.

20.3.5. LIQUID CHROMATOGRAPHY AND ADSORPTION

As discussed in the introduction, adsorption is typically used for the removal of insolubles such as cells or cell debris as well as for the initial isolation of the product, while chromatography is often used for the final purification steps. Different types of chromatography are used to achieve the high purity required, as is the case for bioproducts such as monoclonal antibodies (see the subsection Bioprocess Design and Economics for a discussion of the purification of monoclonal antibodies). Detailed information about the theory and equipment for liquid chromatography and adsorption can be found in Sec. 16. In the current section, chromatography and adsorption topics are discussed that have particular relevance to bioproducts: (1) adsorbents that are commonly used to purify biomolecules; (2) the length of unused bed (LUB) method for scaling up adsorption of biomolecules that obey the Langmuir isotherm, which has often been used to correlate equilibrium adsorption data for proteins; (3) agitated-bed adsorption for processing cell suspensions in which it is desired to selectively remove a bioproduct that has been secreted by the cells; (4) membrane chromatography, which has applications for macromolecules such as proteins and DNA; and (5) the scale-up of the chromatography of proteins.

Adsorbents for Purification of Bioproducts Many adsorbent resins have been developed for adsorptive and chromatographic separation of bioproducts. There are two basic resin materials: polymer and silica. Many types of ligand chemistries can be conjugated to either resin material. Typically, however, silica resins most commonly have hydrophobic coatings and are used for reversed-phase chromatography. Polymer resins are more often used in aqueous applications and are conjugated with ion exchange, hydrophobic interaction, or affinity-type ligands. More detailed information about polymer and silica adsorbents can be found in the subsection Adsorbents and Ion Exchangers in Sec. 16.

Surface area and particle size are very important properties of adsorbent resins. The resin provides the surface area for the adsorption, which is generally 100 to 1500 m^2/g. The surface area on the outer surface of a 10-μm-diameter solid sphere is 1.7 m^2/g, so it follows that most of the surface area is in the internal porosity of the particle. Since this surface area is accessed by molecular diffusion (one class of resins, called *perfusion resins*, allows convection through some macropores), the path length for this diffusion is important. This path length is the radius of the resin particle. Therefore, both the diameter of the particle and its internal surface area are important for the resin performance. Resins have large ranges of surface areas and particle sizes, and they do not necessarily co-vary.

The various adsorbents used for adsorption and chromatography of biomolecules are discussed below based on the type of operation that is carried out.

Ion Exchange Adsorption and Chromatography A comprehensive discussion of ion exchange adsorbents is given in the subsection Adsorbents and Ion Exchangers in Sec. 16.

Reversed-Phase Chromatography Reversed-phase chromatography employs a hydrophobic phase bonded to the surface of the resin. Typically, reversed-phase resins are silica based. Reversed phase is so named because the partitioning of solutes between the mobile phase and stationary phase is opposite to that observed with bare silica. In other words, hydrophobic solutes bind in higher proportions in reversed phase, while hydrophilic solutes bind in higher proportion in “normal phase.” Solutes are typically introduced into reversed-phase columns in water, or with minimal amounts of organic solvent, so that most solutes partition to the stationary phase. The organic content of the mobile phase is slowly increased, typically as a percent of acetonitrile, methanol, or isopropanol, thereby decreasing the polarity of the mobile phase.

Hydrophobic phases that are bonded to silica are typically aliphatic octyl (C_8), octyldecyl (C_{18}), phenyl (C_6 aromatic), and methyl (C_1). The different chain lengths and densities (called *coverage* in the commercial literature) of the different bonded phases obviously lead to more or less hydrophobicity. The entire surface of the silica cannot be fully covered with a monolayer of the desired phase, however, because of steric effects. Bare silica remains exposed, and this bare silica can participate in the separation by interacting with hydrophilic molecules, or hydrophilic domains of large molecules, thereby altering the binding. The strategy employed for covering this exposed silica surface depends almost as much on the specifics of the separation achieved as it does on the chain length of the bonded phase. Polymerized phases represent an attempt to cover the surface by polymerizing the alkyl chains together at their point of attachment to the silica. End-capped resins use a short chain length group, such as methyl or ethyl, to cover the unreacted surface sites. Resins that do not utilize either method are left so intentionally to take advantage of the "mixed-mode" separation that may result. The separation characteristics of these resins are difficult to reproduce precisely, leading to considerable variation in separation between different manufacturers' resins, and within one manufacturer's resin from one lot of material to another.

Ions do not partition well in hydrophobic phases. It is common, therefore, to choose a counterion for reversed-phase chromatography. For biological mixtures, the counterion is nearly always a strong acid anion, such as trifluoroacetate, acetate, or chloride. The counterion has a strong effect on the separation, by partitioning along with the co-ion of interest. The counterion can be used to make solutes more or less hydrophobic and will not affect all solutes equally.

Hydrophobic Interaction Chromatography Hydrophobic interaction chromatography is often used for protein separations. It employs derivatized polymer resins, with phenyl, butyl, or octyl ligand groups, typically. Proteins adhere to the hydrophobic surface under high-salt conditions and redissolve into the mobile phase as the salt concentration is reduced. Hydrophobic interaction chromatography differs from reversed-phase in that the mobile phase is kept aqueous (polar), and the salt concentration is used to effect the partitioning to the surface. The mechanism of partition is related to precipitation as opposed to two-phase partitioning (reversed-phase) or ionic interaction (ion exchange). This is due to the use of salts that strip proteins of their solvation water. As the concentration of "lyophilic" salts increases, the probability increases that the protein will aggregate, or nucleate on the surface of the resin [Roettger et al., *Biotechnol. Prog*. **5:** 79 (1989)]. Hydrophobic interaction chromatography is sensitive to pH, salt used, buffer type, and temperature. Each of these must be carefully controlled to achieve reproducible separation but also to represent an opportunity for increased selectivity.

Affinity Chromatography and Adsorption Affinity chromatography and adsorption take advantage of biological interactions to effect binding of specific solutes. Antibodies, antigens, or dyes are conjugated to polymer resins for the purpose of binding specific solutes from a mixture. For instance, an antibody could be raised against a target protein. The antibody would be conjugated to a resin, usually via cyanogen bromide activation. The antibody then captures the solute out of the mixture, and the impurities flow through the column. The solute can be recovered by changing the pH, increasing the salt concentration, or adding a displacer, that is, a molecule that also has some affinity for the antibody, or other binding agent (affinity ligand) on the stationary phase.

Other examples of specific interactions that can be used to isolate proteins are enzyme–ligand, enzyme–cofactor, and receptor–agonist (antagonist). In each case, one member of any of these pairs may be immobilized to a resin to isolate the desired partner. Affinity chromatography is often coupled with cloning techniques to synthesize the target molecule with an "epitope" or recognition sequence that can be captured by the affinity ligand. Affinity chromatography is used from small-scale research (e.g., high-throughput screening) to large-scale purification.

An example of a type of affinity chromatography that has had a major impact on the purification of monoclonal antibodies is the use of immobilized protein A in process scale purification [Vunnum, in U. Gottschalk (ed.), *Process Scale Purification of Antibodies*, Wiley, Hoboken, N.J., 2009, p. 79]. Protein A is often used as the first chromatography step in the purification, which gives a large purification factor and results in simplifying the purification process. Protein A has affinity for the constant region of Ig-G antibodies, so it is generally applicable to the capture and purification of most monoclonal antibodies. It is a polypeptide with a molecular mass of 54 kDa that is found in the cell wall of *Staphylococcus aureus.* Recombinant protein A that lacks the membrane-binding region is used in affinity purification.

One of the drawbacks of the protein A and other affinity methods is that low levels of the affinity ligand or its fragments can co-elute with the target molecule. In particular, when an affinity step is used as the first step in the purification process, it is exposed to significant levels of extracellular proteases that liberate fragments of the ligand into the column effluent. However, trace amounts of affinity ligands and others such as high-molecular-weight aggregates of the antibody and host cell protein can be removed in one or two subsequent chromatography steps. More information about the process scale purification of monoclonal antibodies using protein A is found in the Bioprocess Design and Economics subsection.

Immobilized Metal Affinity Chromatography Some proteins have high affinities for specific metals. This affinity may be either structural, as in the case of metalloproteins, which require metal centers for their biological activity, or based on the content of specific amino acid residues, such as histidine, tryptophan, and cysteine, which have increased affinity for transition metals such as nickel and copper. Techniques have been developed to immobilize metal ions with spacer arms onto polymer resins. These resins are referred to as IMAC resins, and they are used to purify proteins that have one of the two characteristics mentioned above. Genetic engineering has also been used to enable IMAC to be performed, with cloned target biomolecules being fused to polyhistidine tags [Arnold, *Bio/Technology* **9:** 152 (1991)].

Size Exclusion Chromatography Sometimes referred to as *gel filtration*, size exclusion chromatography (SEC) separates solutes on the basis of their size. There is no derivatization of the polymer gel, and there is no binding between the solutes and the resin. Molecules larger than the largest pores in the gel (the exclusion limit) cannot enter the gel and are eluted first. Smaller molecules enter the gel to varying extents, depending on their size and shape, and thus are retarded on their passage through the bed. In general, SEC resins are hydrophilic polymer gels with a broad distribution of pore sizes. The pore size is dependent on the degree of polymerization of the gel. Size exclusion chromatography is a useful technique, especially for changing buffers or for removing small molecules from protein solutions. Because of the lack of binding between the solute and the resin, however, the capacity of this technique is low. Size exclusion effects may be in action in all the above-described techniques, since all resins are macroporous.

Agitated-Bed Adsorption Agitated-bed adsorption processes have been developed to allow removal of a product secreted by the cells without first having to remove the cells. In this type of process, cell culture broth is passed through a series of agitated columns containing an adsorbent, as shown in Fig. 20-53. Each column has screens at the inlet and outlet that are designed to retain the adsorbent within the column but allow the broth to pass through. When the concentration of the product in the effluent of the last column in the series reaches a certain value, the flow is stopped, and the lead column is taken out of the train. Periodic countercurrent operation is obtained by advancing each of the remaining columns in the train, placing a regenerated column of adsorbent in the last position, and restarting the feed flow. The lead column taken out of the train is washed with the adsorbent agitated to remove the broth solids, and the product is eluted from the adsorbent, usually in the fixed-bed mode.

This process has advantages over filtration, in that there is no filter aid to dispose of and it is not necessary to wash a filter cake containing the cells, so losses of the product are often less. The equipment for this process is less expensive and easier to maintain than that used for centrifugation. The disadvantage is that expensive solid adsorbents are more easily fouled by the dirtier feed stream and so require harsher or more expensive regeneration procedures and more frequent replacement compared to adsorbents utilized with streams with fewer impurities. Also, resin attrition can be an issue.

A useful mathematical model for this process has been developed [Belter et al.,*Biotechnol. Bioeng.* **15:** 533 (1973)]. The continuity equation for the *n*th column in the train can be written for separand*i* as

Rate of separand in − rate of separand out = rate of accumulation of separand

$$Qc_{i,n-1} - Qc_{i,n} = V_L \frac{dc_{i,n}}{dt} + V_R \frac{dq_{i,n}}{dt}$$

(20-82)

where Q = volumetric flow rate

$c_{i,n-1}$, $c_{i,n}$ =

separand concentration in feed to and effluent from column n, respectively

V_L = liquid volume in column

V_R = volume of adsorbent in column

$q_{i,n}$ = separand concentration in adsorbent phase of column n averaged over an adsorbent particle

t = time

The rate of mass transfer of separand to the adsorbent phase is described by a linear driving force expression

$$\frac{dq_{i,n}}{dt} = K_a(c_{i,n} - c^*_{i,n})$$

(20-83)

where $c^*_{i,n}$ is the separand concentration in the bulk liquid when it is at equilibrium with $q_{i,n}$, and K_a is an overall mass-transfer coefficient that can be correlated to experimental data as

$$K_a = Ae^{-B(q_i/q_{i,\text{sat}})} + De^{-E(q_i/q_{i,\text{sat}})}$$

(20-84)

Here A, B, D, and E are constants, and $q_{i,\text{sat}}$ is the adsorbent phase concentration which is in equilibrium with the separand concentration c_{i0} in the feed to the train of mixed columns. In the use of this model for the recovery of an antibiotic, equilibrium was modeled by the Freundlich isotherm written in the form

$$c^*_{i,n} = bq^a_{i,n}$$

(20-85)

where a and b are constants.

Equations (20-82) to (20-85) constitute a set of mathematical relationships that govern the performance of each column in the train. These simultaneous equations can be solved by the Runge-Kutta numerical method to predict the effluent and adsorbent concentrations as a function of time. Excellent agreement between predicted and experimental adsorption data for the recovery of the antibiotic novobiocin in a three-stage train has been obtained using this method (Belter et al., *Bioseparations*, Wiley, Hoboken, N.J., 1988, p. 63).

The scale-up of a series of agitated columns containing adsorbent (Fig. 20-53), operated in the periodic countercurrent mode, follows directly from the mathematical model presented for this process [Eqs. (20-82) to (20-85)] (Belter et al., *Bioseparations*, Wiley, Hoboken, N.J., 1988, p. 63). Besides the increases in the flow rate and volume that occur upon scale-up, the mixing patterns may also change (Harrison et al., *Bioseparations Science and Engineering*, Oxford University Press, Oxford, UK, 2015, p. 305).

Figure 20-53 Train of agitated-bed adsorption columns for the processing of cell culture broth. [Reproduced from Bioseparations Science and Engineering, 2d ed., by Roger G. Harrison, Paul W. Todd, Scott R. Rudge, and Demetri P. Petrides (2015). By Permission of Oxford University Press.]

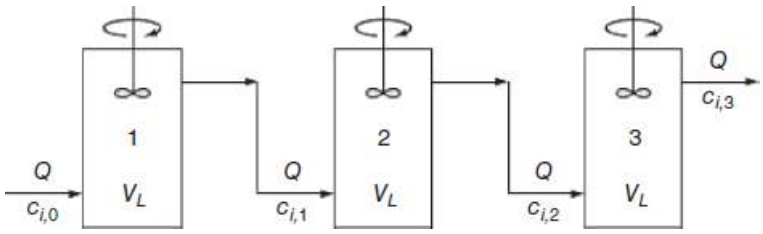

Length of Unused Bed (LUB) Method for Scale-Up of Fixed-Bed Adsorption This method allows scale-up of fixed-bed adsorption based on data from laboratory columns, keeping the particle size and superficial velocity constant (Thomas and Crittenden, Adsorption Technology and Design, Butterworth-Heinemann, Waltham, Mass., 1998, p. 165). In discussing the LUB method of scale-up, it is necessary to define the break-point time t_b and the ideal adsorption time t^* on a breakthrough curve, which are indicated in Fig. 20-54. The break-point time is usually taken at the relative concentration c_i/c_{i0} = 0.05 or 0.10, where c_{i0} is the feed concentration (McCabe et al., *Unit Operations of Chemical Engineering*, McGraw-Hill, New York, 1993, p. 819). Since only the fluid last exiting the column has this concentration, the average fraction of the solute removed from the start of feeding to the break-point time is usually 0.99 or higher. The ideal adsorption time is the time for breakthrough that would occur if the solute were in perfect equilibrium with the bed of adsorbent, which would give a vertical breakthrough curve. For a symmetrical breakthrough curve, the ideal adsorption time is the time at which c_i/c_{i0} = 0.5. At the ideal adsorption time for a bed initially free of the solute to be adsorbed, based on a unit area of bed cross section,

Figure 20-54 Breakthrough curve for a fixed-bed adsorber, showing the break-point time t_b, chosen at 5 percent of the solute feed concentration, and the ideal adsorption time t^*. The ratio of mobile phase concentration of solute to solute concentration in feed to the adsorber is c_i/c_{i0}. [Reproduced from Bioseparations Science and Engineering, 2d ed., by Roger G. Harrison, Paul W. Todd, Scott R. Rudge, and Demetri P. Petrides (2015). By Permission of Oxford University Press.]

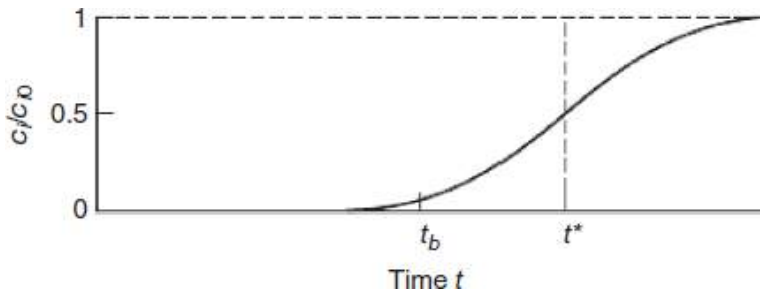

$$vc_{i0}t^* = L\rho_b q_{i,\text{sat}}$$

(20-86)

where L = bed length

$q_{i,\text{sat}}$ = average adsorbent phase concentration of solute i in equilibrium with feed concentration c_{i0}, based on the adsorbent weight (weight of solute i per weight of adsorbent)

v = superficial, or linear, velocity (flow rate divided by the cross- sectional area)

c_{i0} = concentration of solute i in feed

ρ_b = bulk density of adsorbent

The ideal adsorption time is therefore given by

$$t^* = \frac{L\rho_b q_{i,\text{sat}}}{vc_{i0}}$$

(20-87)

The amount of the solute adsorbed at the break point can be determined by integrating the breakthrough curve up to time t_b, as indicated in Fig. 20-55. The width of the breakthrough curve defines the width of the *mass-transfer zone* in the bed.

Figure 20-55 Integration of the breakthrough curve for a fixed-bed adsorber. The area of integration to the left of a vertical line at time t is proportional to the amount of solute adsorbed up to that time. The ratio of mobile phase concentration of solute to solute concentration in feed to the adsorber is c_i/c_{i0}. [Reproduced from Bioseparations Science and Engineering, 2d ed., by Roger G. Harrison, Paul W. Todd, Scott R. Rudge, and Demetri P. Petrides (2015). By Permission of Oxford University Press.]

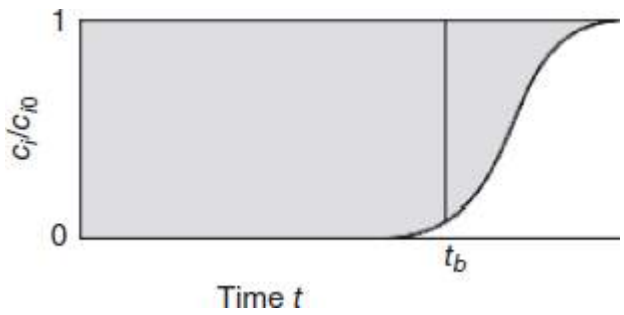

For adsorption where the equilibrium isotherm is favorable, which is true for the Langmuir isotherm that can often be used for protein adsorption, the concentration profile in the mass-transfer zone takes on a characteristic shape that does not change as the zone propagates through the bed [Ruthven, in Kroschwitz (ed.), *Kirk-Othmer Encyclopedia of Chemical Technology*, vol. 1, 4th ed., Wiley-Interscience, Hoboken, N.J., 1991, p. 493]. At the break-point time, the adsorbent between the inlet of the bed and the beginning of the mass-transfer zone is completely saturated (in equilibrium with the solute in the feed). The adsorbent in the mass-transfer zone goes from being completely saturated to being almost free of solute, and the adsorbent could be assumed to be on the average about half-saturated. This would be equivalent to half the adsorbent in the mass-transfer zone being saturated and the other half being unused. The scale-up principle is that the length of the unused bed in the mass-transfer zone does not change as the bed length is changed [Collins, *AIChE Symp.* **74**(63): 31 (1967)].

The length of unused bed (LUB) can be determined directly from the breakthrough curve obtained experimentally. If $q_{i,b}$ is the average adsorbent phase concentration of solute *i* at the break-point time, then the fraction of bed capacity utilized at the break-point time is $q_{i,b}/q_{i,\text{sat}}$. Therefore, the unused fraction of the bed is $1 - q_{i,b}/q_{i,\text{sat}}$. From Eq. (20-86),

$$\frac{q_{i,b}}{q_{i,\text{sat}}} = \frac{t_b}{t^*}$$

(20-88)

so that LUB can be written as

$$\text{LUB} = \left(1 - \frac{q_{i,t_b}}{q_{i,\text{sat}}}\right) L = \left(1 - \frac{t_b}{t^*}\right) L$$

(20-89)

where t_b and t^* are stoichiometric times determined by integration of the breakthrough curve:

$$t^* = \int_0^\infty \left(1 - \frac{c_i}{c_{i0}}\right) dt$$

(20-90)

$$t_b = \int_0^{t_b} \left(1 - \frac{c_i}{c_{i0}}\right) dt$$

(20-91)

In scale-up calculations, the length of column required can easily be found by adding the LUB to the length calculated by assuming local equilibrium, with a shock wave concentration front [Ruthven, in Kroschwitz (ed.), *Kirk-Othmer Encyclopedia of Chemical Technology*, vol. 1, 4th ed., Wiley-Interscience, Hoboken, N.J., 1991, p. 493].

Example

Example 20-8 Scale-Up of the Fixed-Bed Adsorption of a Pharmaceutical Product

The breakthrough data given in the table below were obtained for the adsorption of a pharmaceutical product in a laboratory column (5-cm diameter × 15-cm high) at a feed flow rate of 400 mL/h and feed concentration of 0.75 U/L, where U is units of biological activity of the pharmaceutical product. It is desired to scale up the process to operate in a column 30 cm high. What break-point time can be expected in the 30-cm-high column?

t (h)	c_i (U/L)
20.5	0.01
26.7	0.20
32.0	0.39
36.0	0.53

We use the LUB method, which involves graphical integrations of the breakthrough curve to determine the amount of solute adsorbed at various times. The breakthrough curve with concentration in dimensionless form is therefore plotted, with the curve extended to c_i/c_{i0} = 1.0, assuming that the curve is symmetric about c_i/c_{i0} = 0.5 (Fig. 20-56). By doing graphical integrations of this curve, we find the following:

Figure 20-56 Breakthrough curve for the fixed-bed adsorption of a pharmaceutical product in Example 20-8. [Reproduced from Bioseparations Science and Engineering, 2d ed., by Roger G. Harrison, Paul W. Todd, Scott R. Rudge, and Demetri P. Petrides (2015). By Permission of Oxford University Press.]

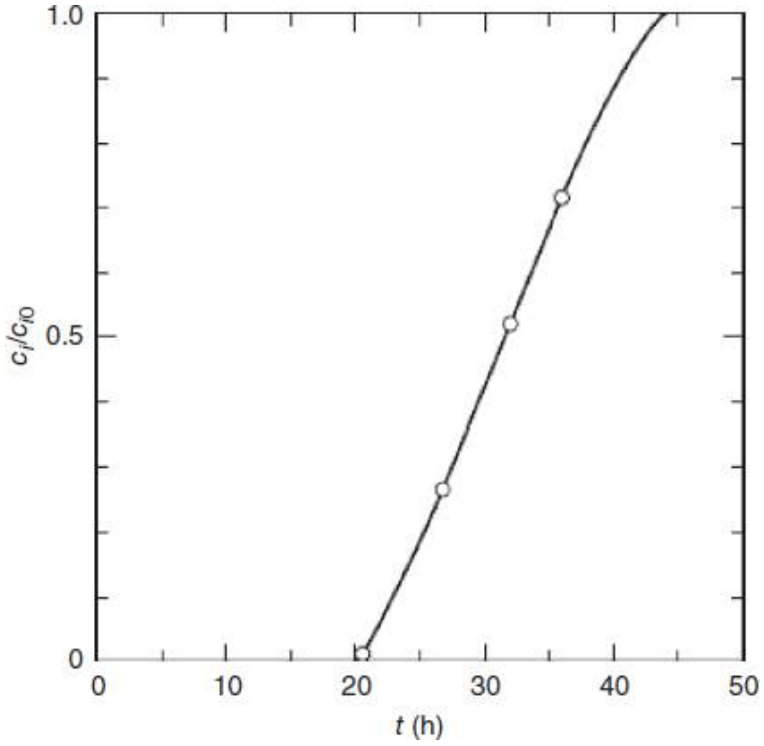

Total solute adsorbed at saturation (c_i/c_{i0} = 1.00)

$$= Qc_{i0}\int_0^{44.0} \left(1 - \frac{c_i}{c_{i0}}\right) dt = Qc_{i0}(31.5\,\text{h})$$

Total solute adsorbed at break point (c_i/c_{i0} = 0.05)

$$= Qc_{i0}\int_0^{21.5} \left(1 - \frac{c_i}{c_{i0}}\right) dt = Qc_{i0}(21.2\,\text{h})$$

where Q is the volumetric flow rate. Thus, t^* and t_b are 31.5 and 21.2 h, respectively, for this column. From Eq. (20-89)

$$\frac{\text{LUB}}{L} = 1 - \frac{Qc_{i0}(21.2\,\text{h})}{Qc_{i0}(31.5\,\text{h})} = 1 - 0.673 = 0.327$$
$$\text{LUB} = 0.327(15\text{ cm}) = 4.90\text{ cm}$$

The adsorbent loading at saturation per total bed volume is

$$\rho_b q_{i,\text{sat}} = \frac{400\frac{\text{cm}^3}{\text{h}} \times 0.00075\frac{\text{U}}{\text{cm}^3} \times 31.5\,\text{h}}{\frac{3.14 \times 5^2\text{cm}^2 \times 15\,\text{cm}}{4}} = 0.0321\frac{\text{U}}{\text{cm}^3}$$

For the column 30 cm high, the LUB does not change, so that

$$\frac{\text{LUB}}{L} = \frac{4.90}{30} = 0.163$$

The superficial velocity stays the same and is

$$v = \frac{400\frac{cm^3}{h}}{\frac{3.14 \times 5^2 cm^2}{4}} = 20.4\frac{cm}{h}$$

From Eq. (20-87),

$$t^* = \frac{L\rho_b q_{i,\text{sat}}}{vc_{i0}} = \frac{30\,\text{cm} \times 32.1\frac{\text{U}}{\text{L}}}{20.4\frac{\text{cm}}{\text{h}} \times 0.75\frac{\text{U}}{\text{L}}} = 62.9\,\text{h}$$

Therefore, from Eq. (20-89),

$$t_b = t * \left(1 - \frac{\text{LUB}}{L}\right) = (62.9\,\text{h})(1 - 0.163) = 52.6\,\text{h}$$

Membrane Chromatography The use of filters and membranes to adsorb substances from a process stream has a long history. Indeed, the classic elementary school experiment, in which India ink is separated into a rainbow of colors as it ascends a wetted strip of filter paper, is a form of membrane chromatography, in which the pigment chemicals have differential binding affinities for the cellulose fibers that form the filter material. However, the use of membranes in chromatography received renewed interest with the development of microporous adsorptive membranes, in which the surfaces of the pores are chemically derivatized with an interactive ligand. Membrane chromatography was first performed in 1988 by [Brandt et al., *Bio/Technology* **6:** 779 (1988)] using hollow fiber membranes functionalized with either the protein gelatin for isolating fibronectin from human plasma or protein A for purifying an IgG antibody. Compared to the equivalent chromatography column packed with 100-μm adsorbent particles, the membrane chromatography column volume and fluid residence time were less by more than 3 orders of magnitude.

The major difference between membrane and packed-bed chromatography is that in membrane chromatography the transport of solutes to their binding sites takes place predominantly by convection through the pores (rather than by diffusion in the stagnant fluid inside the adsorbent particles for packed-bed chromatography), thereby reducing both process time and liquid volume. Much higher flow rates can be used in membrane chromatography than in packed beds, and the binding efficiency is relatively independent of the feed flow rate over a wide range [Ghosh, *J. Chromatogr. A* **952:** 13 (2002)]. Although they have a shorter flow path, membrane chromatography systems have generally been found to achieve resolutions comparable to those with packed beds of adsorbent [Yamamoto and Sano, *J. Chromatogr.* **597:** 173 (1992); Gerstner et al., *J. Chromatogr.* **596:** 173 (1992)]. However, membrane chromatography systems typically are used for adsorption of contaminants in a process stream, such as DNA or endotoxin, or low levels of host cell proteins, rather than for the binding and elution of a product molecule and its closely related variants, such as those caused by oxidation or amino acid misincorporation. For example, in an antibody purification process, a final step may be the reduction of DNA, endotoxin, and certain host cell proteins. In this case, the monoclonal antibody need not bind to the chromatography media (resin or membrane); therefore, a pH may be chosen where the antibody does not bind, while the contaminants do. This is called the *flow-through mode,* or *frontal chromatography.*

Another application where membrane chromatography is particularly suitable is in the purification of large proteins (molecular weight > 250,000) [Ghosh, *J. Chromatogr. A* **952:** 13 (2002)]. Proteins this large diffuse slowly into the pores of chromatography adsorbent media, but this is not a limitation in membrane chromatography since diffusion paths are very short.

In membrane chromatography, there is dispersion in the system due to the flow found in open pores, and the diffusion of molecules in the radial direction across the parabolic flow profile and also in the axial direction. There is some dispersion due to the kinetics of adsorption and desorption, which are a feature of conventional chromatography as well. Finally, there is dispersion due to mixing volumes upstream and downstream of the membrane for flow distribution.

Membranes for chromatography have been fabricated and are commercially available as thin sheets, flat disks, hollow fibers, and monolithic rods, disks, and tubes [Avramescu et al., in A. Pabby et al. (eds.), *Handbook of Membrane Separations*, CRC Press, Boca Raton, fla., 2009, p. 25]. Hollow fibers are usually bundled within a shell using potting material. For large-scale production, thin membrane sheets are usually stacked or spiral-wound. Various configurations of membrane systems are illustrated in Fig. 20-57. The volumetric binding capacities are lower than in conventional chromatography, and the depths are not typically high.

Figure 20-57 Various configurations used in membrane chromatography systems. The arrows represent the direction of flow, and the membrane cross-sectional area is shaded in gray. [Reproduced from Bioseparations Science and Engineering, 2d ed., by Roger G. Harrison, Paul W. Todd, Scott R. Rudge, and Demetri P. Petrides (2015). By Permission of Oxford University Press.]

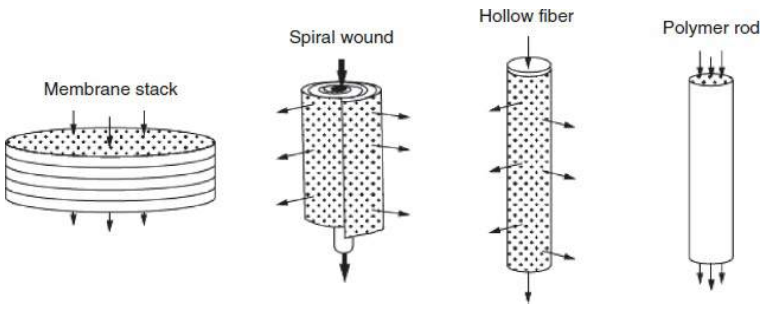

The case typically made for membrane chromatography is that the disposable nature of the filters and the large volumes of water required to operate a fixed column make membrane chromatography a viable alternative to column chromatography for polishing applications for removal of contaminants such as viruses, DNA, and endotoxins [Fraud et al., *BioPharm. Int.* **23:** 44 (2010)]. However, in analyses such as these, the chromatography column is sized at 100 times the size of the membrane; in other words, the chromatography column will be used at 1 percent of its dynamic binding capacity, where the membrane will be used at 100 percent dynamic binding capacity. Furthermore, the dynamic binding capacity of the chromatography resin typically exceeds that of the membrane configuration [70 mg/mL for Sepharose Q-HP (GE Life Sciences Technical Literature, available at www.gelifesciences.com) versus 50 mg/mL for the Sartobind Q (Sartorius technical literature, available at www.sartorius.com), for example]. The actual ligand density in the two formats is approximately 50*mM* for the Sartobind Q versus 140 *mM* for the Sepharose Q-HP. This demonstrates two related points. First, the ligand density achievable in membrane chromatography is much lower (three times in this comparison) because the surface area for adsorption is lower than in resin chromatography. Second, because this internal surface area in resin chromatography is less accessible than for membrane chromatography, the proportion of dynamic binding capacity available to a large molecule such as a protein is much smaller for resin than for membranes.

Another perceived limitation of using membranes as chromatography media is the cleanliness of the feed stream required. For the specific application of stripping extremely low-concentration contaminants from a concentrated antibody solution as the last step (with the cleanest feed stream) in the process, a high solids load could potentially foul the membrane surface and blind pores. Ultimately, only the largest pores will be left open, diffusion path lengths will increase, and flow will deteriorate. This issue is easily overcome by adding a prefilter upstream of the membrane, just as is frequently done for conventional chromatography. The contaminant load on the membrane itself is addressed by sizing the membrane for the anticipated load, again, just as one would with conventional chromatography. For example, in the polishing of antibody solutions using anion exchange, many contaminants, including viruses, nucleic acids, and endotoxins, tend to be negatively charged at neutral pH, while antibodies are positively charged at this pH and flow through without binding [Zhou et al., *BioPharm Int.* **20:** 26 (2007)].

Scale-up of membrane chromatography is typically achieved by increasing the diameter of the filter, conserving the interstitial velocity from scale to scale. However, it is possible to scale up by maintaining the ratio of membrane thickness to interstitial velocity constant [Etzel and Riordan, in Shukla et al. (eds.), *Process Scale Bioseparations for the Biopharmaceutical Industry,* Taylor and Francis, 2007, p. 278], and when this is done, the longer or thicker membranes would have to be able to perform with higher pressure drops and higher velocities than their scaled-down counterparts.

Example

Example 20-9 Comparison of Time for Diffusion Mass Transfer in Conventional Chromatography and Membrane Chromatography

Estimate the time for diffusion mass transfer in conventional chromatography and in membrane chromatography. Assume a typical particle diameter for an adsorbent used in preparative chromatography of 100 μm, pore diffusion coefficient $\mathscr{D}_p$ of 3×10^{-7} cm^2 s^{-1} of a representative protein bovine hemoglobin in size exclusion media at 20 C [Athalye,*J. Chromatog.* **589:** 71 (1992)], superficial velocity of 600 cm/h in the pores in membrane chromatography possible in membrane chromatography with no compromise in efficiency [Zhou et al., *BioPharm Int*. **20:** 26 (2007)], void fraction of 0.6 for the membranes, and a membrane pore size of 1 μm. Assume the fluid has the properties of water.

The time required for diffusion can be calculated using Einstein's diffusion equation

$$t = \frac{\delta^2}{2\mathscr{D}_p}$$

For conventional chromatography, the diffusion length is 50 μm (one-half the particle diameter). The type of convective flow regime in the pores in membrane chromatography can be determined by calculating the Reynolds number in a cylindrical pore:

$$\mathrm{Re} = \frac{d_m \left(\frac{v}{\varepsilon}\right) \rho}{\mu} = \frac{1\ \mu\mathrm{m} \times \frac{600\frac{\mathrm{cm}}{\mathrm{h}}}{0.6} \times 1.0\frac{\mathrm{g}}{\mathrm{cm}^3} \times \frac{1\ \mathrm{cm}}{10^4\ \mu\mathrm{m}} \times \frac{1\ \mathrm{h}}{3600\,\mathrm{s}}}{0.01\frac{\mathrm{g}}{\mathrm{cm}\cdot\mathrm{s}}} = 0.003$$

where d_m is the diameter of a pore in the membrane,v is the fluid superficial velocity, ε is the void fraction, and ρ and μ are the density and viscosity of the fluid, respectively. Thus, this is laminar, creeping flow since Re is less than 0.1, and the velocity in the pore has a parabolic profile. Since the protein is being adsorbed on the surface of the pore, there will be a radial concentration gradient from the surface to the center of the pore, and the maximum diffusion length will therefore be 0.5 μm (one-half the pore diameter).

Therefore, for the conventional chromatography the diffusion time from the Einstein diffusion equation is

$$t = \frac{(50\ \mu\mathrm{m})^2 \times \left(\frac{1\ \mathrm{cm}}{10^4\ \mu\mathrm{m}}\right)^2}{2 \times 3.0 \times 10^{-7}\frac{\mathrm{cm}^2}{\mathrm{s}}} = 42\ \mathrm{s}$$

For membrane chromatography, assuming the diffusion coefficient in the pores of the membrane is the same as in pores of the conventional chromatography adsorbent,

$$t = \frac{(0.5\ \mu\mathrm{m})^2 \times \left(\frac{1\,\mathrm{cm}}{10^4\ \mu\mathrm{m}}\right)^2}{2 \times 3.0 \times 10^{-7}\frac{\mathrm{cm}^2}{\mathrm{s}}} = 0.004\ \mathrm{s}$$

These calculations show that the diffusion time is four orders of magnitude less for membrane chromatography compared to conventional chromatography. A similar result was obtained by Klein (*Affinity Membranes*, Wiley, Hoboken, N.J., 1991, p. 135) for the diffusion time of IgG antibody in membrane chromatography with hollow fibers compared to a fast-flow gel matrix, both using immobilized protein A.

In summary, membrane chromatography is a technology that is growing in importance in bioseparation science. There is a place for low-capacity, high-throughput adsorption media for the stripping of low-level contaminants from a process stream. The membranes are available with virtually all the same chemistries as conventional chromatography. They can be made inexpensively and fit well with disposable technologies currently in favor in the industry.

Scale-Up of the Chromatography of Proteins Chromatography scale-up algorithms typically account for changes in bed height and diameter, linear and volumetric flow rate, and particle size. A general approach to scale-up is based on keeping the resolution constant. Yamamoto et al. [*J. Chromatog.* **409:** 101 (1987); *Ion-Exchange Chromatography of Proteins*, Dekker, 1988, p. 263] have developed the following proportionality for resolution R_s of proteins in linear gradient elution ion exchange chromatography and hydrophobic interaction chromatography:

$$R_s \propto \left[\frac{\mathscr{D}_m L}{g(V - V_0) u d_p^2} \right]^{1/2}$$

(20-92)

where $\mathscr{D}_m$ = diffusion coefficient of protein in solution

L = column length

g = slope of gradient (change in concentration of gradient per volume of gradient)

V = column volume

V_0 = column void volume

u = interstitial fluid velocity = superficial velocity$v$/column void fraction ε

d_p = particle diameter

This equation has been found to be valid over a wide range of experimental conditions (Yamamoto et al., ibid.). To remove the volume terms from the expression for resolution, we make the definitions

$$\overline{Q} = \frac{Q}{V} = \frac{\varepsilon u A_c}{V}$$

(20-93)

$$G = Vg$$

(20-94)

where Q is the inlet flow rate, ε is the column void fraction, and$A$ is the column cross-sectional area. These substitutions lead to

$$R_s \propto \left(\frac{\mathscr{D}\varepsilon}{G(1 - \varepsilon)\overline{Q}\, d_p^2} \right)^{1/2}$$

(20-95)

Thus, for scale-up with constant resolution from scale 1 to scale 2 for the same product and the same column void fraction, the scale-up equation is

$$G_1 \overline{Q}_1 d_{p1}^2 = G_2 \overline{Q}_2 d_{p2}^2$$

(20-96)

Thus, as the particle size increases on scale-up, the flow rate relative to the column volume must decrease and/or the gradient slope must decrease to maintain constant resolution, which seems correct intuitively.

In practice, the gradient and the stationary phase size and chemistry are not changed upon scale-up. This is so because it is easy to develop lab-scale processes that use the same resin and same gradient that can be used at the commercial process scale. Therefore, in practice, only the ratio between column volume and flow rate needs to be addressed:

$$\frac{Q_1}{V_1} = \frac{Q_2}{V_2}$$

(20-97)

Scale-up from a well-designed process development or preparatory column is reasonably straightforward. When the bed height can be maintained on scale-up, the mobile phase linear velocity remains the same, and the column is simply scaled by diameter. Scaling from a column 1 cm in diameter to a column having a diameter of 10 cm would constitute a 100-fold increase in scale. This is the most conservative way to scale up a column, but is not a necessary constraint.

Example

Example 20-10 Scale-Up of Protein Chromatography

A column 20 cm long, with an internal diameter of 5 cm, gives sufficient purification to merit scale-up. The column produces 3.2 g of purified protein per cycle, and a cycle takes 6 h, from equilibration through regeneration. To design a throughput of 10 g/h, what are the new column's dimensions if the superficial velocity is held constant and it is assumed that the gradient and particle size are not changed on scale-up?

Equation (20-97) is applicable since the gradient and particle size remain the same. According to this equation, the residence time is the same at small and large scales, and therefore the cycle time is not changed. Thus, the scaled-up column must produce 6 h/cycle ×10 g/h = 60 g/cycle. Since the flow rate is proportional to the throughput of protein,

$$\frac{Q_2}{Q_1} = \frac{60\,\mathrm{g/cycle}}{3.2\,\mathrm{g/cycle}} = 18.75$$

From Eq. (20-97),

$$\frac{Q_1}{A_1 L_1} = \frac{Q_2}{A_2 L_2}$$

which leads to

$$\frac{v_1}{L_1} = \frac{v_2}{L_2}$$

Since the superficial velocity is constant,

$$L_1 = L_2$$

Therefore,

$$\frac{Q_2}{Q_1} = \frac{V_2}{V_1} = \frac{\pi\left(\frac{D_2}{2}\right)^2 L_2}{\pi\left(\frac{D_1}{2}\right)^2 L_1} = \left(\frac{D_2}{D_1}\right)^2 = 18.75$$

where D_1 and D_2 are the column diameters for columns 2 and 1, respectively. Since D_1 = 5.0 cm, we obtain

$$D_2 = (18.75)^{0.5} D_1 = 21.6\,\text{cm}$$

It is not always necessary to scale according to bed diameter. The flow rate may be normalized against the volume of the empty column, to give units of time^{-1}. This normalized flow rate is held constant from one scale to another, as shown in Eq. (20-97). Considerable research and practice indicate that this technique is equally effective and less restrictive compared to holding linear velocity constant. In this case, column bed height may be increased or decreased, depending on the requirements of pressure drop and mechanical seals. A shallower bed gives a lower linear velocity and a wider diameter. A deeper bed gives a higher linear velocity (and higher pressure drop) and a proportionally narrower bed diameter. Therefore, bed height may need to be scaled on the basis of pressure drop constraints.

20.3.6. BIOPROCESS DESIGN AND ECONOMICS

Given a product and a desired annual production rate (process throughput), bioprocess design endeavors to answer the following and other related questions: What are the required amounts of raw materials and utilities needed for a single batch? What is the total amount of resources consumed per year? What is the required size of process equipment and supporting utilities? Can the product be produced in an existing facility, or is a new plant required? What is the total capital investment? What is the manufacturing cost? What is the optimum batch size? How long does a single batch take? How much product can be generated per year? Which process steps or resources constitute scheduling and throughput bottlenecks? What changes can increase throughput? What is the environmental impact of the process (i.e., amount and type of waste materials)? Which design is the “best” among several plausible alternatives?

Definitions and Background Process design is the conceptual work done prior to building, expanding, or retrofitting a process plant. It consists of two main activities, process synthesis and process analysis. *Process synthesis* is the selection and arrangement of a set of unit operations (process steps) capable of producing the desired product at an acceptable cost and quality. *Process analysis* is the evaluation and comparison of different process synthesis solutions. In general, a synthesis step is usually followed by an analysis step, and the results of analysis determine the subsequent synthesis step.

Process design and project economic evaluation require integration of knowledge from many different scientific and engineering disciplines and are carried out at various levels of detail. Table 20-25 presents a common classification of design and cost estimates and typical engineering costs for a $50 million capital investment for a new plant.

Table 20-25 Types of Design Estimates, Their Cost and Accuracy for a $50 Million Project*

Level	Type of estimate	Error (%)	Cost ($1000)
1	Order-of-magnitude estimate (ratio estimate) based on similar previous projects	≤ 50	
2	Project planning estimate (budget estimation) based on knowledge of major equipment items	≤ 30	30–100
3	Preliminary engineering (scope estimate) based on sufficient data to permit the estimate to be budgeted	≤ 25	250–750
4	Detailed engineering (capital approval stage) based on almost complete process data	≤ 15	1250–2000
5	Procurement and construction (contractor's estimate) based on complete engineering drawings, specifications, and site surveys	≤ 10	3500–7000

*Douglas, *Conceptual Design of Chemical Processes*, McGraw-Hill, New York, 1988, p. 7.

Reproduced from *Bioseparations Science and Engineering*, 2d. ed., by Roger G. Harrison, Paul W. Todd, Scott R. Rudge, and Demetri P. Petrides (2015). By Permission of Oxford University Press.

Figure 20-58 presents the need for design estimates of various types during the life cycle of product development and commercialization. The trapezoidal shape of the diagram represents the drastic reduction in product candidates as we move from feasibility studies to commercialization. In fact, the chances of commercialization at the research stage for a new product are only about 1 to 3 percent, at the development stage they are about 10 to 25 percent, and at the pilot plant stage they are about 40 to 60 percent (Douglas, *Conceptual Design of Chemical Processes*, McGraw-Hill, New York, 1988, p. 4).

Figure 20-58 Types of design estimates during the life cycle of a product [Frohlich, in Biopharmaceutical Process Economics and Optimization (conference proceedings), Sept. 30–Oct. 1, 1999, International Business Communications, Westborough, Mass].

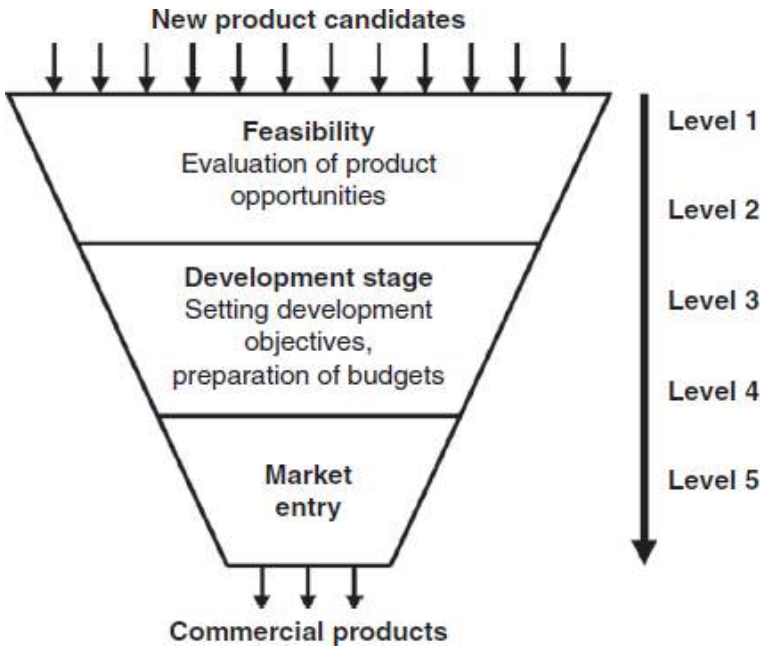

Order-of-magnitude estimates are usually practiced by experienced engineers who have worked on similar projects in the past. They take minutes or hours to complete, but the error in the estimate can be as high as 50 percent. Table 20-26 presents a sample of data typically used by experienced engineers for order-of-magnitude estimates. The table lists the capital investment for five large-scale facilities built to manufacture therapeutic monoclonal antibodies using cell culture (by growing mammalian cells in stirred-tank bioreactors). Column 2 displays the number of the production bioreactors, the working volume of each, and the total working volume. For instance, a Genentech facility includes six production bioreactors, each having a working volume of 15 m^3. Column 4 displays the total capital investment, and column 5 displays the ratio of the total capital investment to the total production bioreactor volume. The ratio ranges from 3.3 to 6.2 with an average value of $4.6 million per cubic meter of bioreactor volume. Based on the data of Table 20-26, an engineer may conclude with some confidence that the capital investment for a new 100 m^3 (total production bioreactor volume) cell culture facility would be in the range of $330 million to $620 million and most likely around $460 million. Please note, however, that advances in technology (e.g., cell lines that generate higher product titers and the use of single-use systems) and other factors may render such data obsolete and reduce the accuracy of order-of-magnitude estimates. As a result, cost estimates are progressively refined as new product candidates move through the development life cycle shown in Fig. 20-58.

Table 20-26 Capital Investments for Cell Culture Facilities

	Bioreactor capacity (m^3)	Completion year	Investment ($ millions)	$ million per m^3
Boehringer Ingelheim (Germany)	6 × 15 = 90	2003	296	3.3
Lonza Biologics (Portsmouth, N.H.)	3 × 20 = 60	2004	207	3.4
Genentech (Oceanside, Calif.)	6 × 15 = 90	2005	450	5.0
Bristol Myers Squibb (Devens, Mass.)	6 × 20 = 120	2009	750	6.2
Roche Pharmaceuticals (Switzerland)	6 × 12.5 = 75	2009	375	5.0

Reproduced from *Bioseparations Science and Engineering*, 2d ed., by Roger G. Harrison, Paul W. Todd, Scott R. Rudge, and Demetri P. Petrides (2015). By Permission of Oxford University Press.

Most engineers employed by operating companies usually perform level 2 and 3 studies. Such studies take weeks or months to complete using appropriate computer aids. The main objective of such studies is to evaluate alternatives and pinpoint the most cost-sensitive areas—the economic "hot spots"—of a complex process. The results of such analyses are used to plan future research and development and to generate project budgets.

Level 4 and 5 studies are usually performed by the engineering and construction companies hired to build new plants for promising new products that are at an advanced stage of development. Such estimates are beyond the scope of this section. Instead, the focus of the material in the rest of this section will be on level 1, 2, and 3 studies. Also note that opportunities for creative process design work are usually limited to preliminary studies. By the time detailed engineering work has been initiated, a process is more than 80 percent fixed. Furthermore, the vast majority of important decisions for capital expenditures and product commercialization are based on results of preliminary process design and cost analysis. This explains why it is so important for a new engineer to master the skills of preliminary process design and cost estimation.

Environmental impact assessment is an activity closely related to process design and cost estimation. Biochemical plants generate a wide range of liquid, solid, and gaseous waste streams that require treatment prior to discharge. The cost associated with waste treatment and disposal has skyrocketed in recent years due to increasingly strict environmental regulations. This cost can be reduced through minimization of waste generation at the source. However, generation of waste from a chemical or biochemical process is dependent on the process design and the manner in which the process is operated. Thus, reducing waste in an industrial process requires intimate knowledge of the process technology. In contrast, waste treatment is essentially an add-on at the end of the process. In addition, minimization of waste generation must be considered by process engineers at the early stages of process development. Once a process has undergone significant development, it is difficult and costly to make major changes. Furthermore, regulatory constraints that are unique to the pharmaceutical industry restrict process modifications after clinical efficacy of the drug has been established. These are only some of the reasons why process synthesis and analysis must be initiated at the early stages of product development.

Synthesis of Bioseparation Processes Rules of thumb, or heuristics, were given in the introduction for use in developing flowsheets for the recovery and purification of biological products, and examples were given of the application of these rules of thumb to the placement of various bioseparation unit operations.

Process Analysis The flowsheets created during process synthesis must be analyzed and compared on the basis of capital investment, manufacturing cost, environmental impact, and other criteria to decide which ideas to consider further. Methodologies for estimating capital investment and manufacturing cost are presented later in the Process Economics subsection. In both cases, estimation is based on the results of material and energy balances and equipment sizing. These calculations are typically done using spreadsheets or process simulators. These tools allow the process design team to characterize a processing scenario, and then quickly and accurately redo the entire series of calculations for a different set of assumptions and other input data.

Spreadsheets Spreadsheet applications, such as Microsoft Excel, have become as easy to use as word processors and graphics packages. In its simplest form, a spreadsheet is an electronic piece of paper with empty boxes, known as *cells*. The user can enter data in those *cells*, perform calculations, and generate results. Results from spreadsheets can be easily plotted in a variety of graphs.

Process Simulators and Their Benefits Process simulators are software applications that enable the user to readily represent and analyze integrated processes. They have been in use in the petrochemical industries since the early 1960s. Established simulators for those industries include Aspen Plus and Aspen HYSYS from Aspen Technology, Inc. (Burlington, Mass.), ChemCAD from Chemstations, Inc. (Houston, Tex.), and PRO/II from SimSci-Esscor, Inc. (Lake Forest, Calif.).

The simulators mentioned above have been designed to model primarily continuous processes and their transient behavior. Most biological products, however, are produced in batch and semicontinuous mode (Korovessi and Linningerr, *Batch Processes*, Taylor and Francis, Oxford, UK, 2006; Heinzle et al., *Development of Sustainable Bioprocesses*, Wiley, Hoboken, N.J., 2006). Such processes are best modeled with batch process simulators that account for time dependency and sequencing of events. The first simulator designed specifically for batch processes was called Batches (from Batch Process Technologies in West Lafayette, Ind.). It was commercialized in the mid-1980s. All its operation models are dynamic, and simulation always involves integration of differential equations over a period of time. In the mid-1990s, Aspen Technology (Burlington, Mass.) introduced Batch Plus (now called Aspen Batch Process Developer), a recipe-driven simulator that targeted batch pharmaceutical processes. Around the same time, Intelligen, Inc. (Scotch Plains, N.J.) introduced SuperPro Designer [Petrides et al., *Pharm. Eng.* **22:** 56 (2002); Toumi et al., *Pharm. Eng.* **20**, March/April 2010]. SuperPro Designer is a flowsheet-driven simulator that handles material and energy balances, equipment sizing and costing, economic evaluation, environmental impact assessment, process scheduling, and debottlenecking of batch and continuous processes.

Discrete-event simulators have also found applications in the bioprocessing industries. Established tools of this type include ProModel from ProModel Corporation (Orem, Utah), Arena and Witness from Rockwell Automation, Inc. (Milwaukee, Wis.), Extend from Imagine That, Inc. (San Jose, Calif.), and flexSim from flexSim Software Products, Inc. (Orem, Utah). The focus of models developed with such tools is usually on the minute-by-minute time dependency of events and the animation of the process. Material balances, equipment sizing, and cost analysis tasks are usually out of the scope of such models.

The benefits from the use of process simulators depend on the type of product, stage of development, and size of the investment. For commodity biological products, such as biofuels, minimization of capital and operating costs is the primary benefit. For high-value biopharmaceuticals, systematic process development that shortens the time to commercialization is the primary motivation. Figure 20-59 shows a pictorial representation of the benefits from the use of such tools at the various stages of the commercialization process.

Figure 20-59 Benefits of using process simulators. [Reproduced fromBioseparations Science and Engineering, 2d ed., by Roger G. Harrison, Paul W. Todd, Scott R. Rudge, and Demetri P. Petrides (2015). By Permission of Oxford University Press.]

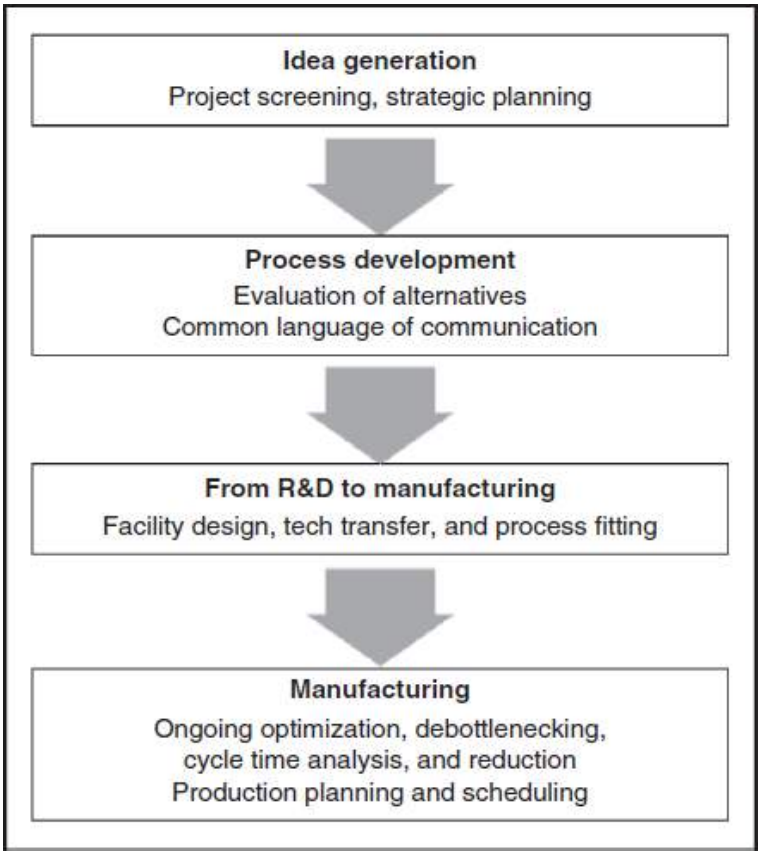

When product and process ideas are first conceived, process modeling tools are used for project screening, selection, and strategic planning based on preliminary economic analyses. During this phase, the company's process development groups are looking into the various options available for synthesizing, purifying, characterizing, and formulating the final product. The process undergoes constant changes during development. Typically, a large number of scientists and engineers are involved in the improvement and optimization of individual processing steps. The use of process simulators at this stage can introduce a common language of communication and facilitate team interaction. A computer model of the entire process can provide a common reference and evaluation framework to facilitate process development. The impact of process changes can be readily evaluated and documented in a systematic way. Once a reliable model is available, it can be used to pinpoint the cost-sensitive areas of a complex process. These are usually steps of high capital and operating cost or low yield and production throughput. The findings from such analyses can focus further lab and pilot plant studies to optimize those portions of the process. The ability to experiment on the computer with alternative process setups and operating conditions reduces the costly and time-consuming laboratory and pilot plant effort. A simulator can also evaluate the environmental impact of a process. For instance, material balances calculated for the projected large-scale manufacturing reveal environmental hot-spots. These are usually process steps that utilize organic solvents and other regulated materials with high disposal costs. Environmental issues not addressed during process development may lead to serious drawbacks during manufacturing.

With process development near completion at the pilot plant level, simulation tools are used to systematically design and optimize the process for commercial production. Availability of a good computer model can greatly facilitate the transfer of a new process from the pilot plant to the large-scale facility. If a new facility needs to be built, process simulators can size process equipment and supporting utilities and estimate the required capital investment. In transferring production to existing manufacturing sites (technology transfer), process simulators can be used to evaluate the various sites from a capacity and cost point of view and to select the most appropriate one.

In large-scale manufacturing, simulation tools are mainly used for on-going process optimization and debottlenecking studies. Furthermore, tools that are equipped with batch process scheduling capabilities can be used to generate production schedules on an ongoing basis in a way that does not violate constraints related to the limited availability of equipment, labor resources, utilities, inventories of materials, etc.

Using a Biochemical Process Simulator The minimum requirements for a biochemical process simulator are the ability to handle batch as well as continuous processes and the ability to model the unit operations that are specific to bioprocessing. Because SuperPro Designer (from Intelligen, Inc.) has the ability to satisfy these requirements, we will use it to illustrate the role of such tools in bioprocess design. A functional evaluation version of SuperPro Designer and additional information on bioprocess simulation can be obtained at the website www.intelligen.com. Tutorial videos on the use of SuperPro Designer can be viewed at www.intelligen.com/videos.

To model an integrated process using a simulator, the user starts by developing a flowsheet that represents the overall process. For instance, the flowsheet of a hypothetical process can be drawn on the main window of SuperPro Designer. The flowsheet is developed by putting together the required unit operations (sometimes referred to as *unit procedures,* as explained later in this section) and joining them with material flow streams. Next, the user initializes the flowsheet by registering (selecting from the component database) the various materials used in the process and specifying operating conditions and performance parameters for the various operations.

Most biochemical processes operate in batch or semicontinuous mode. This is in contrast to continuous operation, which is typical in the petrochemical and other industries that handle large throughputs. In continuous operations, a piece of equipment performs the same action all the time, which is consistent with the notion of unit operations. In batch processing, however, a piece of equipment goes through a cycle of operations. For instance, a typical chromatography cycle includes *equilibration, loading, washing, elution,* and *regeneration.* In SuperPro Designer, the set of operations that comprise a processing step is called a *unit procedure* (versus a *unit operation*). Each unit procedure contains individual tasks (e.g., equilibration, loading) called *operations.* A unit procedure is represented on the screen with a single equipment icon. In essence, a unit procedure is the recipe of a processing step that describes the sequence of actions required to complete that step. The significance of the unit procedure is that it enables the user to describe and model the various activities of batch processing steps in detail.

For every operation within a unit procedure, SuperPro includes a mathematical model that performs material and energy balance calculations. Based on the material balances, SuperPro performs equipment-sizing calculations. If multiple operations within a unit procedure dictate different sizes for a certain piece of equipment, the software reconciles the different demands and selects an equipment size that is appropriate for all operations. In other words, the equipment is sized to ensure that it will not be overfilled during any operation but is no larger than necessary (to minimize capital costs). In addition, the software checks to ensure that the vessel contents will not fall below a user-specified minimum volume (e.g., a minimum impeller volume) for applicable operations.

Before any simulation calculations can be done, the user must initialize the various operations by specifying operating conditions and performance parameters through appropriate dialog windows. After initialization of the operations, the simulator performs material and energy balances for the entire process and estimates the required sizes of equipment. Optionally, the simulator may be used to carry out cost analysis and economic evaluation calculations. The fundamentals of process economics are described in the next subsection.

Other tasks that can be handled by process simulators include process scheduling, environmental impact assessment, debottlenecking, and throughput analysis. Issues of process scheduling and environmental impact assessment are addressed in the Illustrative Examples subsection. Throughput analysis and debottlenecking is the analysis of the capacity and time utilization of equipment and resources (e.g., utilities, labor, raw materials). The objective is to identify opportunities for increasing throughput with the minimum possible capital investment (see Illustrative Examples for additional information on the subject).

Having developed a good model using a process simulator or a spreadsheet, the user may conduct virtual experiments with alternative process setups and operating conditions. This may potentially reduce costly and time-consuming laboratory and pilot plant effort. One must be aware, however, that the GIGO (garbage in, garbage out) principle applies to all computer models. More specifically, if some assumptions and input data are incorrect, the outcome of the simulation will not be reliable. Consequently, validation of the model is necessary. In its simplest form, a review of the results by an experienced engineer can play the role of validation.

Process Economics The preliminary economic evaluation of a project for manufacturing a biological product usually involves estimation of capital investment, estimation of operating costs, and analysis of profitability. For biopharmaceuticals, another figure worth considering is the average cost of new drug development, which is in the range of $500 million to $1 billion [DiMasi et al., *J. Health Econ.* **22:** 151 (2003); Gilbert et al., *The Business and Medicine Report* **21:** Nov. 2003]. Much of this figure represents research and development (R D) spending for all unsuccessful products. In other words, the actual average development cost per successful drug may be $100 to $200 million, but because more than 90 percent of new projects never reach commercialization, the average overall R D cost skyrockets. This order-of-magnitude cost increase reinforces the need for effective process design tools and methodologies that assist engineers and scientists in efficiently evaluating and eliminating nonpromising project ideas at the very early stages of product and process development.

Capital Cost Estimation The capital investment for a new plant includes three main items: *direct fixed capital* (DFC), working capital, and start-up and validation cost. The DFC for small to medium biotechnology facilities is usually in the range of $50 to $200 million, whereas for large facilities it is in the range of $250 to $750 million. For preliminary design purposes, the various items of DFC are estimated based on the total equipment *purchase cost* (PC) using several multipliers sometimes called *Lang factors*. Table 20-27 provides ranges and average values for the multipliers and a skeleton for the calculations. Detailed definitions of the various cost items and additional information can be found in traditional process design textbooks and the technical literature [Turton et al., *Analysis, Synthesis, and Design of Chemical Processes*, 5th ed., Pearson, Upper Saddle River, N.J., 2018; Douglas, *Conceptual Design of Chemical Processes*, McGraw-Hill, New York, 1988; Peters and Timmerhaus, *Plant Design and Economics for Chemical Engineers*, 5th ed., McGraw-Hill, New York, 2002; Ulrich et al., *A Guide to Chemical Process Design and Economics, Wiley*, Hoboken, N.J., 1984; Valle-Riestra et al., *Project Evaluation in the Chemical Process Industries*, McGraw-Hill, New York, 1983; Garrett, *Chemical Engineering Economics*, Van Nostrand Reinhold, New York, 1989; Seider et al., *Process Design Principles—Synthesis, Analysis, and Evaluation*, Wiley, Hoboken, N.J., 1999; Towler and Sinnott, *Chemical Engineering Design; Principles, Practice and Economics of Plant and Process Design*, Butterworth-Heinemann (Elsevier), Oxford, U.K., 2008].

Table 20-27 Fixed Capital Cost Estimation

Cost item	Average multiplier	Range of multiplier values
Total plant direct cost (TPDC)		
Equipment purchase cost (PC)		
Installation	0.50 × PC	0.2–1.5
Process piping	0.40 × PC	0.3–0.6
Instrumentation	0.35 × PC	0.2–0.6
Insulation	0.03 × PC	0.01–0.05
Electrical	0.15 × PC	0.1–0.2
Buildings	0.45 × PC	0.1–3.0
Yard improvement	0.15 × PC	0.05–0.2
Auxiliary facilities	0.50 × PC	0.2–1.0
Total plant indirect cost (TPIC)		
Engineering	0.25 × TPDC	0.2–0.3
Construction	0.35 × TPDC	0.3–0.4
Total plant cost (TPC)	TPDC + TPIC	
Contractor's fee	0.05 × TPC	0.03–0.08
Contingency	0.10 × TPC	0.07–0.15
Direct fixed capital (DFC)	TPC + contractor's fee and contingency	

Reproduced from *Bioseparations Science and Engineering*, 2d ed., by Roger G. Harrison, Paul W. Todd, Scott R. Rudge, and Demetri P. Petrides (2015). By Permission of Oxford University Press.

Notice the wide range of multiplier values in Table 20-27 for estimating the cost of buildings. Plants for commodity biochemicals, such as ethanol and citric acid, fall on the low end of the range. Conversely, biopharmaceutical facilities with their expensive heating, ventilation, and air conditioning (HVAC) requirements fall on the high end. The average value of 0.45 corresponds to relatively large plants that produce medium- to high-value products (e.g., industrial enzymes).

For more accurate estimation of building costs, it is necessary to estimate the process area required based on the footprint of the equipment and the space required around the equipment for safe and efficient operation and maintenance. Then the building cost is estimated by multiplying the area of the various sections (e.g., process, laboratory, office) of a plant by an appropriate unit cost provided in Table 20-28. This table, which was developed by DPS Biometrics (Framingham, Mass.), also provides information on air circulation rates for the various process areas, which determine the sizing and power requirements of HVAC systems.

Table 20-28 Building Cost Estimation (Year 2012 Prices)*

Space function	Unit cost ($/m^2)	Air circulation rates (volume changes/h)
Process area†		
ISO Grade 8	3000–3750	10–20
ISO Grade 7	3750–5200	30–70
ISO Grade 6	6700–9000	70–160
ISO Grade 5	9000–12,000	200–600
Mechanical room (utilities)	450–900	
Laboratory	1500–3000	
Office	750–900	

*Frolich, in *Biopharmaceutical Process Economics and Optimization* (conference proceedings), International Business Communications, Sept. 30–Oct. 1, 1999.

†The ISO Grade refers to ISO 14644, "Cleanrooms and associated controlled environments." An earlier system uses a "class number" that refers to the maximum number of particles 0.5 μm or larger per cubic foot. Classes 100,000, 10,000, 1000, and 100 are similar to ISO Grades 8, 7, 6, and 5, respectively.

Reproduced from *Bioseparations Science and Engineering*, 2d ed., by Roger G. Harrison, Paul W. Todd, Scott R. Rudge, and Demetri P. Petrides (2015). By Permission of Oxford University Press.

Table 20-27 indicates a wide range in the equipment installation cost multipliers. Using multipliers that are specific to individual equipment items leads to the most accurate estimates. In general, equipment delivered mounted on skids has a lower installation cost.

For preliminary cost estimates, Table 20-27 clearly shows that the fixed capital investment of a plant is a multiple (usually 3 to 10 times) of its equipment purchase cost. The low end of the range applies to large-scale facilities that produce biofuels and commodity biochemicals. The high end applies to biopharmaceutical facilities.

The equipment purchase cost can be estimated from vendor quotations, published data, company data compiled from earlier projects, and the use of process simulators that are equipped with appropriate costing capabilities. Vendor quotations are time-consuming to obtain and are, therefore, usually avoided for preliminary cost estimates. Instead, engineers tend to rely on the other three sources. Figures 20-60 to 20-63 provide equipment cost data for disk-stack centrifuges, membrane filtration systems, chromatography columns, and vertical agitated tanks that meet the specifications of the biopharmaceutical industry. The cost of the membrane filtration systems includes the cost of the skid, tank, pumps, and automation hardware and software. The tanks are appropriate for buffer preparation. They include a low-power agitator, but no heating/cooling jacket. The data represent average values from several vendors.

Figure 20-60 *Purchase cost of disk-stack centrifuges versus Σ factor (2012 prices). [Reproduced from Bioseparations Science and Engineering, 2d ed., by Roger G. Harrison, Paul W. Todd, Scott R. Rudge, and Demetri P. Petrides (2015). By Permission of Oxford University Press.]*

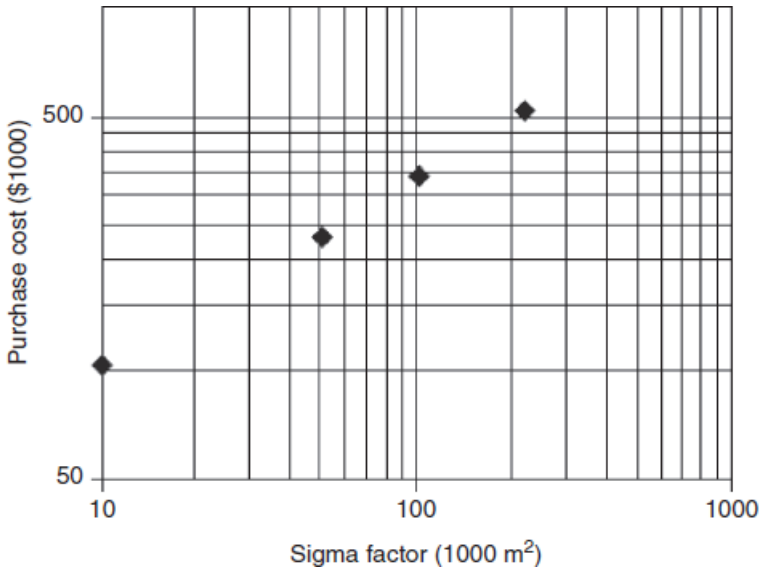

Figure 20-61 *Purchase cost of membrane filtration systems (2012 prices). [Reproduced from Bioseparations Science and Engineering, 2d ed., by Roger G. Harrison, Paul W. Todd, Scott R. Rudge, and Demetri P. Petrides (2015). By Permission of Oxford University Press.]*

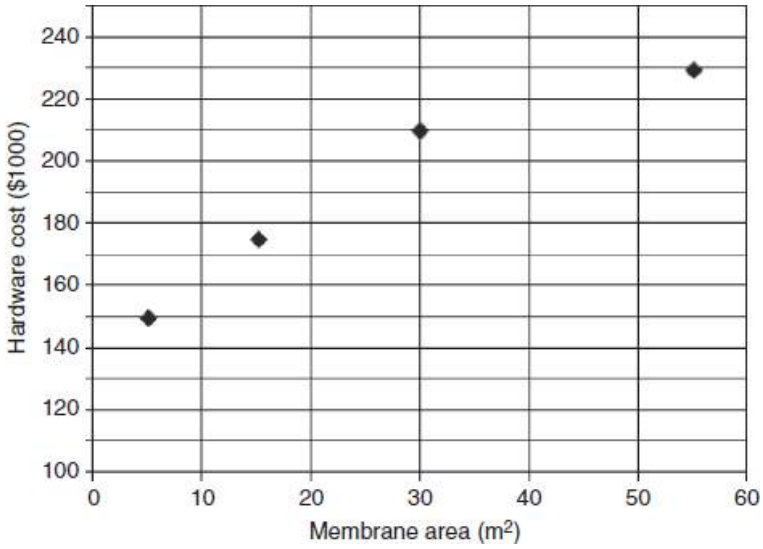

Figure 20-62 Purchase costs of chromatography columns made of acrylic tube and stainless-steel bed supports (2012 prices). [Reproduced from Bioseparations Science and Engineering, 2d ed., by Roger G. Harrison, Paul W. Todd, Scott R. Rudge, and Demetri P. Petrides (2015). By Permission of Oxford University Press.]

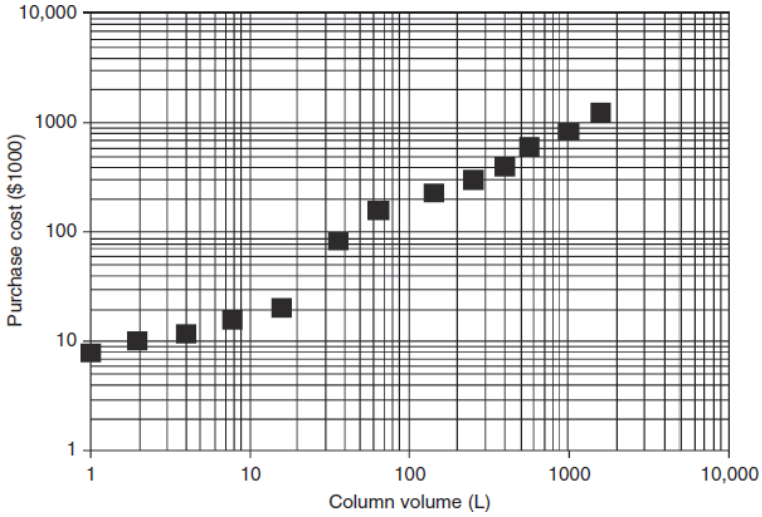

Figure 20-63 Purchase cost of agitated tanks made of stainless steel (2012 prices). [Reproduced from Bioseparations Science and Engineering, 2d ed., by Roger G. Harrison, Paul W. Todd, Scott R. Rudge, and Demetri P. Petrides (2015). By Permission of Oxford University Press.]

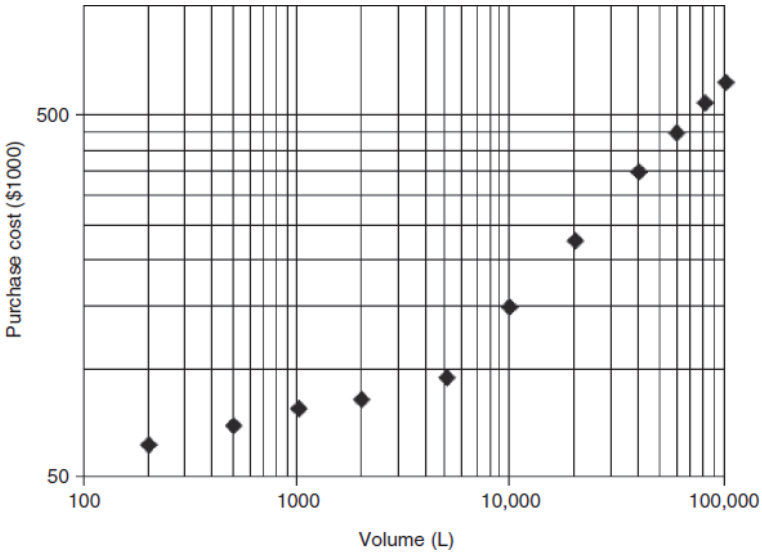

Note that equipment purchase cost is a strong function of industrial application and plant location. The data of Figs. 20-60 to 20-63 are applicable to biopharmaceutical facilities in developed countries. The cost of membrane filtration systems used in the food, biofuel, and water purification industries is more than an order of magnitude lower compared to the biopharmaceutical industry. The much larger equipment scale and the less stringent equipment specifications relative to biopharmaceuticals are responsible for the large difference in cost. The same trend applies to the cost of chromatography columns, storage tanks, reactor vessels, and most other equipment items. A good source of cost data for equipment used in the biofuel and biomaterial industries is available from the U.S. Department of Energy [DOE/NETL-2002/1169 (2002). Process Equipment Cost Estimation. Available at http://www.osti.gov/bridge/purl.cover.jsp?purl=/797810-Hmz80B/native/]. Additional sources for bioprocessing equipment cost data are available in the literature [Kalk and Langlykke, in Demain and Solomon (eds.), *Manual of Industrial Microbiology and Biotechnology*, American Society for Microbiology, Washington D.C., 1986, p. 363; Reisman, *Economic Analysis of Fermentation Processes,* CRC Press, Boca Raton, fl, 1988, p. 55].

Often, cost data for one or two discrete equipment sizes are available, but the cost for a different-size piece of equipment must be estimated. In such cases, the *scaling law* (expressed by the following equation) can be used:

$$\text{Cost}_2 = \text{Cost}_1 \left(\frac{\text{Size}_2}{\text{Size}_1} \right)^a$$

(20-98)

The mathematical form of the scaling law explains why cost-versus-size data graphed on logarithmic coordinates tend to fall on a straight line. The value of the exponent *a* in Eq. (20-98) ranges between 0.5 and 1.0, with an average value for vessels of around 0.6 (this explains why the scaling law is also known as the "0.6 rule"). According to this rule, when the size of a vessel doubles, its cost will increase by a factor of $(2/1)^{0.6}$, or approximately 52 percent. This result is often referred to as the *economy of scale*. In using the scaling law, it is important to make sure that the piece of equipment whose cost is being estimated has a size that does not exceed the maximum available size for that type of equipment.

The prices of equipment change with time owing to inflation and other market conditions. That change in price is captured by the Chemical Engineering Plant Cost Index (CE Index) that is published monthly by *Chemical Engineering* magazine. The index *I* is used to update equipment cost data according to the following equation:

$$\text{Cost}_2 = \text{Cost}_1 \left(\frac{I_2}{I_1} \right)$$

(20-99)

Another factor that affects equipment purchase cost is the material of construction. For instance, a tank made of stainless steel costs approximately 2.5 to 3 times as much as a carbon-steel tank of the same size. A tank made of titanium costs around 15 times the cost of a carbon-steel tank of the same size. Other factors that affect equipment cost include the finishing of the metal surface and the instrumentation that is provided with the equipment.

Working capital accounts for cash that must be available for investments in ongoing expenses and consumable materials. These expenses may include raw materials for 1 to 2 months, labor for 2 to 3 months, utilities for 1 month, waste treatment/disposal for 1 month, and other miscellaneous expenses. The required amount of working capital for a process is usually 10 to 20 percent of the DFC.

Start-up and validation costs can also represent a significant capital investment for a biopharmaceutical plant. A value of 20 to 30 percent of DFC is quite common.

Operating Cost Estimation The operating cost to run a biochemical plant is the sum of all ongoing expenses including raw materials, labor, consumables, utilities, waste disposal, and facility overhead. Dividing the annual operating cost by the annual production rate yields the unit production cost (e.g., in dollars per kilogram). The unit cost and selling prices of bioproducts are inversely proportional to market size (Harrison et al., *Bioseparations Science and Engineering*, Oxford University Press, Oxford, UK, 2015, p. 2). Low-molecular-weight commodity biochemicals and biofuels that are produced in large quantities cost around $1 to $5/kg to make. Citric acid, whose production is analyzed later in this section, is a product of this type. Specialty biochemicals that are used as food supplements (e.g., vitamins) and flavoring agents have a manufacturing cost of $5 to $100/kg. The manufacturing cost of therapeutic proteins produced in large quantities is in the range of $1/g to $1000/g. Human serum albumin (HSA) which is extracted from blood plasma and has an annual production volume of more than 500 metric tons lies close to the low end. The manufacturing cost of therapeutic proteins with annual production volume ranging from a few hundreds of kilograms to a few metric tons is in the range of $50 to $1000/g. The insulin and monoclonal antibody processes analyzed later in this section represent products of this type. The manufacturing cost of interferons, erythropoietin (EPO), and other therapeutic proteins with very low annual production volume (from hundreds of grams to a few kilograms) is more than $10,000/g [Jagschies, *BioPharm Int*. **21:** 72 (2008)].

Table 20-29 displays the various types of operating cost, their direct or indirect nature, and ranges for their values relative to the total operating cost. Sometimes cost items are categorized as either fixed or variable. Fixed costs are incurred regardless of the volume of product output. The clearest case of a fixed cost is depreciation, which is part of the equipment-dependent cost. The clearest case of a variable cost would be the cost of raw materials. Most other costs have a fixed component and a variable component. It is obvious from the wide range of values in Table 20-29 that industry averages cannot predict the operating cost of a process; a certain level of detailed calculations is required.

Table 20-29 Operating Cost Items and Ranges

Cost item	Type of cost	Range of values (% of total)
Raw materials	Direct	10–80
Labor	Direct	10–50
Consumables	Direct	1–50
Lab/QC/QA	Direct	1–50
Waste disposal	Direct	1–20
Utilities	Direct	1–30
Facility overhead	Indirect	10–70
Miscellaneous	Indirect	0–20

Reproduced from *Bioseparations Science and Engineering*, 2d ed., by Roger G. Harrison, Paul W. Todd, Scott R. Rudge, and Demetri P. Petrides (2015). By Permission of Oxford University Press.

The raw materials cost includes the cost of all fermentation media, recovery chemicals, and cleaning materials. For commodity biochemicals, such as ethanol, the cost of fermentation media is the main component. For high-value products, the solutions used for product recovery and equipment cleaning can be a major part of the raw materials cost. Table 20-30 provides a list of commonly used raw materials in the biochemical industries. Note that the price of a raw material can vary widely depending on its required purity. This can be clearly seen in the case of water. *Water for injection* (WFI), for instance, costs 100 to 500 times as much as city water. Raw materials for biopharmaceuticals are typically required to be USP/NF grade. Prices for a wide range of chemicals are available online at www.spectrumchemicals.com.

Table 20-30 Common Bioprocessing Raw Materials (Year 2012 Prices)

Raw material	Comments	Price ($/kg)
C Source		
Glucose	Solution 70% w/v	0.30–0.40
Corn syrup	95% Dextrose equivalent	0.40–0.50
Molasses	50% Fermentable sugars	0.12–0.20
Soybean oil	Refined	1.10–1.30
Corn oil	Refined	1.30–1.40
Ethanol	USP tax-free	0.80–0.90
Methanol	Gulf Coast	0.40–0.45
n-Alkanes		0.75–0.90
N Source		
Ammonia	Anhydrous, fertilizer grade	0.30–0.60
Soybean flour	44% protein	0.45–0.50
Cottonseed flour	62% protein	0.50–0.60
Casein	13.5% w/w total N	10.00–12.00
Ammonium sulfate	Technical	0.17–0.25
Ammonium nitrate	Fertilizer grade 33.5% N, bulk	0.20–0.30
Urea	46% N, agricultural grade	0.55–0.65
Yeast	Brewers, debittered	1.25–1.40
Whey	Dried, 4.5% w/w N	1.25–1.40
Salts		
KH_2PO_4	USP, granular	1.65–1.85
K_2SO_4	Granular, purified	2.80–3.00
Na_2HPO_4		1.40–1.80
$MgSO_4 \cdots 7H_2O$		0.45–0.55
$ZnSO_4 \cdots 7H_2O$	Agricultural grade, powder	0.65–0.75
Other		

Raw material	Comments	Price ($/kg)
Process water		0.0001–0.001
RO water		0.005–0.01
Water for injection		0.02–0.5
H_3PO_4 (85% w/w)	Food grade	3.5 – 4.5
NaOH		0.2–0.5
HCl (37% w/w)		0.7–0.8
H_2SO_4 (98% w/w)		0.15–0.25

Reproduced from *Bioseparations Science and Engineering*, 2d ed. by Roger G. Harrison, Paul W. Todd, Scott R. Rudge, and Demetri P. Petrides (2015). By Permission of Oxford University Press.

Labor is estimated based on the total number of operators, which in turn is calculated by summing the operator requirements of the various operations as a function of time. As will become clear in the examples discussed later, the labor requirement in a batch manufacturing facility varies with time. In a single-product facility, the number of operators in each shift must be based on maximum demand during that shift. In multiproduct facilities, each product line can employ a certain number of dedicated operators and rely on floating operators during periods of peak demand. In general, smaller facilities tend to utilize a larger number of operators per processing step because these plants are less automated. For instance, a small biotech company may utilize two or three operators to set up a fermenter, whereas in a large, highly automated fermentation facility, a single operator may handle the setup of six different fermenters remotely from the control room. In general, a typical biotech company that deals with high-value products will allocate at least one operator to each processing step (centrifugation, membrane filtration, chromatography, etc.) during its operation. The setup of a step may require multiple operators for a short period. The annual cost of an operator (including salary and benefits) varies widely around the globe. It is in the range of $4000 to $10,000 in developing nations and can exceed $50,000 in developed countries (Pollak et al., *Contract Pharma*, Jan./Feb. 2012).

Consumables are items that may be used up, fouled, or otherwise damaged during processing, such as membranes, chromatography resins, and activated carbon. These items must be replaced periodically. As the examples later in this section will illustrate, the high unit cost of chromatography resins and their frequent replacement can make them a major component of the manufacturing cost. The unit cost of typical ion exchange and hydrophobic interaction chromatography resins used for the purification of proteins is in the range of $500 to $2000 per liter of resin. The unit cost of protein A affinity resins that are commonly used for the purification of monoclonal antibodies is in the range of $5000 to $15,000 per liter of resin. The replacement frequency of such resins is in the range of 50 to 200 cycles of usage (the high-end resins have a longer useful life). In contrast, the unit cost of polymeric chromatography resins used for the purification of small biomolecules (e.g., amino acids) is substantially lower (under $100 per liter of resin), and their life is longer (1000 to 2000 h of operation). Likewise, the unit cost of silica-based resins used for water demineralization is around $0.5 per liter, and their life is in the range of 2000 to 6000 h of operation (the life strongly depends on the composition of the treated materials).

Regarding membrane filtration operations, the unit cost of MF/UF membranes used in the biopharmaceutical industry (in the form of hollow fiber cartridges or cassettes) is in the range of $300 to $800/$m^2$. Such membranes typically handle 10 to 50 filtration cycles before disposal. The unit cost of related membranes used in industrial biotechnology (e.g., for production of industrial enzymes) is considerably lower (under $200/$m^2$), and the expected life is more than 2000 h of operation. The cost of membranes used for large-scale water purification is under $50/$m^2$, and their useful life is at least 6000 h of operation. In general, ceramic membranes cost more than polymeric ones, but they last longer.

The cost of disposable bags or containers, also known as single-use systems, is part of the consumables cost as well. Disposable bags have become popular in biopharmaceutical manufacturing because they eliminate the need for cleaning and sterilization in place (Papavasileiou et al., *BioPharm Int. Suppl.,* Nov. 2008, p. 16). Other advantages of single-use systems include increased processing flexibility and shorter validation, start-up, and commercialization times. Table 20-31 provides information on disposable bags used for the preparation and storage of buffer solutions and fermentation media. Bags with mixing capability are required for solution preparation. Similar bags are used for inoculum preparation in rocking and stirred-tank bioreactors. Bags for stirred-tank bioreactors are available with working volumes of up to 2000 L. A number of biopharmaceuticals are produced exclusively in single-use systems. Note that large disposables bags (larger than 50 L) utilize appropriate supporting skids.

Table 20-31 Disposable Bags for Preparation and Storage of Solutions (Year 2012 Prices)

Volume (L)	Bags for storage ($)	Bags for mixing ($)
50	310	600
100	340	690
200	360	820
500	460	930
1000	650	1180

Reproduced from *Bioseparations Science and Engineering*, 2d ed., by Roger G. Harrison, Paul W. Todd, Scott R. Rudge, and Demetri P. Petrides (2015). By Permission of Oxford University Press.

Laboratory, QC, and QA activities include off-line analysis, quality control (QC), and quality assurance (QA) costs. Chemical and biochemical analysis and physical property characterization, from raw materials to final product, are a vital part of biochemical operations. The laboratory/QC/QA cost is usually 10 to 20 percent of the operating labor cost. However, for certain biopharmaceuticals that require a large number of very expensive assays, this cost can be as high as the operating labor. For such cases, it is important to account for the number and frequency of the various assays in detail, since changes in lot size that can reduce the frequency of analysis can have a major impact on profit margins.

The treatment of wastewater and the disposal of solid and hazardous materials are other important operating costs. The amount and composition of the various waste streams are derived from the material balances. Multiplying the amount of each waste stream by the appropriate unit cost yields the cost of treatment and disposal. Treatment of low biological oxygen demand (BOD) wastewater (< 1000 mg/L) by a municipal wastewater treatment facility usually costs \$0.2 to \$0.5/m^3. This is not a major expense for most biotech facilities that deal with high-value products. However, disposal of contaminated solvents (typically generated by chromatography steps) and other regulated compounds can become a major expense because the unit disposal cost can be more than \$1/kg. Waste disposal may also become a problem if an unwanted by-product is generated as part of the recovery chemistry of a process (see the citric acid example). Disposal of single-use systems via incineration costs \$100 to \$200 per metric ton of material.

Utilities costs include the cost of heating and cooling agents as well as electricity. The amounts are calculated as part of the material and energy balances. Aerobic fermenters are major consumers of electricity, but downstream processing equipment generally does not consume much electricity. In terms of unit cost, electricity costs $0.05 to $0.15/kWh. The cost of heat removal using cooling water is in the range of $0.002 to $0.01 per 1000 kcal of heat removed. The cost of cooling using chilled water and refrigerants is in the range of $0.05 to $0.1 per 1000 kcal of heat removed. The cost of producing steam for use as a heating medium is around $5 to $15/1000 kg depending on pressure (low, medium, high), type of fuel used for its generation, and scale of production. The cost of clean steam (generated utilizing highly purified water) is around $50 to $100/1000 kg (depending on the scale of production and level of water purity). Clean steam is used in biopharmaceutical facilities for sterilizing equipment as part of equipment cleaning (e.g., "steam-in-place" or SIP operations). Note that manufacturers often classify purified water used for buffer preparation and equipment cleaning as a utility and not as a raw material, thus increasing the cost contribution of utilities. The insulin example, presented later in this section, describes a methodology for the systematic sizing of systems that supply purified water.

Facility overhead costs account for the depreciation of the fixed capital investment, maintenance costs for equipment, insurance, local (property) taxes, and possibly other overhead-type expenses. For preliminary cost estimates, the entire fixed capital investment is usually depreciated linearly over a 10-year period. In the real world, the U.S. government allows corporations to depreciate equipment in 5 to 7 years and buildings in 25 to 30 years. The value of land cannot be depreciated. The annual maintenance cost can be estimated as a percentage of the equipment's purchase cost (usually

10 percent) or as a percentage of the overall fixed capital investment (usually 3 to 5 percent). Insurance rates depend to a considerable extent on the maintenance of a safe plant in good repair condition. A value for insurance in the range of 0.5 to 1 percent of DFC is appropriate for most bioprocessing facilities. The processing of flammable, explosive, or highly toxic materials usually results in higher insurance rates. The local (property) tax is usually 2 to 5 percent of DFC. The factory expense represents overhead cost incurred by the operation of non-process-oriented facilities and organizations, such as accounting, payroll, fire protection, security, and cafeteria. A value of 5 to 10 percent of DFC is appropriate for these costs.

Included in miscellaneous costs are ongoing R D, process validation, and other overhead-type expenses that can be ignored in preliminary cost estimates. Other general expenses of a corporation include royalties, advertising, and selling. If any part of the process or any equipment used in the process is covered by a patent not assigned to the corporation undertaking the new project, permission to use the technology covered by the patent must be negotiated, and some form of royalty or license fee is usually required. Advertising and selling covers expenses associated with the activities of the marketing and sales departments.

Profitability Analysis Estimates of capital investment, operating cost, and revenues of a project provide the information needed to assess its profitability and attractiveness from an investment point of view. There are various measures for assessing profitability. The simplest ones include gross margin, return on investment (ROI), and payback time, and they are calculated by using the following equations:

$$\text{Gross margin} = \frac{\text{Gross profit}}{\text{Revenues}}$$

(20-100)

$$\text{Return on investment (ROI)} = \frac{\text{Net profit per year}}{\text{Total investment}} \times 100\ \%$$

(20-101)

$$\text{Payback time (yr)} = \frac{\text{Total investment}}{\text{Net profit per year}}$$

(20-102)

where gross profit is equal to annual revenues minus the annual operating cost, and net profit is equal to gross profit minus income taxes plus depreciation. All variables are averaged over the lifetime of a project.

Other measures that are more involved, such as the net present value (NPV) and internal rate of return (IRR), consider the cash flows of a project over its evaluation life and the time value of money. Detailed definitions for NPV and IRR can be found in the literature [Peters and Timmerhaus, *Plant Design and Economics for Chemical Engineers*, 4th ed., McGraw-Hill, New York, 1991, p. 327; Towler and Sinnott, *Chemical Engineering Design; Principles, Practice and Economics of Plant and Process Design*, Butterworth-Heinemann (Elsevier), Oxford, U.K., 2008, p. 366]. The examples presented next demonstrate how these measures facilitate the decision-making process.

Illustrative Examples In this section, SuperPro Designer is used to illustrate the analysis and evaluation of the production of three biological products. The first example analyzes the production of citric acid, a commodity organic acid heavily used in the beverage industry. The second deals with the bacterial production of recombinant human insulin, the first commercial product of modern biotechnology. The third example focuses on the production of monoclonal antibodies (mAbs) from mammalian cells cultured in stirred-tank bioreactors. The generation of the flowsheets for the production of all three products was based on information available in the patent and technical literature combined with engineering judgment and experience with other biological products. These examples are used to draw general conclusions on the manufacturing cost of biological products. The computer files for these examples are available as part of the evaluation version of SuperPro Designer at the website www.intelligen.com. The flowsheets and charts of the examples are available in color format in the readme files of the corresponding SuperPro Designer examples. Additional examples and pertinent publications are available at www.intelligen.com/literature.

Citric Acid Production A number of organic acids are produced via fermentation. Of these, citric acid is produced in the largest amount [> 1,800,000 metric tons (t) per year]. Citric acid is marketed as citric acid monohydrate or as anhydrous citric acid. The majority of citric acid (> 60 percent) is used in the food and beverage industries to preserve and enhance flavor. In the chemical industries (which represent 25 to 30 percent of total utilization), the uses of citric acid include the treatment of textiles, softening of water, and manufacturing of paper. In the pharmaceutical industry (10 percent of total utilization), citrate is used as a buffer and formulation excipient, iron citrate is used as a source of iron, and citric acid is used as a preservative for stored blood, tablets, and ointments, and in cosmetic preparations (Crueger and Crueger, *Biotechnology—A Textbook of Industrial Microbiology*, 2d ed., Sinauer, Sunderland, Mass., 1989, p. 134). Citric acid is increasingly being used in the detergent industry as a replacement for polyphosphates.

Citric acid was first recovered in 1869 in England from calcium citrate, which was obtained from lemon juice. Its production by filamentous fungi has been known since 1893. The first production via surface culture fermentation was initiated in 1923. Production using stirred-tank fermenters began in the 1930s, and presently this is the preferred method for large-scale manufacturing. The plant considered in this example produces around 18,000 t/yr of crystal citric acid, which represents approximately 1 percent of the current world demand.

The entire flowsheet is shown in Fig. 20-64. Molasses, the carbon source of fermentation, is diluted with water from about 50 percent fermentable sugars content to 20 percent in a blending tank (V-101). Suspended particulate material is then removed by filtration (PFF-101). Metal ions, particularly iron, are subsequently removed by an ion exchange chromatography column (C-101), and the purified raw material solution is then heat-sterilized (ST-101). Nutrients (i.e., sources of ammonium, phosphorus, magnesium, potassium copper, and zinc) are dissolved in water (V-104) and heat-sterilized (ST-101). (It is necessary to sterilize the first three nutrients separately to avoid a precipitate.) The fermentation cycle is 7 days, and the production is handled by seven fermenters that operate in staggered mode. Since the plant operates around the clock, one fermentation batch is initiated daily and another one is completed daily. Each fermenter has a vessel volume of 350 m^3 and generates broth of around 315 m^3. A three-step seed fermenter train (not shown in the flowsheet) supplies inoculum to each production fermenter (FR-101). A pure culture of the mold *Aspergillus niger* is used to inoculate the smallest seed fermenter. When optimum growth of mycelium is reached, the contents of the seed fermenter are transferred to the next stage fermenter, which is approximately 10 times larger. Similarly, this larger seed fermenter inoculates the production fermenter with about 10 percent volume of actively growing mycelium broth. Air is supplied by a compressor (G-101) at a rate that gradually increases from 0.15 vvm (volume of air per volume of liquid per minute) to 1.0 vvm. Cooling water removes the heat produced by the exothermic process (2990 kcal/kg of citric acid formed) and maintains the temperature at 28 C. The fermented broth is discharged into the holding tank (V-105), which acts as a buffer tank between the batch upstream section and the continuous downstream section.

***Figure 20-64** Citric acid production flowsheet. [Reproduced from Bioseparations Science and Engineering, 2d ed., by Roger G. Harrison, Paul W. Todd, Scott R. Rudge, and Demetri P. Petrides (2015). By Permission of Oxford University Press.]*

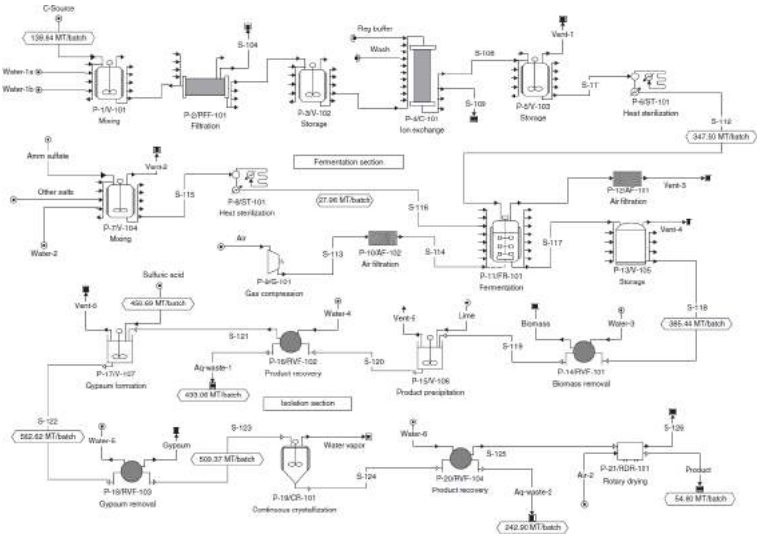

Purification starts with the removal of biomass by a rotary vacuum filter (RVF-101). The clarified fermentation liquor flows to an agitated reactor vessel (V-106) where approximately 1 part of hydrated lime, $Ca(OH)_2$, for every 2 parts of liquor is slowly added to precipitate calcium citrate. The lime solution must be very low in magnesium content to minimize losses due to generation of relatively soluble magnesium citrate. Calcium citrate is separated by a second rotary vacuum filter (RVF-102), and the citrate-free filtrate (Aq-Waste-1) is sent to a wastewater collection tank. The calcium citrate cake is sent to another agitated reactor vessel (V-107), where it is acidified with dilute sulfuric acid to form a precipitate of calcium sulfate (gypsum). A third filter (RVF-103) removes the precipitated gypsum and yields an impure citric acid solution in the filtrate. Careful control of the pH and temperature of each precipitation step is important for maximizing the yield of citric acid. The resulting solution is concentrated and crystallized using a continuous evaporator/crystallizer (CR-101). The crystals formed are separated by rotary vacuum filtration (RVF-104) and dried in a rotary dryer (RDR-101). If the final product is required in high purity, then treatment with activated carbon may precede crystallization to remove colorants. In addition, ion exchange is sometimes used to remove metal ions and other ionic species.

An equipment occupancy chart for consecutive batches can be developed using SuperPro Designer (Harrison et al., *Bioseparations Science and Engineering,* Oxford University Press, Oxford, UK, 2015, p. 475). The process batch time is approximately 200 h (or 8.3 days). This is the time elapsed from the preparation of raw materials to the final product of a single batch (excluding the time required for inoculum preparation). The duration of each fermentation batch is 160 h (6.7 days). The availability of seven production fermenters operating in staggered mode (out of phase) enables the plant to initiate a new batch every 24 h. The upstream portion of the process (i.e., raw material preparation and fermentation) operates in batch mode. The downstream section (product recovery and purification) operates continuously.

A summary of the overall material balances (expressed as input-output component balance) is given in Table 20-32. "CA crystal" stands for crystalline citric acid and represents the final product. Glucose represents the fermentable carbohydrates in molasses (50 percent w/w). Note the large amounts of $Ca(OH)_2$ and sulfuric acid consumed and gypsum (calcium sulfate) generated. The quantities of these compounds depend on the chemistry of the purification process and cannot be reduced without changing the recovery technology. Since this gypsum is contaminated with biomass, it has little or no commercial value. A disposal cost of $50/MT (metric ton) was assumed in this example. The large amount of wastewater is also worth noting.

Table 20-32 Overall Material Balances for Citric Acid (CA) Production (kg/yr)

Component	In	Out	Out – In
Ammonium sulfate	278,000	26,000	−252,000
Biomass	0	2,014,000	2,014,000
CA crystal	0	18,250,000	18,250,000
$Ca(OH)_2$	11,717,000	558,000	−11,159,000
Calcium citrate	0	623,000	623,000
CO_2	0	3,861,000	3,861,000
Citric acid	0	657,000	657,000
Glucose	22,934,000	275,000	−22,659,000
Gypsum	0	19,972,000	19,972,000
Impurities	459,000	459,000	0
Nutrients	1,894,000	383,000	−1,511,000
Oxygen	65,171,000	57,994,000	−7,177,000
NaOH	185,000	185,000	0
Sulfuric acid	14,979,000	576,000	−14,403,000
Water	308,879,000	320,663,000	11,784,000
Total	426,496,000	426,496,000	0

Reproduced from *Bioseparations Science and Engineering*, 2d ed., by Roger G. Harrison, Paul W. Todd, Scott R. Rudge, and Demetri P. Petrides (2015). By Permission of Oxford University Press.

A list of major equipment items along with their purchase costs (generated by SuperPro Designer) is shown in Table 20-33. The total equipment cost for a plant of this capacity is around $10.4 million. Note that approximately 30 percent of the equipment cost is associated with the seven production fermenters. The fermenters are made of stainless steel to minimize leaching of heavy metals that affect product formation. The final item, cost of unlisted equipment, accounts for the cost of the seed fermenters, pumps, and other secondary equipment that is not considered explicitly. Table 20-34 displays the various items of the direct fixed capital (DFC) investment. The total DFC for a plant of this capacity is around $43.6 million or approximately 4.2 times the total equipment cost.

Table 20-33 Equipment Specification and Purchase Costs for Citric Acid Production (Year 2012 Prices)

Quantity	Name	Description	Unit cost ($)	Cost ($)
1	AF-101	Air filter	100,000	100,000
		Rated throughput = 7.7 m^3/s		
1	AF-102	Air filter	37,000	37,000
		Rated throughput = 3.0 m^3/s		
1	C-101	Chromatography column	150,000	150,000
		Column volume = 4.66 m^3		
1	CR-101	Crystallizer	542,000	542,000
		Vessel volume = 130 m^3		
7	FR-101	Fermenter	436,000	3,052,000
		Vessel volume = 350 m^3		
1	G-101	Centrifugal compressor	1,560,000	1,560,000
		Compressor power = 1,430 kW		
1	PFF-101	Plate & frame filter	145,000	145,000
		Filter area = 335 m^2		
1	RDR-101	Rotary dryer	475,000	475,000
		Drying area = 85 m^2		
1	RVF-101	Rotary vacuum filter	154,000	154,000
		Filter area = 46 m^2		
1	RVF-102	Rotary vacuum filter	214,000	214,000
		Filter area = 83 m^2		
1	RVF-103	Rotary vacuum filter	195,000	195,000

Quantity	Name	Description	Unit cost ($)	Cost ($)
		Filter area = 71 m^2		
1	RVF-104	Rotary vacuum filter	137,000	137,000
		Filter area = 35 m^2		
1	ST-101	Sterilizer	308,000	308,000
		Rated throughput = 34 m^3/h		
1	V-101	Blending tank	503,000	503,000
		Vessel volume = 300 m^3		
1	V-102	Blending tank	503,000	503,000
		Vessel volume = 300 m^3		
1	V-103	Blending tank	503,000	503,000
		Vessel volume = 300 m^3		
1	V-104	Blending tank	139,000	139,000
		Vessel volume = 35 m^3		
2	V-105	flat bottom tank	198,000	396,000
		Vessel volume = 350 m^3		
1	V-106	Neutralizer	126,000	126,000
		Vessel volume = 42 m^3		
1	V-107	Neutralizer	94,000	94,000
		Vessel volume = 15 m^3		
		Unlisted Eequipment		1,037,000
		Total		**10,370,000**

Reproduced from *Bioseparations Science and Engineering*, 2d ed., by Roger G. Harrison, Paul W. Todd, Scott R. Rudge, and Demetri P. Petrides (2015). By Permission of Oxford University Press.

Table 20-34 Fixed Capital Estimate Summary for Citric Acid Production (Year 2012 Prices, $)

Total plant direct cost (TPDC)		
Equipment purchase cost	10,370,000	
Installation	3,726,000	
Process piping	3,111,000	
Instrumentation	2,074,000	
Insulation	311,000	
Electrical	1,037,000	
Buildings	2,074,000	
Yard improvement	1,556,000	
Auxiliary facilities	1,037,000	
TPDC		25,295,000
Total plant indirect cost (TPIC)		
Engineering	5,059,000	
Construction	7,589,000	
TPIC		12,648,000
Total plant cost (TPC = TPDC + TPIC)		37,943,000
Contractor's fee	1,897,000	
Contingency	3,794,000	
Direct fixed capital (DFC)		43,634,000
TPC + contractor's fee and contingency		

Reproduced from *Bioseparations Science and Engineering*, 2d ed., by Roger G. Harrison, Paul W. Todd, Scott R. Rudge, and Demetri P. Petrides (2015). By Permission of Oxford University Press.

A summary of the operating costs is shown in Table 20-35. The raw materials cost is the most important, accounting for 40.9 percent of the overall operating cost. This is quite common for commodity biochemicals. Molasses is the most expensive raw material, accounting for 67 percent of the raw materials cost. The purification chemicals, sulfuric acid and calcium hydroxide, account for 18.7 percent and 9.3 percent of the overall raw materials cost, respectively. The following prices were assumed: \$0.15/kg of molasses, \$0.013/kg of 10 percent w/w H_2SO_4 solution, \$0.08/kg of $Ca(OH)_2$, and \$0.1/m^3 of process water. The facility-dependent cost is the second most important, accounting for 28.7 percent of the overall cost. Depreciation of the fixed capital investment and maintenance of the facility are the main contributors to this cost. Utilities are the third largest expense, accounting for 14.8 percent of the overall cost. Electricity and cooling water utilized by the fermenters are the main contributors to this cost. Labor lies in the fourth position, and the environmental cost (waste treatment/disposal) is fifth. Disposal unit costs of \$1/m^3 and \$50/MT (metric ton) were assumed for liquid and solid (gypsum) waste streams, respectively. The disposal of gypsum accounts for 85 percent of the overall environmental cost. The overall unit production cost is approximately \$1.4/kg, which is roughly equal to the early 2012 selling price of citric acid [Saleem, http://www.prlog.org/11293569-china-citric-acid-price-trend-outlook-2011.html (2011)]. This can be explained by noting the excess citric acid production capacity around the world (which keeps profit margins low), and the fact that most operating citric acid plants are rather old and partially depreciated. If depreciation is ignored, the facility-dependent cost is reduced by more than 80 percent, and the overall unit cost drops to around \$1/kg.

Table 20-35 Operating Cost Summary for Citric Acid Production (Year 2012 Prices)

Cost item	Citric acid crystals (\$/kg)	Annual cost (\$/yr)	Proportion of total (%)
Raw materials	0.57	10,310,000	40.92
Facility-dependent	0.40	7,223,000	28.67
Labor	0.12	2,102,000	8.34
Consumables	0.00	15,000	0.06
Lab/QC/QA	0.01	210,000	0.83
Waste treatment and disposal	0.09	1,611,000	6.39
Utilities	0.21	3,724,000	14.78
Total	1.40	22,195,000	100.00

Reproduced from *Bioseparations Science and Engineering*, 2d ed., by Roger G. Harrison, Paul W. Todd, Scott R. Rudge, and Demetri P. Petrides (2015). By Permission of Oxford University Press.

Based on the preliminary evaluation of this project idea, one should not recommend investing in new citric acid production capacity unless there is a combination of favorable conditions. Obviously, availability of inexpensive equipment (e.g., by acquiring an existing facility) and raw materials (e.g., by locating the plant near a source of low-cost molasses) are the most important factors. Development or adoption of a superior technology may also change the attractiveness of citric acid production. Such a technology is actually available; it utilizes extraction for citric acid recovery [Roberts, in McKetta and Cunningham (eds.), *Encyclopedia of Chemical Processing and Design*, vol. 8, Dekker, New York, 1979, p. 324]. Recovery by extraction eliminates the consumption of $Ca(OH)_2$ and H_2SO_4 and the generation of the unwanted $CaSO_4$. Butanol has been used as an extractant, as has tributyl phosphate. Ion pair extraction by means of secondary or tertiary amines dissolved in a water-immiscible solvent (e.g., octyl alcohol) provides an alternative route. Developments in electrodialysis membranes could lead to recovering citric acid directly from the fermentation broth by this technique (Blanch and Clark, *Biochemical Engineering*, Dekker, New York, 1997, p. 611).

Human Insulin Production Insulin facilitates the metabolism of carbohydrates and is essential for the supply of energy to the cells of the body. Impaired insulin production leads to the disease diabetes mellitus, which is a significant cause of death and health problems in industrialized and developing countries [Barfoed, *Chem. Eng. Prog.* **83:** 49 (1987); World Health Organization, fact sheet no. 310, 2011].

Human insulin is a polypeptide consisting of 51 amino acids arranged in two chains: chain A with 21 amino acids and chain B consisting of 30 amino acids. The A and B chains are connected by two disulfide bonds. Human insulin has a molecular weight of 5808 and an isoelectric point of 5.4. Human insulin can be produced by four different methods:

- Extraction from human pancreas
- Chemical synthesis via individual amino acids
- Conversion of pork insulin, or "semisynthesis"
- Fermentation of genetically engineered microorganisms

Extraction from the human pancreas cannot be practiced because the availability of raw material is so limited. Total synthesis, while technically feasible, is not economically viable because the yield is very low. Production based on pork insulin, also known as *semisynthesis*, transforms the porcine insulin molecule into an exact replica of the human insulin molecule by substituting a single amino acid, threonine, for alanine in the G-30 position. This technology has been developed and implemented by Novo Nordisk A/S (Denmark). However, this option is also quite expensive because it requires the collection and processing of large amounts of porcine pancreases. In addition, the supply is limited by the availability of porcine pancreas.

At least three alternative technologies have been developed for producing human insulin based on fermentation and utilizing recombinant DNA technology [Ladisch and Kohlmann, *Biotechnol. Prog*. **8:** 469 (1992)]. The first successful technique of *biosynthetic human insulin* (BHI) production based on recombinant DNA technology was the two-chain method. This technique was developed by Genentech, Inc. (South San Francisco) and scaled up by Eli Lilly and Company (Indianapolis, Ind.). Each insulin chain is produced as a β-galactosidase fusion protein in *Escherichia coli,* forming inclusion bodies. The two peptide chains are recovered from the inclusion bodies (IBs), purified, and combined to yield human insulin. Later, the β-galactosidase operon was replaced with the tryptophan (Trp) operon, resulting in a substantial yield increase.

The so-called intracellular method of making proinsulin eliminates the need for the separate fermentation and purification trains required by the two-chain method. Intact proinsulin is produced instead. The proinsulin route has been commercialized by Eli Lilly [Kehoe, in Sikdar et al., (eds.), *Frontiers in Bioprocessing*, CRC Press, Boca Raton, Fla., 1989, p. 45]. Figure 20-65 shows the key transformation steps. The *E. coli* cells overproduce Trp-LE'-Met-proinsulin (Trp-LE'-Met is a 121-amino acid peptide signal sequence; proinsulin, with 82 amino acids, is a precursor to insulin) in the form of inclusion bodies, which are recovered and solubilized. Proinsulin is released by cleaving the methionine linker using cyanogen bromide (CNBr). The proinsulin chain is subjected to a folding process to allow intermolecular disulfide bonds to form; and the C peptide, which connects the A and B chains in proinsulin, is then cleaved with enzymes to yield human insulin. A number of chromatography and membrane filtration steps are required to purify the product.

Figure 20-65 Human insulin from proinsulin fusion protein. [Reproduced from Bioseparations Science and Engineering, 2d ed., by Roger G. Harrison, Paul W. Todd, Scott R. Rudge, and Demetri P. Petrides (2015). By Permission of Oxford University Press.]

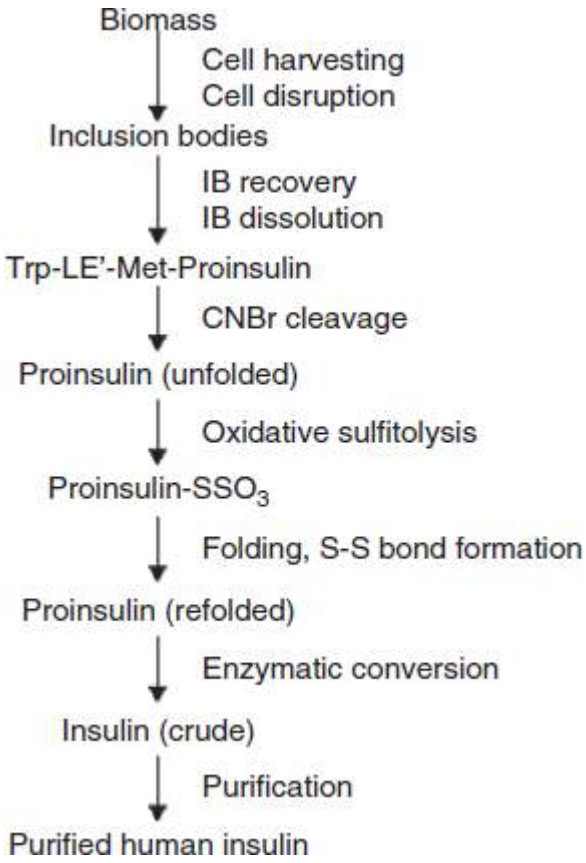

A second (extracellular) method of producing proinsulin was developed by Novo Nordisk A/S. It is based on yeast cells that secrete insulin as a single-chain insulin precursor [Barfoed, *Chem. Eng. Prog.* **83:** 49 (1987); World Health Organization, fact sheet no. 310, 2011]. Secretion simplifies product isolation and purification. The precursor contains the correct disulfide bridges and is therefore identical to those of insulin. It is converted to human insulin by transpeptidation in organic solvent in the presence of a threonine ester and trypsin followed by deesterification. Another advantage of the secreted proinsulin technology is that by employing a continuous bioreactor–cell separator loop, it is possible to reuse the cells.

In this example, we analyze a process based on the intracellular proinsulin method. The economics of this process were studied previously by Datar and Rosen, in Asenjo (ed.), *Separation Processes in Biotechnology*, Dekker, New York, 1990, p. 741, and by Petrides et al., *Biotechnol. Bioeng.* **5:** 529 (1995).

The annual world demand for insulin and insulin analogs was over 50,000 kg in 2010 and was growing at an annual rate of around 20 percent [Nair, *BioPharm Int*. **24:** 11 (2011)]. The plant analyzed in this example has a capacity of around 1800 kg of purified *biosynthetic human insulin* (BHI) per year. This is a relatively large plant for producing polypeptide-based biopharmaceuticals. The plant operates around the clock, 330 days a year. A new batch is initiated every 48 h, resulting in 160 batches per year. The fermentation broth volume per batch is approximately 37.5 m^3.

The entire flowsheet for the production of BHI is shown in Fig. 20-66. It is divided into four sections: fermentation, primary recovery, reactions, and final purification. *Note:* A "section" in SuperPro is simply a set of unit procedures (processing steps). If you open the file "insulin.spf" in SuperPro, you will see that all the unit procedures within a given section have their own distinctive color (blue, green, purple, and black for fermentation, primary recovery, reactions, and final purification, respectively).

Figure 20-66 ***Insulin production flowsheet. [Reproduced from Bioseparations Science and Engineering, 2d ed., by Roger G. Harrison, Paul W. Todd, Scott R. Rudge, and Demetri P. Petrides (2015). By Permission of Oxford University Press.]***

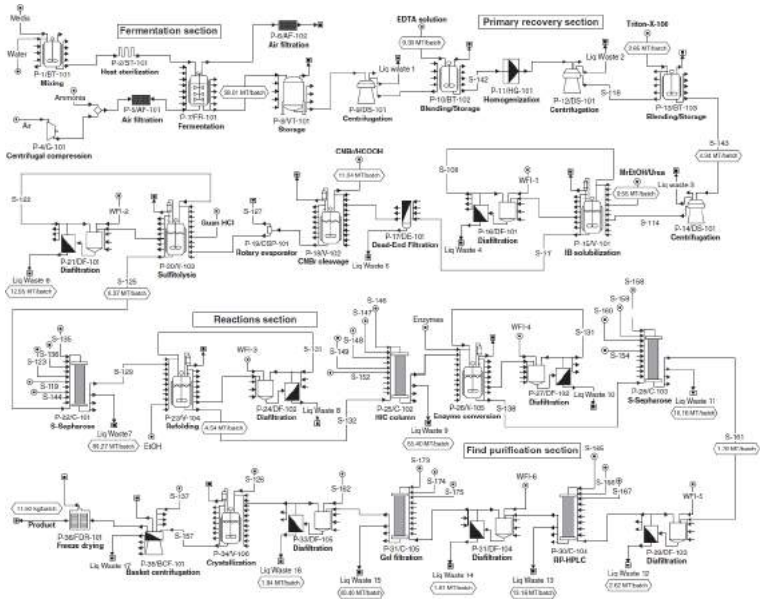

Fermentation media are prepared in a stainless-steel tank (BT-101) and sterilized in a continuous heat sterilizer (ST-101). The axial compressor (G-101) and the absolute filter (AF-101) provide sterile air and ammonia to the fermenter at an average rate of 0.5 vvm. A two-step seed fermenter train (not shown in the flowsheet) is used to inoculate the 50-m^3 production fermenter (FR-101) with transformed *E. coli* cells. These cells are used to produce the Trp-LE'-Met-proinsulin precursor of insulin, which is retained in the cellular biomass. The fermentation time in the production fermenter is about 18 h, and the fermentation temperature is 37 C. The final concentration of *E. coli* in the production fermenter is about 30 g/L (dry cell weight). The Trp operon is turned on when the *E. coli* fermentation runs out of tryptophan. The chimeric protein Trp-LE'-Met-proinsulin accumulates intracellularly as insoluble aggregates (inclusion bodies), and this decreases the rate at which the protein is degraded by proteolytic enzymes. In the base case, it was assumed that the inclusion bodies (IBs) constitute 20 percent of total dry cell mass. At the end of fermentation, the broth is cooled down to 10 C to minimize cell lysis. After completion of each processing step in the fermentation section (and subsequent sections), the equipment is washed to prepare for the next batch of product.

After the end of fermentation, the broth is transferred into a surge tank (VT-101), which isolates the upstream section from the downstream section of the plant. Three disk-stack centrifuges (DS-101) operating in parallel are used for cell harvesting. Note that a single unit procedure icon in the SuperPro model may represent multiple equipment items operating in parallel. During centrifugation, the broth is concentrated from 37,000 L to 9157 L, and most of the extracellular impurities are removed. The cell recovery yield is 98 percent. The cell sludge is diluted with an equal volume of buffer solution (buffer composition: 96.4 percent w/w water for injection (WFI), 0.7 percent EDTA, and 2.9 percent Tris-base) in a blending tank (BT-102). The buffer facilitates the separation of the cell debris particles from inclusion bodies. Next, a high-pressure homogenizer (HG-101) is used to break the cells and release the inclusion bodies. The exit temperature is maintained at around 10 C. The same centrifuges as before (DS-101) are then used for inclusion body recovery (P-12). The reuse of these centrifuges can be seen by noting that procedures P-9 and P-12 have the same equipment name, DS-101. The IBs are recovered in the heavy phase (with a yield of 98 percent), while most of the cell debris particles remain in the light phase. This is possible because the density (1.3 g/cm^3) and size (diameter about 1 μm) of the IBs are significantly greater than those of the cell debris particles. The IB sludge, which contains approximately 20 percent solids w/w, is washed with WFI containing 0.66 percent w/w Triton-X100 detergent (the volume of solution is twice the volume of inclusion body sludge) and recentrifuged (P-14) using the same centrifuges as before (DS-101). The detergent solution facilitates purification (dissociation of debris and soluble proteins from inclusion bodies). The exit temperature is maintained at 10 C. The slurry volume at the end of the primary recovery section is around 1440 L.

The inclusion body suspension is transferred to a glass-lined reaction tank (V-101) and is mixed with urea and 2-mercaptoethanol to final concentrations of 300 g/L (5 *M*) and 40 g/L, respectively. Urea is a chaotropic agent that dissolves the denatured protein in the inclusion bodies, and 2-mercaptoethanol is a reductant that reduces disulfide bonds. A reaction time of 8 h is required to reach a solubilization yield of 95 percent. The inclusion bodies are composed of 80 percent w/w Trp-LE'-Met-proinsulin, with the remainder being other (contaminant) proteins. At the end of the solubilization reaction, a diafiltration unit (DF-101) is used to replace urea and 2-mercaptoethanol with WFI and to concentrate the solution. This operation is performed in 6 h with a recovery yield of 98 percent. All remaining fine particles (biomass, debris, and inclusion bodies) are removed by means of a polishing dead-end filter (DE-101). This polishing filter protects the chromatographic units that are used further downstream. The solution volume at this point is around 2200 L.

The fusion protein is cleaved with CNBr (cyanogen bromide) into the signal sequence Trp-LE'-Met, which contains 121 amino acids, and the denatured proinsulin (82 amino acids) in a glass-lined reactor (V-102). The reaction is carried out in a 70 percent formic acid solution containing 30-fold molar excess CNBr (stoichiometrically, 1 mol of CNBr is required per mole of Trp-LE'-Met-proinsulin). The reaction takes 12 h at 20 C and reaches a yield of 95 percent. The mass of the released proinsulin is approximately 30 percent of the mass of Trp-LE'-Met-proinsulin. A small amount of cyanide gas is formed as a by-product of the cleavage reaction. Detailed information on CNBr cleavage is available in the patent literature (Di Marchi, U.S. Patent 4,451,396, 1984). The formic acid, unreacted CNBr, and generated cyanide gas are removed by applying vacuum and raising the temperature to around 35 C (the boiling point of CNBr). This operation is carried out in a rotary vacuum evaporator (CSP-101) and takes 1 h. Since cyanide gas is toxic, all air exhausted from the vessels is scrubbed with a solution of hypochlorite, which is prepared and maintained in situ (Bobbit and Manetta, U.S. Patent 4,923,967, 1990).

Sulfitolysis of the denatured proinsulin takes place in a glass-lined reactor (V-103) under alkaline conditions (pH 9–11). This operation is designed to unfold proinsulin, break any disulfide bonds, and add SO_3 moieties to all sulfur residues on the cysteines. The product of interest is human proinsulin$(S{-}SO_3{-})_6$ (protein–S–sulfonate). The sulfitolysis step is necessary for two reasons: (1) The proinsulin probably is not folded in the correct configuration when expressed in *E. coli* as part of a fusion protein, and (2) the cyanogen bromide treatment tends to break existing disulfide bonds. The final sulfitolysis mixture contains 50 percent w/w guanidine HCl (6 *M*), 0.35 percent ammonium bicarbonate (NH_4HCO_3), 3 percent Na_2SO_3, and 1.5 percent $Na_2S_4O_6$ (Di Marchi, U.S. Patent 4,451,396, 1984). A reaction time of 12 h is required to reach a yield of 95 percent. The presence of the denaturing reagent (guanidine HCl) prevents refolding and cross-folding of the same protein molecule onto itself or two separate protein molecules onto each other. Urea may also be used as a denaturing reagent. Upon completion of the sulfitolysis reaction, the sulfitolysis solution is exchanged with WFI to a final guanidine HCl concentration of 20 percent w/w. This procedure, P-21, utilizes the DF-101 diafilter that also handles buffer exchange after IB solubilization. The human proinsulin$(S{-}SO_3{-})_6$ is then chromatographically purified by means of three ion exchange columns (C-101) operating in parallel and each running four cycles per batch. Each column has a diameter of 140 cm and a bed height of 25 cm. A cation exchange resin is used (SP Sepharose Fast flow from GE Healthcare Biosciences) operating at pH 4.0. The eluant solution contains 69.5 percent w/w WFI, 29 percent urea, and 1.5 percent NaCl. Urea, a denaturing agent, is used to prevent incorrect refolding and cross-folding of proinsulin$(S{-}SO_3{-})_6$. The following operating assumptions were made: (1) The column is equilibrated for 30 min prior to loading. (2) The total resin binding capacity is 20 mg/mL. (3) The eluant volume is equal to 5 *column volumes* (CVs). (4) The total volume of the solutions for column wash, regeneration, and storage is 15 CVs. (5) The protein of interest is recovered in 1.5 CVs of eluant buffer with a recovery yield of 90 percent.

A refolding operation catalyzes the removal of the SO_3 moiety and then allows disulfide bond formation and correct refolding of the proinsulin to its native form. It takes place in a reaction tank (V-104). This process step involves treatment with mercaptoethanol (MrEtOH), a reductant that facilitates the disulfide interchange reaction. It is added at a ratio of 1.5 mol of mercaptoethanol to 1 mol of SO_3. Dilution to a proinsulin$(S—SO_3—)_6$ concentration of less than 1 g/L is required to prevent cross-folding of proinsulin molecules. The reaction is carried out at 8 C for 12 h and reaches a yield of 85 percent. After completion of the refolding step, the refolding reagents are replaced with WFI, and the protein solution is concentrated using a diafiltration unit (DF-102), which has a product recovery yield of 95 percent (5 percent of the protein denatures). The volume of the solution at this point is around 4500 L. Next, the human proinsulin is chromatographically purified in a *hydrophobic interaction chromatography* (HIC) column (C-102). The following operating assumptions were made: (1) The column is equilibrated for 30 min prior to loading. (2) The total resin binding capacity is 20 mg/mL. (3) The eluant volume is equal to 6 CVs. (4) The total volume of the solutions for column wash, regeneration, and storage is 15 CVs. (5) The protein of interest is recovered in 1 CV of eluant buffer with a recovery yield of 90 percent. (6) The material of a batch is handled in three cycles.

The removal of the C-peptide from human proinsulin is carried out enzymatically (using trypsin and carboxypeptidase B) in a reaction vessel (V-105). Trypsin cleaves at the carboxy-terminus of internal lysine and arginine residues, and carboxypeptidase B removes terminal amino acids. The amount of trypsin used is rate-limiting and allows intact human insulin to be formed. Carboxypeptidase is added to a final concentration of 4 mg/L, while trypsin is added to a final concentration of 1 mg/L. The reaction takes place at 30 C for 4 h and reaches a conversion yield of 95 percent. The volume of the solution at this point is around 4300 L.

A purification sequence based on multimodal chromatography, which exploits differences in molecular charge, size, and hydrophobicity, is used to isolate biosynthetic human insulin. A description of all the purification steps follows.

The enzymatic conversion solution is exchanged with WFI and concentrated by a factor of 4 in a diafilter (DF-102). An ion exchange column (C-103) is used to purify the insulin solution. The following operating assumptions were made: (1) The column is equilibrated for 30 min prior to loading. (2) The total resin binding capacity is 20 mg/mL. (3) The eluant volume is equal to 8 CVs, and the eluant is an 11.5 percent w/w solution of NaCl in WFI. (4) The total volume of the solutions for column wash, regeneration, and storage is 14 CVs. (5) The protein of interest is recovered in 1.5 CV of eluant buffer with a recovery yield of 95 percent. (6) The material from each batch is handled in four cycles. The solution volume at this point is around 1780 L.

Next, the ion exchange eluant solution is exchanged with WFI in a diafilter (DF-103) and is concentrated by a factor of 2.0. A recovery yield of 98 percent was assumed for this step (2 percent denatures).

The purification of the insulin solution proceeds with a*reversed-phase high-performance liquid chromatography* (RP-HPLC) step (C-104). Detailed information on the use of RP-HPLC for insulin purification is available in the literature. Analytical studies with a variety of reversed-phase systems have shown that an acidic mobile phase can provide excellent resolution of insulin from structurally similar insulinlike components. Minor modifications in the insulin molecule, resulting in monodesamido formation at the 21st amino acid of the A chain, or derivatization of amines via carbamylation or formylation results in insulin derivatives having significantly increased retention. Derivatives of this nature are typical of the kind of insulinlike components that are found in the charge stream going into the reversed-phase purification. The use of an acidic mobile phase results in the elution of all the derivatives after the insulin peak, while the use of mildly alkaline pH results in derivatives eluted on either side of the parent insulin peak. An ideal pH for insulin purification is in the region of 3.0 to 4.0, since this pH range is far enough below the isoelectric pH of 5.4 to provide for good insulin solubility. An eluant buffer with an acetic acid concentration of 0.25 *M* meets these operational criteria because it is compatible with the chromatography and provides good insulin solubility. A 90 percent insulin yield was assumed in the RP-HPLC step with the following operating conditions: (1) the column is equilibrated for 30 min prior to loading; (2) the total resin binding capacity is 15 mg/mL; (3) the column height is 25 cm; (4) the eluant volume is 6 CVs and its composition is 25 percent w/w acetonitrile, 1.5 percent w/w acetic acid, and 73.5 percent w/w WFI; (5) the total volume of the solutions for column wash, equilibration, regeneration, and storage is 6 CVs; and (6) the protein of interest is recovered in 1 CV of eluant buffer with a recovery yield of 90 percent.

The RP-HPLC buffer is exchanged with WFI and concentrated by a factor of 2.0 in a diafilter (DF-104) that has a product recovery yield of 98 percent (2 percent denatures). Purification is completed by a gel filtration chromatography column (C-105). The following operating assumptions were made: (1) The column is equilibrated for 30 min prior to loading. (2) The sample volume is equal to 5 percent of the column volume. (3) The eluant volume is equal to 4 CVs. (4) The total volume of the solutions for column wash, depyrogenation, stripping, and storage is 6 CVs. (5) The protein of interest is recovered in 0.5 CV of eluant buffer with a recovery yield of 90 percent. The mobile phase is a solution of acetic acid.

Next, a diafilter (DF-105) is used to concentrate the purified insulin solution by a factor of 10. The solution volume at this point is around 180 L, which contains approximately 12.8 kg of insulin. This material is pumped into a jacketed and agitated tank (V-106). Ammonium acetate and zinc chloride are added to the protein solution until each reaches a final concentration of 0.02 *M* [Datar and Rosen, in Asenjo (ed.), *Separation Processes in Biotechnology*, Dekker, New York, 1990, p. 741]. The pH is then adjusted to between 5.4 and 6.2. The crystallization is carried out at 5 C for 12 h. Insulin crystallizes with zinc with the following stoichiometry: $insulin_6$-Zn_2. Step recovery on insulin is around 90 percent.

The crystals are recovered with a basket centrifuge (BCF-101) with a yield of 95 percent. Finally, the crystals are freeze-dried (FDR-101). The purity of the crystallized end product is between 99.5 and 99.9 percent as measured by analytical high-performance liquid chromatography (HPLC). Approximately 11.5 kg of product is recovered per batch. The overall recovery yield is around 32 percent.

Table 20-36 displays the material requirements in kilograms per year, per batch, and per kilogram of main product (MP = purified insulin crystals). The solutions of H_3PO_4 (5 percent w/w) and NaOH (0.5 *M*) are used for equipment cleaning. WFI is used for preparing all the buffers utilized in product purification as well as all the cleaning solutions. Note the large amounts of formic acid, urea, guanidine hydrochloride, acetic acid, and acetonitrile required per kilogram of final product. All these materials end up in waste streams.

Table 20-36 Raw Material Requirements for Human Insulin Production: 1 Batch = 11.5 kg Main Product (MP = Purified Insulin Crystals)

Raw material	kg/year	kg/batch	kg/kg MP
Glucose	782,200	4,889	425.1
Salts	71,400	446	38.8
Water	9,715,000	60,719	5,279.9
H_3PO_4 (5% w/w)	3,979,000	24,869	2,162.5
NaOH (0.5 *M*)	3,842,000	24,013	2,088.0
WFI	51,890,000	324,313	28,201.1
Ammonia	81,600	510	44.3
EDTA	10,420	65	5.7
TRIS base	43,160	270	23.5
Triton-X-100	3,035	19	1.6
MrEtOH	98,660	617	53.6
Urea	3,054,000	19,088	1,659.8

Raw material	kg/year	kg/batch	kg/kg MP
CNBr	15,270	95	8.3
Formic acid	1,752,000	10,950	952.2
Guanidine-HCl	805,600	5,035	437.8
$Na_2O_6S_4$	24,160	151	13.1
NH_4HCO_3	5,551	35	3.0
Sodium sulfite	48,320	302	26.3
Sodium chloride	775,500	4,847	421.5
Acetic acid	975,700	6,098	530.3
Sodium hydroxide	137,200	858	74.6
Enzymes	3	0	0.0
Acetonitrile	764,700	4,779	415.6
Ammonium acetate acetate	181	1	0.1
Zinc chloride	320	2	0.2
Total	78,874,980	492,943	42,866.8

Reproduced from *Bioseparations Science and Engineering*, 2d ed., by Roger G. Harrison, Paul W. Todd, Scott R. Rudge, and Demetri P. Petrides (2015). By Permission of Oxford University Press.

In the base case, this waste is treated and discarded. However, opportunities may exist for recycling some chemicals for in-process use and recovering others for off-site use. For instance, formic acid (HCOOH), acetonitrile, and urea are good candidates for recycling and recovery. Formic acid is used in large quantities (11 tons per batch) in the CNBr cleavage step (V-102), and it is removed by means of a rotary vacuum evaporator (CSP-101), along with small quantities of CNBr, H_2O, and urea. The recovered formic acid can be readily purified by distillation and recycled in the process. Around 2.2 metric tons per batch of urea is used for the dissolution of inclusion bodies (V-101), and 17 metric tons per batch is used in the first chromatography step (C-101) to purify proinsulin$(S—SO_3)_6$ before its refolding. Approximately 90 percent of the urea appears in just two waste streams (Liq Waste 4 and 8). It is unlikely that these urea-containing streams can be purified economically for in-process recycling. However, these solutions can be concentrated, neutralized, and shipped off site for further processing and utilization as a nitrogen fertilizer.

Approximately 4.8 metric tons (MT) per batch of acetonitrile is used in the reversed-phase HPLC column (C-104), and most of it ends up in the waste stream of the column (Liq Waste 13) along with 6.8 MT of water, 1.85 MT of acetic acid, and small amounts of NaCl and other impurities. It is unlikely that acetonitrile can be recovered economically to meet the high-purity specifications for a step so close to the end of the purification train. However, there may be a market for off-site use.

The scheduling and equipment utilization for consecutive batches can be determined using SuperPro Designer (Harrison et al., *Bioseparations Science and Engineering,* Oxford University Press, Oxford, UK, 2015, p. 489). The batch time is approximately 11 days. This is the time required to go from the preparation of raw materials to final product for a single batch (excluding inoculum preparation). However, since most of the equipment items are utilized for much shorter periods within a batch, a new batch is initiated every 48 h. The equipment with the least idle time between consecutive batches is the *time* (*or scheduling*) *bottleneck* (V-104 in this case) that determines the maximum number of batches per year. Its occupancy time (approximately 45 h) is the minimum possible time between consecutive batches. The production line operates around the clock and processes 160 batches per year.

Process scheduling is closely related to the determination of the annual capacity of a batch process. The last part of this example discusses how changes in scheduling and installation of additional equipment can be used to increase process throughput and reduce manufacturing cost.

Another characteristic of batch processing is the variable demand for resources (e.g., labor, utilities, and raw materials) as a function of time. For example, SuperPro Designer can be used for tracking the use of WFI and for sizing the equipment for WFI needed to produce insulin by this process (Harrison et al., *Bioseparations Science and Engineering,* Oxford University Press, Oxford, UK, 2015, p. 490).

The results of the economic evaluation are shown in Table 20-37. The detailed tables for these calculations are available as part of the evaluation version of SuperPro Designer. For a plant of this capacity, the total capital investment is $178 million. The unit production cost is $61 per gram of purified insulin crystals. Assuming a selling price of $100/g, the project yields an after-tax internal rate of return (IRR) of 35 percent and a net present value (NPV) of $250 million (assuming a discount interest rate of 7 percent). Based on these results, this project represents a very attractive investment. However, if amortization of up-front R D costs is considered in the economic evaluation, the numbers change drastically. For instance, a modest amount of $100 million for up-front R D cost amortized over a period of 10 yr reduces the IRR to 16.8 percent and the NPV to $153 million.

Table 20-37 Key Economic Evaluation Results for Human Insulin Production

Direct fixed capital	$145 million
Total capital investment	$178 million
Plant throughput	1803 kg/yr
Manufacturing cost	$110 million/yr
Unit production cost	$61/g
Selling price	$100/g
Revenues	$180 million/yr
Gross profit	$70 million/yr
Taxes (40%)	$28 million/yr
IRR (after taxes)	35%
NPV (for 7% discount interest rate)	$250 million

Reproduced from *Bioseparations Science and Engineering*, 2d ed., by Roger G. Harrison, Paul W. Todd, Scott R. Rudge, and Demetri P. Petrides (2015). By Permission of Oxford University Press.

The operating cost is broken down in Fig. 20-67. The cost of consumables is the most important, accounting for 31.9 percent of the overall manufacturing cost. Consumables represent the expense of periodically replacing the resins of the chromatography columns and the membranes of the membrane filters. The cost of raw materials is the second most important, accounting for 27.3 percent of the overall cost. The facility-dependent cost is third, accounting for 24.1 percent of the overall cost. This cost item accounts for the depreciation and maintenance of the facility and other overhead expenses. Labor and Lab/QC/QA account for 9.1 percent. The treatment and disposal of waste materials accounts for 7.3 percent of the total cost. As mentioned in the material balance section, recycling and reuse of some of the waste materials may reduce this cost.

Figure 20-67 Breakdown of manufacturing cost for human insulin production. [Reproduced from Bioseparations Science and Engineering, 2d ed., by Roger G. Harrison, Paul W. Todd, Scott R. Rudge, and Demetri P. Petrides (2015). By Permission of Oxford University Press.]

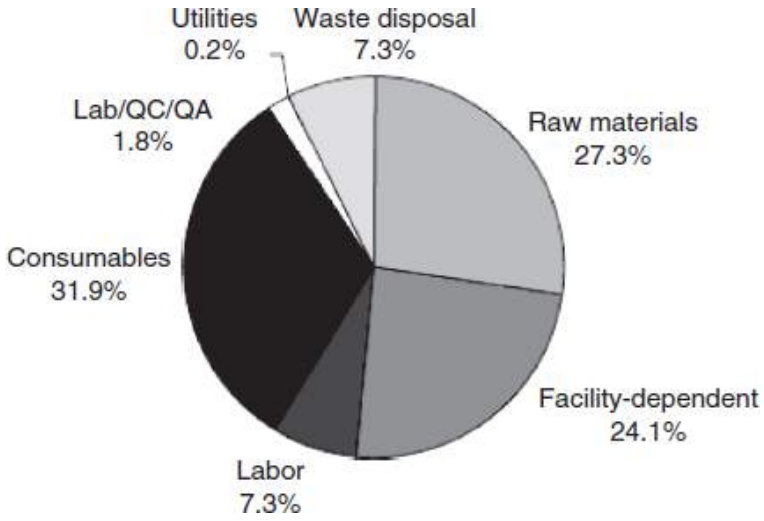

The percentage of the operating cost associated with each flowsheet section is displayed inFig. 20-68. Only 7.3 percent of the overall cost is associated with fermentation. The other 92.7 percent is associated with the recovery and purification sections. Most of the cost is associated with the reactions section because of the large amounts of expensive chemicals and consumables required for purification.

Figure 20-68 Cost distribution per flowsheet section for human insulin production. [Reproduced from Bioseparations Science and Engineering, 2d ed., by Roger G. Harrison, Paul W. Todd, Scott R. Rudge, and Demetri P. Petrides (2015). By Permission of Oxford University Press.]

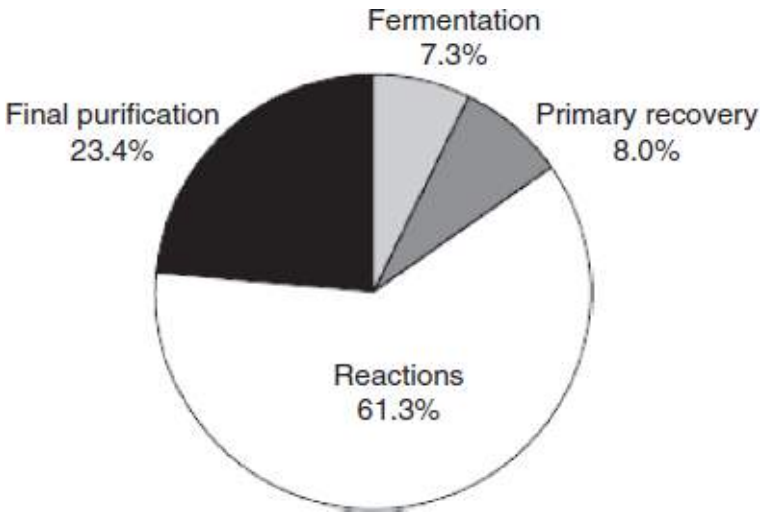

Finally, for each raw material used in the process, Table 20-38 displays the price, annual cost, and contribution to the overall raw materials cost. WFI, urea, and H_3PO_4 (5 percent w/w) are the top three contributors to the raw materials cost. The H_3PO_4 and NaOH solutions are used for equipment cleaning.

Table 20-38 Cost of Raw Materials for Human Insulin Production (Year 2012 Prices)

Bulk material	Unit cost ($/kg)	Annual cost ($)	Percent
Glucose	0.60	469,300	1.56
Salts	1.00	71,400	0.24
Water	0.05	485,800	1.61
H_3PO_4 (5% w/w)	1.00	3,979,000	13.19
NaOH (0.5 *M*)	0.50	1,921,200	6.37
WFI	0.10	5,188,500	17.20
Ammonia	0.70	57,100	0.19
EDTA	18.50	192,700	0.64
TRIS base	6.00	259,000	0.86
Triton-X-100	1.50	4,600	0.02
MrEtOH	3.00	296,000	0.98
Urea	1.52	4,642,200	15.38
CNBr	11.00	168,000	0.56
Formic acid	1.60	2,802,400	9.29
Guanidine-HCl	2.15	1,732,000	5.74
$Na_2O_6S_4$	0.60	14,500	0.05
NH_4HCO_3	1.00	5,600	0.02
Sodium sulfite	0.40	19,300	0.06
Sodium chloride	1.23	954,000	3.16
Acetic acid	2.50	2,439,400	8.08
Sodium hydroxide	3.50	480,300	1.59
Enzymes	500,000	1,691,100	5.60
Acetonitrile	3.00	2,294,200	7.60

Bulk material	Unit cost ($/kg)	Annual cost ($)	Percent
Ammonium acetate	15.00	2,700	0.01
Zinc chloride	12.00	3,800	0.01
Total		30,174,100	100.00

Reproduced from *Bioseparations Science and Engineering*, 2d ed., by Roger G. Harrison, Paul W. Todd, Scott R. Rudge, and Demetri P. Petrides (2015). By Permission of Oxford University Press.

Other assumptions for the economic evaluation include the following: (1) A new manufacturing facility will be built and dedicated to production of 1800 kg/yr of purified insulin. (2) The entire direct fixed capital is depreciated linearly over a period of 10 yr. (3) The project life-time is 15 yr. (4) The unit cost of membranes is $800/m^2 and they are replaced every 50 cycles. (5) The average unit cost of chromatography resins is $1500/L. (6) The waste disposal cost is $5/m^3 for low BOD streams and $150/m^3 for streams containing significant amounts of solvents and other regulated chemicals.

In the base case, a new batch is initiated every 48 h. Most of the equipment items, however, are utilized for less than 24 h per batch. If the market conditions are favorable, this provides the opportunity for increasing plant throughput without major capital expenditures. A realistic improvement is to initiate a batch every 24 h. This will require a new fermenter of the same size as the original fermenter, whose operation will be staggered relative to the existing unit so that one fermenter is ready for harvesting every day. Such a production change will also require additional equipment of the following types: (1) disk-stack centrifuges to reduce the occupancy of DS-101 to less than 24 h, (2) two reaction vessels to reduce the occupancy of V-103 and V-104, and (3) membrane filters to reduce the occupancy of DF-104 and DF-105.

The additional capital investment for such a change is around $55 million. This additional investment will allow the plant's capacity to be doubled, and the new unit production cost will be around $55/g. The reduction in the unit production cost is rather small because the majority of the manufacturing cost is associated with consumables and raw materials that scale approximately linearly with production.

Therapeutic Monoclonal Antibody Production Monoclonal antibodies are large protein molecules that consist of two main regions, the Fab (fragment antigen binding) region and the Fc (fragment crystallizable) region. Monoclonal antibodies (mAbs) are the fastest-growing segment in the biopharmaceutical industry. Currently mAbs are used to treat various types of cancer, rheumatoid arthritis, psoriasis, severe asthma, macular degeneration, multiple sclerosis, and other diseases. More than 20 mAbs and Fc fusion proteins are approved for sale in the United States and Europe, and approximately 200 mAbs are in clinical trials for a wide variety of indications [Walsh, *Trends Biotechnol.* **23:** 553 (2005); Pavlou and Belsey, *Eur. J. Pharm. Biopharm.* **59:** 389 (2005)]. The market size for mAbs in 2010 was in excess of $35 billion [Rader, *Contract Pharma*, July/Aug. 2012].

The high-dose demand for several mAbs translates into annual production requirements for purified product in the metric ton range. This example illustrates the analysis of a large-scale mAb process. Again, the modeling and calculations are performed with SuperPro Designer.

The flowsheet of the overall process is displayed in Fig. 20-69. The generation of the flowsheet was based on information available in the patent and technical literature combined with the authors' engineering judgment and experience with such processes [Kelley, *Biotechnol. Prog.* **23:** 995 (2007)]. The process in this example produces 1544 kg/yr of purified mAb. The flow diagram of Fig. 20-69 is a simplified representation of the actual process because it lacks all the buffer preparation and holding activities. Such processes require 20 to 30 buffer solutions for product purification. These solutions are prepared in mixing tanks and then stored in holding tanks located close to the purification train. The tanks required for buffer preparation and holding add to the capital investment of the facility, while the required labor adds to the manufacturing cost. The model files for this example that are part of the evaluation version of SuperPro Designer (available at www.intelligen.com) include the tanks for buffer preparation and holding. In addition, the capital and operating costs associated with buffer preparation activities were considered in the cost analysis results presented in this example. Additional information on this example in the form of two tutorial videos is available at www.intelligen.com/videos. The upstream part is split into two sections: the Inoculum Preparation section and the Bioreaction section. The inoculum is initially prepared in 225-mL T-flasks (TFR-101). Next, the material from the T-flasks is moved to 2.2-L roller bottles (RBR-101; shake flasks are frequently used instead of roller bottles for suspension cultures), then to 100-L and subsequently to 200-L rocking bioreactors that utilize disposable bags (BBS-101 and BBS-102). Sterilized media are fed at the appropriate amount in all four initial steps (3.6, 11.4, 43.6, 175.4 kg/batch, respectively). The broth is then moved to the first stirred seed bioreactor (DSBR-101), which utilizes 1000-L disposable bags. The second seed bioreactor (SBR-102) is a 5000-L stainless-steel vessel. For the two seed bioreactors, the media powder is dissolved in WFI in two prep tanks (MP-101 and MP-102) and then sterilized/fed to the reactors through 0.2-μm dead-end filters (DE-101 and DE-102). In the cell culture section, serum-free low-protein media powder is dissolved in WFI in a stainless-steel tank (MP-103). The solution is sterilized using a 0.2-μm dead-end polishing filter (DE-103). A 20,000-L stainless stirred-tank bioreactor (BR-101) is used to grow the cells, which produce the therapeutic monoclonal antibody (mAb). The production bioreactor operates in fed-batch mode. High media concentrations are inhibitory to the cells, so one-half of the media is added at the start of the process and the rest is fed at a variable rate during fermentation. The concentration of dry media powder in the initial feed solution is 17 g/L. The cell culture time is 12 days. The volume of broth generated per bioreactor batch is approximately 15,000 L, which contains roughly 30.5 kg of product (the product titer is approximately 2 g/L).

Figure 20-69 Monoclonal antibody production flowsheet (L = liters). [Reproduced from Bioseparations Science and Engineering, 2d ed., by Roger G. Harrison, Paul W. Todd, Scott R. Rudge, and Demetri P. Petrides (2015). By Permission of Oxford University Press.]

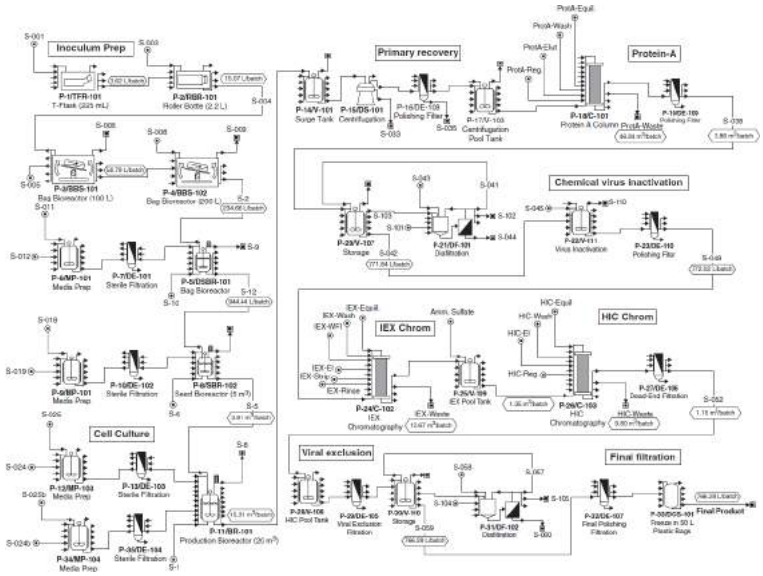

Between the downstream unit procedures there are 0.2-μm dead-end filters to ensure sterility. The generated biomass and other suspended compounds are removed using a disk-stack centrifuge (DS-101). During this step, roughly 5 percent of mAb is lost in the solids waste stream. The bulk of the contaminant proteins are removed using a protein A affinity chromatography column (C-101) which processes a batch of material in four cycles. The following operating assumptions were made for each chromatography cycle: (1) Resin binding capacity is 15 g of product per liter of resin. (2) The eluant or elution buffer is a 0.6 percent w/w solution of acetic acid, and its volume is equal to 5 column volumes (CVs). (3) The product is recovered in 2 CVs of eluant with a recovery yield of 90 percent. (4) The total volume of the solution required for column equilibration, wash and regeneration is 14 CVs. The entire procedure takes approximately 27 h and requires a resin volume of 502 liters. The protein solution is then concentrated fivefold and diafiltered with two volumes of buffer (in P-21/DF-101). This step takes approximately 8.4 h and requires a membrane of 21 m^2. The product yield is 97 percent. The concentrated protein solution is then chemically treated for 1.5 h with Polysorbate 80 to inactivate viruses (in P-22/V-111). The ion exchange (IEX) chromatography step (P-24/C-102) that follows processes one batch of material in three cycles. The following operating assumptions were made for each cycle: (1) The resin's binding capacity is 40 g of product per liter of resin. (2) A gradient elution step is used with a sodium chloride concentration ranging from 0.0 to 0.1 *M* and a volume of 5 CVs. (3) The product is recovered in 2 CVs of eluent buffer with a mAb yield of 90 percent. (4) The total volume of the solutions required for column equilibration, wash, regeneration, and rinse is 16 CVs. The step takes approximately 22.3 h and requires a resin volume of 210 L. Ammonium sulfate is then added to the IEX eluate (in P-25/V-109) to a concentration of 0.75 *M*. This increases the ionic strength of the eluate in preparation for the hydrophobic interaction chromatography (HIC, P-26/C-103) step that follows. Like the IEX step which preceded it, the HIC step processes one batch of material in three cycles. The following operating assumptions were made for each cycle of the HIC step: (1) The resin binding capacity is 40 g of product per liter of resin. (2) The eluant is a sodium chloride (4 percent w/w) sodium dihydrogen phosphate (0.3 percent w/w) solution, and its volume is equal to 5 CVs. (3) The product is recovered in 2 CVs of eluant buffer with a recovery yield of 90 percent. (4) The total volume of the solutions required for column equilibration, wash, and regeneration is 12 CVs. The step takes approximately 22 h and requires a resin volume of 190 L. A viral filtration step (DE-105) follows. It is a dead-end type of filter with a pore size of 0.02 μm. Finally, the HIC elution buffer is exchanged for the *product bulk storage* (PBS) buffer and concentrated 1.5-fold (in DF-102). This step takes approximately 20 h and requires a membrane area of 10 m^2. The approximately 800 L of final protein solution is stored in twenty 50-L disposable storage bags (DCS-101). The overall yield of the downstream operations is 63.2 percent, and 19.3 kg of mAb is produced per batch.

The equipment occupancy chart of the process for consecutive batches can be drawn using SuperPro Designer (Harrison et al., *Bioseparations Science and Engineering,* Oxford University Press, Oxford, UK, 2015, p. 498). The schedule represents a plant that has a single production train. The batch time is approximately 50 days. This is the time required from the start of inoculum preparation to the final product purification of a single batch. A new batch is initiated every 2 weeks (14 days). The production bioreactor (BR-101) is the time (scheduling) bottleneck. On an annual basis, the plant processes 20 batches and produces approximately 386 kg of purified mAb. The analysis revealed that under these conditions the downstream train is underutilized, and the cycle time of the process—the time between consecutive batches—is relatively long. The cycle time of the process can be reduced and the plant throughput increased by installing multiple bioreactor trains that operate in staggered mode (out of phase) and feed the same purification train. For a case of four bioreactor trains feeding the same purification train, the new cycle time is 3.5 days, which is one-fourth of the original. Under these conditions, the plant processes 80 batches per year and produces 1544 kg/yr of mAb. Some biopharmaceutical companies have installed more than four bioreactor trains per purification train in order to achieve cycle times as low as 2 days.

The material requirements of the process are summarized in Table 20-39. Note the large amount of WFI utilized per batch. The majority of WFI is consumed for cleaning and buffer preparation.

Table 20-39 Raw Material Requirements for mAb Production: 1 Batch = 19.3 kg Main Product (MP= Purified mAb)

Material	kg/yr	kg/batch	kg/kg MP
Inoc. media solution	18,630	232.88	12.066
WFI	8,430,000	105,375.00	5,459.845
Serum-free media	37,340	466.75	24.184
H_3PO_4 (5% w/w)	2,277,000	28,462.50	1,474.741
NaOH (0.5 *M*)	2,054,000	25,675.00	1,330.311
NaOH (0.1 *M*)	7,815,000	97,687.50	5,061.528
Amm. sulfate	12,160	152.00	7.876
Polysorbate 80	6	0.08	0.004
Protein A equil. buffer	1,967,000	24,587.50	1,273.964
Protein A elution buffer	800,200	10,002.50	518.264
Protein A reg. buffer	480,400	6,005.00	311.140
NaCl (1 *M*)	184,200	2,302.50	119.301
IEX elution buffer	16,130	201.63	10.447
IEX equil. buffer	664,900	8,311.25	430.635
HIC elution buffer	239,200	2,990.00	154.922
HIC equil. buffer	449,600	5,620.00	291.192
Concentrated PBS	14,370	179.63	9.307
EtOH (10% w/w)	363,000	4,537.50	235.104
Total	**25,823,136**	**322,789.20**	**16,724.83**

Reproduced from *Bioseparations Science and Engineering*, 2d ed., by Roger G. Harrison, Paul W. Todd, Scott R. Rudge, and Demetri P. Petrides (2015). By Permission of Oxford University Press.

Key economic evaluation results generated using the built-in cost functions of SuperPro Designer are displayed in Table 20-40. The total capital investment (for the case with the four bioreactor trains) is around $477 million. The total annual operating cost is $130 million, resulting in a unit production cost of around $84/g (1544 kg of purified mAb is produced annually). Assuming a selling price of $200/g, the project yields an after-tax internal rate of return (IRR) of 24.3 percent and a net present value (NPV) of $560 million (assuming a discount interest rate of 7 percent).

Table 20-40 Key Economic Evaluation Results for mAb Production

Direct fixed capital	$365 million
Total capital investment	$477 million
Plant throughput	1544 kg of mAb/yr
Manufacturing cost	$130 million/yr
Unit production cost	$84/g of mAb
Selling price	$200/g of mAb
Revenues	$309 million/yr
Gross profit	$179 million/yr
IRR (after taxes)	24.3%
NPV (for 7% discount interest rate)	$560 million
Reproduced from *Bioseparations Science and Engineering*, 2d ed., by Roger G. Harrison, Paul W. Todd, Scott R. Rudge, and Demetri P. Petrides (2015). By Permission of Oxford University Press.	

A breakdown of the operating cost contributors is presented in Table 20-41. The facility-dependent cost is the most important item, accounting for 46.7 percent of the manufacturing cost or $39.2/g of final product. This is common for high-value products that are produced in small quantities in expensive facilities. Depreciation of the fixed capital investment and maintenance of the facility are the main contributors to this cost. Consumables are the second most important operating cost, accounting for 18.2 percent of the total or $15.3/g of final product. Consumables include chromatography resins, membrane filters, and disposable bags that need to be replaced on a regular basis. Labor and raw materials costs come third and fourth, accounting for 14.6 percent and 12.9 percent of the total cost, respectively. The miscellaneous cost item (4.2 percent of total) accounts for heating/cooling utilities, electricity, and environmental costs. The cost of WFI, commonly classified as a utility cost in industry, is accounted for in the cost of raw materials in this example. In terms of cost distribution per section, 62 percent of the cost is associated with the upstream section and 38 percent with the downstream.

Table 20-41 Breakdown of the Manufacturing Cost for mAb Production

Cost item	$ million/yr	$/g	%
Raw materials	16.67	10.8	12.86
Facility-dependent	60.54	39.2	46.71
Labor	18.89	12.2	14.58
Consumables	23.58	15.3	18.19
Lab/QC/QA	4.45	2.9	3.43
Miscellaneous	5.47	3.5	4.23
Total	**129.60**	**83.9**	**100.00**

Reproduced from *Bioseparations Science and Engineering*, 2d ed., by Roger G. Harrison, Paul W. Todd, Scott R. Rudge, and Demetri P. Petrides (2015). By Permission of Oxford University Press.

The economic evaluation relies on the following key assumptions: (1) A new manufacturing facility will be built and dedicated to production of 1544 kg/yr of mAb. (2) The entire direct fixed capital is depreciated linearly over a period of 12 yr. (3) The project lifetime is 16 yr. (4) The unit cost of WFI is $0.15/L. (5) The cost of the serum-free media (in powder form) is $300/kg. (6) All the chemicals used are high-purity grade. (7) The unit cost of membranes is $400/$m^2$. (8) The unit cost of chromatography resins is $6000/L, $1200/L, and $2050/L for columns C-101, C-102, and C-103, respectively. (9) The chromatography resins are replaced every 60, 50, and 50 cycles for columns C-101, C-102, and C-103, respectively.

After a model of the entire process has been developed on the computer, tools such as SuperPro Designer can be used to ask and readily answer “what if?” questions and to carry out sensitivity analysis with respect to key design variables. In this example, the impact of product titer (varied from 1 to 10 g/L) and bioreactor size (10,000 and 20,000 L) on unit production cost is evaluated. Figure 20-70 displays the results of the analysis. All points correspond to four production bioreactors feeding a single purification train. For low product titers, the bioreactor volume has a considerable effect on the unit production cost. For instance, for a product titer of 1 g/L, going from 10,000 to 20,000 L of production bioreactor volume reduces the unit cost from $230/g to $162/g. On the other hand, for high product titers (e.g., around 5 g/L), the impact of bioreactor scale is not as important. This can be explained by the fact that at high product titers, the majority of the manufacturing cost is associated with the purification train. It is therefore wise to shift R D efforts from cell culture to product purification as the product titer in the bioreactor increases. A key assumption underlying the sensitivity analysis is that the composition and cost of the cell culture media are independent of product titer.

Figure 20-70 The mAb production cost as a function of product titer and production bioreactor volume (L = liters). The arrow indicates the product titer for this example. [Reproduced from Bioseparations Science and Engineering, 2d ed., by Roger G. Harrison, Paul W. Todd, Scott R. Rudge, and Demetri P. Petrides (2015). By Permission of Oxford University Press.]

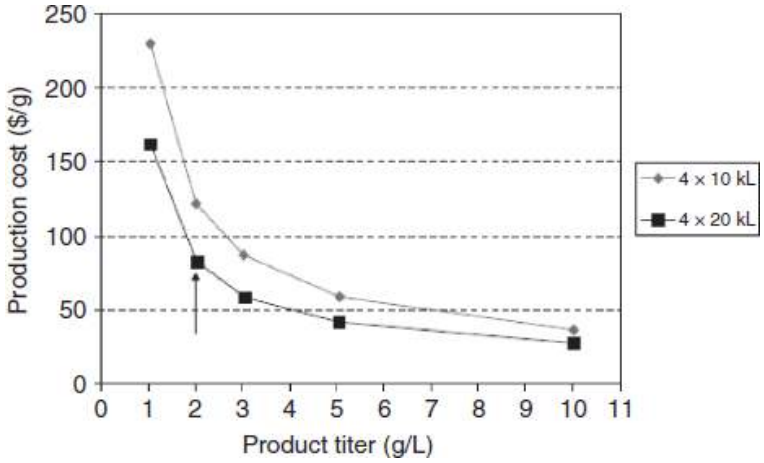

[1] Portions of this section have been reproduced from *Bioseparations Science and Engineering,* 2d ed., by Roger G. Harrison, Paul W. Todd, Scott R. Rudge, and Demetri P. Petrides (2015). By Permission of Oxford University Press.